School of Molecular and Life Sciences

Ancient DNA Archives In Marine Sediments

Kuldeep Dilip More

This thesis is presented for the Degree of

Doctor of Philosophy

of

Curtin University

December 2018

DECLARATION

To the best of my knowledge and belief this thesis contains no material previously published by any other person except where due acknowledgment has been made.

This thesis contains no material which has been accepted for the award of any other degree or diploma in any university.

Kuldeep D. More

Perth, December 13th, 2018

ABSTRACT

Analysing the response of past ecosystems to paleoclimate variations will help us gauge the effects of ongoing and long-term climate change on similar ecosystem in long term. Marine sediments provide ideal settings for such studies as they form an archive of changing benthic and pelagic ecosystem in the form of a deposited biomass. Traditional approaches employed in paleoecological studies rely heavily on the ability of plankton to form microsopic or chemical fossils (i.e. biomarkers). However, most plankton fail to produce or preserve any diagnostic features and/or molecules upon burial and hence provide incomplete picture of the past. Therefore, a more reliable method is required to include the majority of planktonic and benthic taxa in paleoenvironmental studies, and to elucidate a more complete picture of climate-driven paleoecological changes. DNA has been shown to be well-preserved in marine and lake sediments covering at least the last glacial interglacial cycle, and can be analysed in correlation with geochemical proxies to reveal the species-specific ecosystem responses to past climate. This emerging field of analysing sedimentary ancient DNA is called "sedimentary paleogenomics" and was employed in this thesis to investigate paleo-ecology-climate dynamics in three different oceanic settings.

In chapter 2, these techniques were employed to investigate how past protist communities responded to alternating strong and weak oxygen minimum zones (OMZs) that occurred in the north-eastern (NE) Arabian Sea during last glacial interglacial cycle. Protists form the base of marine food chain and any change in protist community reflects itself in higher trophic levels. The NE Arabian Sea currently harbours the most extensive oxygen minimum zone and how oxygen stress affects the protist community is known from few modelling experiments. However, the long-term effects of oxygen stress on pelagic as well as benthic protist communities is not known. Prior geochemical proxy records revealed that the NE Arabian sea experienced alternate strengthening and weakening of the OMZ in response to north Atlantic climate oscillations known as Dansgaard–Oeschger (D/O) events and varying monsoon intensity during the last glacial-interglacial cycle. 18S rDNA sequencing of the protistal DNA isolated from sediment intervals spanning last 43 kyrs revealed that strong OMZ conditions shaped past protist communities by creating isolated habitats for those capable of sustaining oxygen depletion either by adapting a parasitic life cycle or by establishing mutualistic connections with others or by forming cysts.

In chapter 3, a metagenomic approach was used to investigate if sedimentary microbial communities reflect the changes in paleodepositional conditions that occurred during known

climate stages and their transitions since the deglacial in the anoxic Black Sea. The Black Sea functioned as lake during last glacial lowstands and was reconnected to the Mediterranean Sea ~9.0 ka BP as a result of post-glacial sea level rise. Parallel analysis of geochemical proxies revealed the hydrological changes associated with known dry (younger-dryas, preboreal, subboreal) and wet (Allerød, Holocene climate optimum, and Subatlantic) climate stages. Previous ancient DNA profiling revealed significant shifts in planktonic eukaryotic communities (e.g. photosynthetic plankton and zooplankton) with these paleoclimate stages and their transitions. Here, I investigated the downcore distribution of sedimentary bacteria in the Black Sea in the context of paleoenvironmental proxies. The metagenomic survey revealed that taxonomic as well as functional diversity of sedimentary microbiome changed in response to paleo-environmental changes associated with climate transitions in the Black Sea. Presumably active obligate anaerobes responded to the establishment of modern environmental conditions. In contrast, obligate aerobes, likely to be seeded from the past water column, showed a more direct response to paleo-depositional changes.

Chapter 4 describes the use of 16S rDNA survey to analyse how sedimentary archaea reflect the changes in paleodepositional environment that occurred due to drastic variations in sea level and salinity during the last and the previous glacial-interglacial cycles in the Red Sea. Sea level lowstands and hypersaline conditions in the Red Sea occurred during the last and penultimate glacial maximum while sea level highstands and modern-day salinity occurred during the Holocene and the Eemian (i.e., the previous interglacial). These drastic changes were expected to have had a selective effect on the distribution of pelagic and/or benthic archaeal communities in the Red Sea. I used 16S rDNA sequencing to analyse how these variations were mirrored in the sub-seafloor archaeal composition. Sedimentary archaeal 16S profiling revealed a strong significant response of subseafloor archaeal communities to changes in paleodepositional conditions associated with marine isotope stages and their transitions and only a moderately significant response to changes in sediment lithology. Along with an indigenous archaeal community, most likely actively involved in methane cycling and biodegradation of organic matter, the Red Sea sediments contained preserved DNA from taxa that were seeded from the past overlying water column and also of past terrestrial origin.

These results demonstrate the importance of the ancient DNA approach in climate-driven paleoenvironmental reconstructions. Furthermore, the data generated through this study will be an invaluable asset to develop models for prediction of future climate-ecosystem dynamics.

ACKNOWLEDGEMENTS

If this was a separate chapter, it would have been the longest one. Even after writing all the thesis, I find writing acknowledgments very difficult…so many people to thank in such a little space. All of them have transformed my PhD into a wonderful experience.

Firstly, my main supervisor Marco Coolen and his wife Cornelia have been the greatest support system of my PhD life. Marco has shown an incredible amount of patience and trust in me and most importantly he gave me the time and space to develop my ideas. I know Marco and Cornelia for 7 years now and they have been very parental towards me during all these years. Marco is a true guru and not just a teacher. In India, we say, "There is difference between a teacher and a Guru. Teacher teaches you techniques he knows, but Guru makes you so able that you can replace him" Teaching someone is easy but teaching someone without holding back is something very difficult. Every little thing that I know in the field of paleomics, I owe to Marco. I am extremely lucky to have done my PhD under his guidance. I can say a lot of nice things about Cornelia, but on top of all those things she is the most genuine human being ever. Getting to know her is a blessing. I will never forget the lengthy discussions I had with her on all the topics ranging from world history to science to spirituality. I would also like to thank my co-supervisor Kliti Grice, without whose support I wouldn't have been able to finish my PhD. She is the backbone of our group. I also like to thank my chair-person Franca Jones who always answered every query I had in detail and with a pleasant smile.

A huge thank goes to my research group at WA- Organic and Isotope Geochemistry Centre (WA-OIGC). First and foremost thanks to Bettina (Superbetty) for being there to help me whenever I needed and for cheering me up all the time. I would also like to thank Alan, Calum, Matt, Su, Megan, Yali, Chloe, Gemma, Nannan, Danlei, Peter, Alex and Mattia.

Now is the time to thank my friends- Kaushik, Kiran, Swati, Ajay and Sayali. Their mere presence in my life makes me the most fortunate person on the planet. The moments I spent with Kaushya in Europe during my PhD, were one of the best ones in my life. Kirya and Swati have been the emergency support system. I want to thank them just for being there…it's a huge favour. I would also like to thank my Aussie family who are very close to me- Buddhika, Chandramalika, Shamika, Abby, Jossie, Darren, Karin and Jaime. I thank Jaime for introducing me to Buddhi who later gave me my Aussie family. I appreciate Buddhi and Jaime even more, now that I have been through the same journey as they have. Buddhi gave us all the delicious food and is the ultimate "host". We all shared one of the most joyful moments of our lives in

her house. I will never forget my weekend trips to beach with Malika and Shamika….those were the good times! I am very lucky to have them as my close friends. Thanks to Abby and Jossie for being the constant source of positivity. I can make any type of joke without any barrier with Darren and that really helps a lot. Karin and her family are one of the kindest people ever. I was welcomed with warm heart by them during my visits to Rockingham. I want to thank Khiraj, Saee, Pinky Pathak and Daad for making sure that I am doing alright all the time. I want to thank my teachers Mrs. Bhingarde, Mrs. Shirke, Mrs. P. P. Kulkarni, Mrs. M. Kadekar, Dr. Amar Lawate, Mrs. Pathak, Mrs. J. J. Jankar. All of them prepared me for this journey and bestowed their blessings upon me. A huge thanks to my sitar Guru Dr. Hemant Desai for not giving up on me and motivating me to play sitar more and more during stressful times.

I want to thank three most important women in my life- my sister, my aunt and my mother. My sister Nonya and I are so close that we finish each other's sentences and often wonder whose memories belong to whom. I thank her for being the lovely sister that she is. My aunt is my second mother, worries more about me than her own son and turns my every trip to India into a festival. Kahlil Gibran once said "Mother: the most beautiful word on the lips of mankind." How true….what can I say; how can I thank my mother for her unconditional love. She has sacrificed so much for me that no words in any language are good enough to show my gratitude. All that I am, or hope to be, I owe to my angel mother.

I would like to dedicate this dissertation to my country, "India". May She stand free and continue to prosper in eons to come! I also dedicate my dissertation to all those Indian scientists whose innovations went unrecognized.

Primary publications

The chapters integrating this thesis correspond to papers published or submitted or in preparation and are listed below. I warrant that I have obtained, where necessary, permission from the copyright owners to use the journal articles in this dissertation.

Chapter 2

More K.D., Orsi W.D., Galy V., Giosan L., He L., Grice K. and Coolen M.J.L.(2018) A 43 kyr record of protist communities and their response to oxygen minimum zone variability in the Northeastern Arabian Sea. Earth and Planetary Science Letters, 496, 248–256.

https://doi.org/10.1016/j.epsl.2018.05.045

Chapter 3

More K.D., Giosan L., Galy V., Grice K. and Coolen M.J.L. (2018) Holocene paleodepositional changes reflected in the deep biosphere microbiome of the Black Sea sediments. Geobiology.

https://doi.org/10.1111/gbi.12338

Chapter 4

More K.D., Giosan L., Galier V. and Coolen M.J.L. Deep biosphere archaeal communities in the Red Sea sediments reflect depositional changes during marine isotope stages. Quaternary Science Reviews, (in preparation for submission).

Contribution of others

The work presented in this thesis was primarily experimentally executed, interpreted and individual manuscripts were prepared by the first author (Kuldeep D. More) under main supervision and guidance of A/Prof. Marco Coolen.

Chapter 2

Marco Coolen, Valier Galy and Liviu Giosan initiated and designed the study. Kuldeep developed ideas and performed experiments. Kuldeep More and Marco Coolen developed analytical tools. Kuldeep More and William Orsi analyzed data. Kuldeep More wrote the paper. Kuldeep More interpreted the data and all authors provided editorial comments on the manuscript and thesis chapter.

Chapter 3

Marco Coolen and Liviu Giosan initiated and designed the study. Kuldeep More developed ideas and performed experiments. Kuldeep More developed analytical tools, analysed and interpreted the data. Kuldeep More wrote the paper. All authors provided editorial feedback on the manuscript and thesis chapter.

Chapter 4

Marco Coolen and Xabier Irigoien initiated and designed the study. Marco Coolen and Kuldeep More developed ideas. All authors contributed in the experiments. Kuldeep More developed analytical tools, analysed and interpreted the data. Kuldeep More wrote the paper. All authors provided editorial feedback on thesis chapter.

Secondary publications

The following correspond to manuscripts based on research conducted during the preparation of this thesis and abstracts for conference presentations

Peer reviewed journal articles not part of this thesis:

Orsi W.D., Coolen M.J.L., Wuchter C., He L.J., More K.D., Irigoien X., Chust G., Johnson C., Hemingway J.D., Lee M., Galy V. and Giosan L. (2017) Climate oscillations reflected within the microbiome of Arabian Sea sediments. Scientific Reports, 6040.

Laber C. P., Hunter J.E., Carvalho F., Collins J. R., Hunter E.J., Schieler B.M., Boss E., More K.D., Frada M., Thamatrakoln K., Brown C.M., Haramaty L., Ossolinski J., Fredricks H., Nissimov J.I., Vandzura R., Sheyn U., Lehahn Y., Chant R.J., Martins A.M., Coolen M.L.J., Vardi A., DiTullio G.R., Van Mooy B.A.S. and Bidle K. (2018) Coccolithovirus facilitation of carbon export in the North Atlantic. Nature Microbiology, 3, pages 537–547.

Conference abstracts

More K.D., Grice K., Coolen M.J.L. (2016) Planktonic and benthic eukaryotic community responses to glacial-interglacial climate variability in the Arabian Sea. Australian Organic Geochemistry Conference, Fremantle, accepted in September, 2016, oral presentation.

More K.D., Orsi W.D., Galy V., Giosan L., He L., Grice K. and Coolen M.J.L.(2018) A 43 kyr record of protist communities and their response to oxygen minimum zone variability in the Northeastern Arabian Sea. Goldschmidt International Conference, Paris, accepted in May 2017, Poster presentation.

More K.D., Orsi W.D., Galy V., Giosan L., He L., Grice K. and Coolen M.J.L.(2018) A 43 kyr record of protist communities and their response to oxygen minimum zone variability in the Northeastern Arabian Sea. International Meeting on Organic Geochemistry (IMOG), accepted in June 2017, Poster presentation.

Science magazine articles

Kuldeep More and Marco Coolen (2018) Ghosts of the climate past and of climate future. Australasian Science 39 (6), Nov/Dec 2018, 34-35.

Table of Contents

List of figures

List of tables

Abbreviations

AAnP	Aerobic anoxygenic phototrophs
aDNA	Ancient DNA
AGRF	Australian Genomic Research Facility
ANOSIM	Analysis of similarity
ATP	Adenosine tri-phosphate
B/A	Bølling-Allerød interstadial
BLAST	Basic local alignment search tool
BP	Before present
bp	Basepairs
CoA	Coenzyme A
DCM	Dichloromethane
DHVEG1	Deep Hydrothermal Vent Euryarchaeota Group 1
Dia/Dino index	Diatom/Dinoflagellate ratio
DNA	Deoxyribonucleic acid
DO	Dansgaard-Oeschger event
DSEG	Deep Sea Euryarchaeotal Group
GDGT	Glycerol dialkyl glycerol tetraether
GGC	Giant gravity core
GSB	Green sulfur bacteria
H event	Heinrich event
HCO	Holocene climate optimum
HPLC-MS	High performance liquid chromatography-Mass spectroscopy
IS	Interstadial
ISA	Indicator species analysis
ka	Kiloannum
kyrs	Kiloyears
LGM	Last glacial maximum
MBGA	Marine Benthic Group A
MBGB	Marine Benthic Group B
MC	Multicore
MCG	Miscellaneous Crenarchaeota group
MeOH	Methanol

MHVG	Marine Hydrothermal Vent Group
MIS	Marine isotope stage
NE	North-eastern
NGS	Next generation sequencing
NMDS	Nonmetric multidimensional scaling
OIS	Oxygen isotope stage
OM	Organic matter
OMZ	Oxygen minimum zone
ORF	Open reading frames
OTUs	Operational taxonomic units
PCR	Polymerase chain reaction
PFOR	Pyruvate ferredoxin oxidoreductase
ppt	Parts per thousand
qPCR	Quantitative PCR
rDNA	Ribosomal DNA
RNA	Ribonucleic acid
rRNA	Ribosomal RNA
S	Stadial
SMTZ	Sulfate-methane transition zone
SRB	Sulfate reducing bacteria
SSS	Sea surface salinity
SW	South-western
THSCG	Terrestrial Hot Spring Crenarchaeota Group
TMEG	Terrestrial Miscellaneous Euryrchaeota Group
TOC	Total organic carbon
WHOI	Woods Hole Oceanographic Institution
XRF	X-ray fluorescence
YD	Younger dryas

CHAPTER 1

INTRODUCTION

1.1 PALEOCLIMATE AND PALEOECOLOGY

A great majority of studies have concentrated on investigating the effects of climate change on the distribution, diversity, and abundance of different species. Due to spatial as well temporal overlap between species, such perturbations are spread and augmented throughout the food web (Walther, Post et al. 2002, Parmesan 2006, Walther 2010, Rammig and Mahecha 2015). Yet, long term effects of climate change on current ecosystem are not known. Understanding how past ecosystem responded to long-term paleoclimate variability will help to predict these effects in the near future in the context of ongoing climate change. Paleoecology applies geological and biological data to investigate the past occurrence, distribution, and abundance of different ecological units (species, populations, and communities) on a variety of timescales. Precisely dated marine settings provide ideal platform for palaeoecological studies since, upon death a fraction of pelagic as well as benthic biomass is buried in the underlying sediments. Therefore, marine sediments provide an archive of the relics from the past ecosystem as well as climatic or environmental conditions that prevailed at the time of deposition. Traditionally, fossil records of marine planktonic ecosystems have mainly been reconstructed through the microsocopic analysis of microfossils (micropalaeontology) or through lipid biomarkers and their isotopic signatures (organic and isotope geochemistry).

1.1.1 Micropaleontology

Analysis of microfossils of pelagic and benthic taxa is the traditional approach employed to reconstruct the response of past aquatic ecosystems to paleoenvironmental conditions. For example, foraminiferal microfossils are being widely used as a proxy for variations in paleo-oceanographic conditions. Past sea surface temperatures can be inferred from the oxygen isotopic composition of the planktonic foraminifera *Orbulina universa* and *Globigerina bulloides* (Bemis, Spero et al. 1998). Sea surface paleotemperatures throughout the Pleistocene (27–0 Ma) have been reconstructed using the the combined analysis of the oxygen isotopic composition and the Mg/Ca ratio of foraminiferal fossils of Cibicidoides (Billups and Schrag 2002). Mg/Ca paleothermometry on multiple foraminiferal species was used to reconstruct deep-sea temperatures and global ice volumes during the Cenozoic (50 ma) (Lear, Elderfield et al. 2000). A similar multispecies approach was also applied to reconstruct the sea surface temperatures during Last Glacial Maximum (LGM) in the North Atlantic Ocean (Elderfield and Ganssen 2000) and during late Oligocene warming event in the southern North Sea (De Man and Van Simaeys 2004). In addition, roughly 20% of known dinoflagellates also produce preservable calcareous or organic-walled hypnozygotic resting cysts (dinocysts) (William 1986). These cysts are usually associated with sexual reproduction of dinoflagellates and their formation is influenced by key surface water parameters such as seasonal pelagic nutrient depletion (Taylor 1987). Therefore, dinocycst fossils have been used to reconstruct Sea-surface productivity, temperature, salinity, stratification and paleo-oxygenation in global oceans during the Paleogene have been reconstructed using dinocyst fossils (Sluijs, Pross et al. 2005). Furthermore, dinocyst assemblages of *Thalassiphora pelagica* have been employed as oxygenation proxy to reconstruct paleo-oxygenation status of the Mainz Embayment during Tertiary period (Pross 2001). In addition, a complex fossil dinocyst assemblage was used to reconstruct Holocene oxygenation conditions in the Madeira Abyssal Plain (Zonneveld, Versteegh et al. 1997). Furthermore, sedimentary siliceous diatom frustules are frequently being used to infer past sea surface salinities (Sancetta and Silvestri 1986, Bond, Heinrich et al. 1992, Jiang, Seidenkrantz et al. 2002, Yun, Lee et al. 2017). However, the paleontological approach is biased towards the identification and quantification of only fossilizing species whereas the majority of the marine plankton are soft bodied and hence don't preserve microscopic diagnostic features upon burial. Furthermore, a variety of factors alter the chemical composition of fossils after deposition such as calcite dissolution, which affects the Mg/Ca ratios. The Mg-rich carbonate phase is more soluble than pure calcite and thus foraminiferal shells that are subject to dissolution

will appear to be depleted in Mg content (Brown and Elderfield 1996). Two or more different species can produce almost identical fossils and can be indistinguishable from one another. For example, fossilized marine resting eggs have been used for paleontological analysis, but many species produce similar looking resting stages (Marcus 1996). Hence even though elemental compositions in fossils can be studied to investigate the paleo-environmental conditions, they fail to help in paleoecological reconstruction.

1.1.2 Organic and isotopic geochemistry

Biomarkers are "molecular fossils" preserved in sediments or petroleum which originate from biolipids and pigments of once living organisms (Johns 1986, Simoneit 2004). The vast majority of biomass is generated by algae, cyanobacteria and terrestrial and aquatic plants *via* oxygenic photosynthesis. This biomass is deposited under various environments yielding different sedimentary rock types. After deposition biomass undergoes variety of different degradation and transformation processes such as eogenesis, diagenesis, catagenesis, and metagenesis, depending upon the paleodepositional conditions and type of organic matter. Different biolipids and pigments originating from variety of organisms, lose their functional groups and can become saturated during such processes, but still preserve the basic carbon skeleton and hence can be identified using traditional organic geochemical techniques like gas chromatography-mass spectrometry (GC-MS). These biomarkers can encode information about ancient biodiversity, food chain associations and environmental conditions. Biomarkers can either be species specific (e.g. botrycoccane is biomarker for freshwater alga *Botryococcus braunii*), group specific (e.g. isorenieratane as biomarkers green sulfur bacteria) (Summons and Powell 1986; Grice et al. 1996) or can be shared amongst a variety of different organisms (e.g. cholestane is a biomarker found in a wide range of animals and is derived from the diagenesis of cholesterol) (Volkman 1986). The identification and quantification of biomarkers in geological samples is of great significance for the reconstruction of recent and ancient environments since the biomarker composition may reflect the ecological communities and organic matter sources in the depositional environment *e.g.* specific maleimides (methyl iso-butyl maleimide) as molecular indicators of anoxygenic photosynthesis in the ancient water column (Grice et al. 1996; Grice et al. 2005; gammacerane as an indicator of water column stratification (Damsté, Kenig et al. 1995); diagenetic products of aromatic carotenoids of purple and/or green sulfur bacteria as an indicator of permanently stratified waters and the development of photic zone euxinia (Summons and Powell 1986, Brocks, Love et al. 2005, Grice, Cao et al. 2005). Furthermore, isotopic composition of certain biomarkers if analysed can be used as paleo-environmental

proxy (Hayes, Freeman and Popp 1990). For example, Long-chain (C_{37}-C_{39}) unsaturated methyl and ethyl ketones (alkenones) are produced by Prymnesiophytic algae (Marlowe, Green et al. 1984). Variations in Deuterium to Hydrogen (D/H) ratio of these alkenones, known as δD index, reflect the changes in the paleohydrological conditions of the source water where these alkenones were biosynthesized (Van der Meer et al., 2008). In addition, the relative proportion of di-, tri-, and tetra- unsaturated C_{37} alkenones (U^{K}_{37} index) produced by these algae depends on the growth temperature and this relationship can be employed in reconstructing past sea surface temperatures from alkenones preserved in marine sediment cores (Brassell 1993).

A detailed assessment of biomarkers and their elemental compositions assists in paleoecological as well as paleoclimate reconstructions especially in the absence of microfossils. However, the majority of plankton don't produce species specific biolipids and hence escape paleo-ecological analysis. Furthermore, the same biomarker can be produced by a variety of unrelated groups. For example, dinosterane (the diagenic product of dinosterol) is generally used as an indicator for the presence of dinoflagellates, but some diatoms can also produce this biomarker, which adds to the ambiguity of its source (Volkman et.al. 1993).

1.2 NEW APPROACH: ANCIENT DNA STRATIGRAPHY

Since most species lack the capacity to fossilize or to produce specific biomarkers, neither approaches can provide a holistic overview of past ecosystems. Therefore, paleontological and biomarker-independent methods are required to include the majority of planktonic and benthic taxa in paleoecological studies to refine climate-driven paleoenvironmental reconstructions. Fortunately, the analysis of genetic signatures preserved in geological samples, defined as the paleome (Inagaki, Okada et al. 2005), are since recently increasingly being included in paleoenvironmental studies. Fully hydrated DNA spontaneously decays over hundreds of years, mainly through hydrolysis and oxidation (Lindahl 1993, Hofreiter, Serre et al. 2001). However, low temperatures, high ionic strength, and anoxic conditions in sediments can increase the half-life of intact DNA by orders of magnitude (Poinar, Hoss et al. 1996, Willerslev, Hansen et al. 2004). In addition, adsorption of DNA to minerals and organic particles in the sediments increases the preservation potential of the extracellular DNA pool (Coolen and Overmann 2007). Increased longevity of DNA is exemplified by studies which involved analysis of ancient DNA from 560-780 kyrs old horse bone preserved in permafrost (Orlando, Ginolhac et al. 2013), mitochondrial DNA from 300 kyr old fossils of now extinct

mammal *Ursus deningeri* (Dabney, Knapp et al. 2013), and up to 1.4 Ma-old chloroplast and diatom DNA from anoxic marine sediments (Kirkpatrick, Walsh et al. 2016).

Analysis of ancient DNA can reveal genus specific information on the diversity and relative abundance of past biota. For example, the analysis of ancient copepod DNA from Antarctic lake sediments revealed the presence of a different species during early-mid Holocene that is no longer present in the isolated lakes today (Bissett, Gibson et al. 2005). Moreover, ancient DNA revealed a shift towards an increase in sea ice dinoflagellates (*Polarella glacialis*) during the late Holocene In Antarctic Ellis Fjord (Vestfold Hills), which could not be identified through traditional methods since their small cysts were not preserved and *Polarella* is not a source of the traditional lipid biomarker dinosterol (Boere, Abbas et al. 2009). Another example includes the analysis of sedimentary planktonic DNA that revealed shifts in planktonic community in response to paleoclimate variations that occurred during the Holocene in the Black Sea including the marine reconnection and establishment of the modern day salinity (Coolen, Orsi et al. 2013).

This approach is known as sedimentary paleogenomics and involves extraction and purification of ancient DNA inside a clean lab facility, followed by library preparations for subsequent Next Generation Sequencing (NGS). NGS allows sequencing of up to 1 billion of small fragments of DNA in parallel. Bioinformatics analyses are used to piece together these fragments by mapping the individual reads to short sequences or full genomes in reference databases and hence to reveal the species-specific abundance. Two different types of library preparations are generally used for paleogenomic surveys:

1. Target Amplicon sequencing
2. Shotgun Metagenomics

1.2.1 Target amplicon sequencing

Amplicon sequencing refers to ultra-deep sequencing of PCR amplified barcoding genes for analysing taxonomic diversity. In this approach, the targeted gene is first amplified using selective primers through real time-polymerase chain reaction (RT-PCR), which is followed by attaching multiplexing identifiers (MIDs) or barcodes to the amplified gene (amplicon) via another round of PCR. These barcoded amplicons are then sequenced via next generation sequencing and thus obtained sequences are aligned with known reference sequence via alignment tools such as Basic Local Alignment Search Tool (BLAST). This approach can be used to analyse taxonomic variation at each level of hierarchy- from strain to phyla. For example, Cytochrome Oxidase subunit I (COI) gene of host *Emiliania huxleyi* and Major Capsid Protein

(MCP) gene of *Coccolithovirus* were used to track the strain level variations of this host-virus system in the Black Sea during last 7000 years (Coolen 2011). In contrast, 18S rDNA and 16S rDNA sequencing are used to analyse the taxonomic variation in entire eukaryotic vs prokaryotic communitues (Coolen, Orsi et al. 2013, Orsi, Coolen et al. 2017). 18S rRNA is the structural component of the small eukaryotic ribosomal subunit found in all eukaryotes and is transcribed from genomic 18S rDNA. Evolutionarily 18S rDNA gene is highly conserved compared to other genes in eukaryotes and hypervariable regions V1-V3 and the short 130 base pair long V9 are generally used for eukaryotic taxonomic surveys (Fig 1.1). Most recently, sedimentary 18S-V9profiling was used to reconstruct multidecadal scale changes in the diversity and relative abundance of past planktonic communities in the Black Sea as a result of paleoenvironmental changes since the deglacial (Coolen et al. 2013).

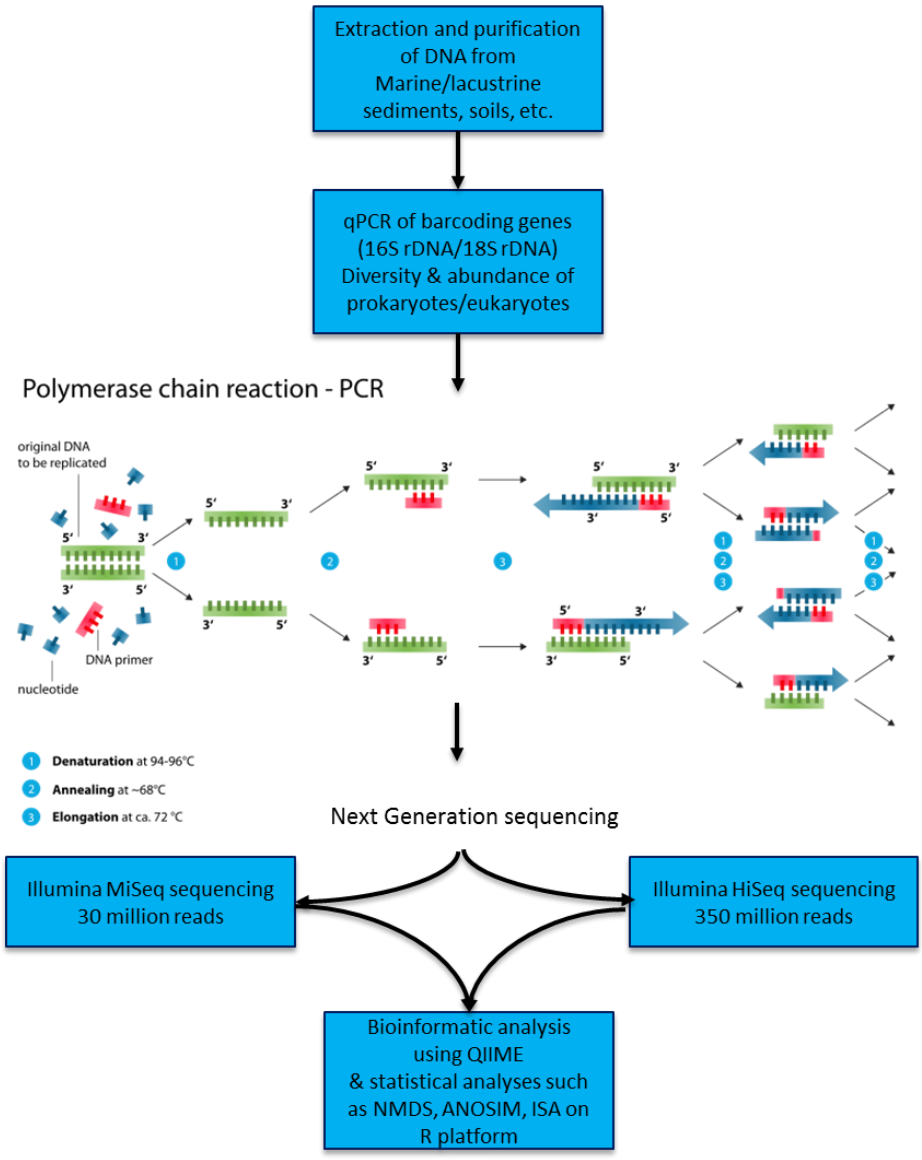

Figure 1.1 16S and 18S rDNA survey

Bacteria and archaea contain ribosomes with 16S rRNA and genomic 16S rDNA profiling yields prokaryotic taxonomic distribution and abundance in environmental samples. Hypervariable regions V6 or V4 of the 16S rDNA are most frequently being used for bacterial and archaeal species level taxonomic diversity (Fig 1.1). For example, combined lipid and 16S rDNA stratigraphy of up to 10,400-yr-old sediments from Ace lake, Antarctica revealed a clear shift in the species composition of archaea and aerobic methanotrophic bacteria after freshwater lake's transformation to open marine system at 9.4 ka BP (Coolen, Hopmans et al. 2004). Recent paired analyses of 16S rDNA surveys with paleoceanographic proxies revealed that paleodepositional selection plays a role in shaping the distribution and taxonomic composition of subsurface microbial communities. For example, it was observed that sub-seafloor bacterial community compositions reflect the alternating strong and weak Oxygen Minimum Zones (OMZ) that occurred in the last glacial-interglacial cycle in the NE Arabian Sea sediments (Orsi et al., 2017).

1.2.2 Shotgun metagenomics

The taxonomic relationship with cultivated closest relatives based on amplicon sequencing of structural genes only provides indirect information about the potential functioning of the source organisms. This problem can be overcome by sequencing of functional metagenomes from complex communities in environmental samples, which is also referred to as environmental genomics or community genomics (Song, Jarvie et al. 2013).

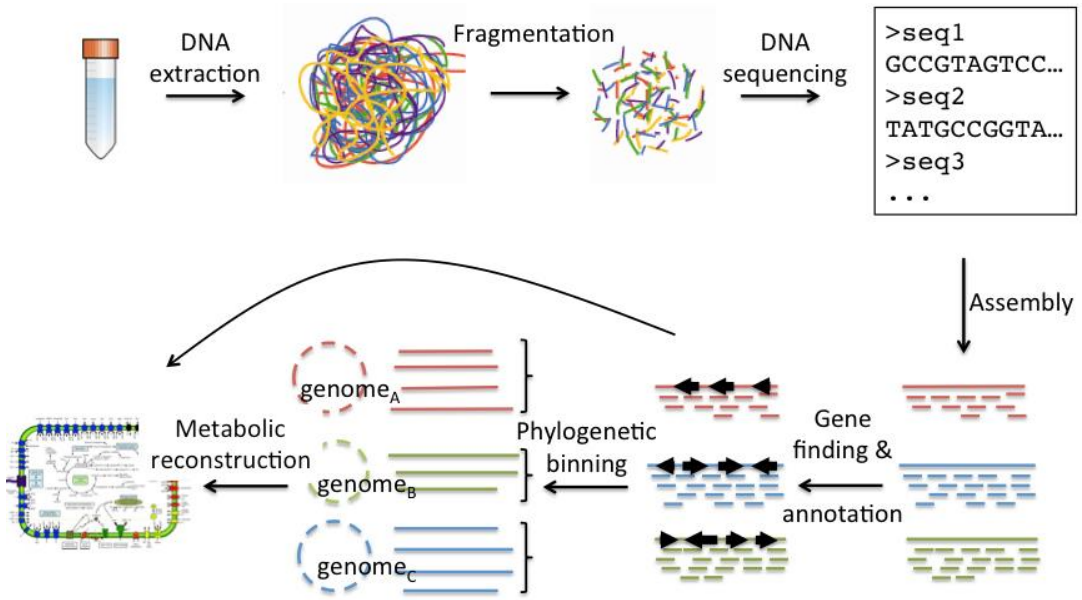

Figure 1.2 Metagenomics (modified from environmental genomics, ENVGEN at KTH. Source: https://envgen.github.io/metagenomics.html)

The sequencing analysis of functional genes provides information on metabolic pathways as well as taxonomic information of the source organisms. The experimental approach for shotgun metagenomics involves the extraction of total genomic DNA from environment samples followed by fragmentation, library preparation, and subsequent NGS (Fig. 1.2). Sequences are then processed using bioinformatic pipelines such as MGRAST to subsequently produce taxonomy x samples and function x samples abundance matrices. These matrices form the basis for subsequent biostatistical and ordination analyses in, for example, the R environment (https://www.r-project.org/). A highly resolved metagenomics survey recently revealed that in paleodepositionally selected subseafloor microbial communities, genomic potential for denitrification correlated with palaeo-OMZ proxies, irrespective of sediment depth and availability of nitrate and nitrite (Orsi, Coolen et al. 2017). Furthermore, metagenomes suggested the fermentation pathway as major subsistence mechanism for these communities (Orsi, Coolen et al. 2017)

1.3 GEOLOGICAL SETTINGS

Sediment samples analysed in this study came from three different marine settings.

1. The north-eastern (NE) Arabian Sea
2. The Black Sea
3. The Red Sea

1.3.1 The north-eastern (NE) Arabian Sea

The Arabian Sea is the northernmost portion of the Indian Ocean bound on the north by Pakistan and Iran, on the west by the Gulf of Aden, Guardafui Channel and the Arabian Peninsula, and on the east by India. The northeast part of the Arabian Sea lies between south Pakistan and north-west India and harbors the Indus river delta. The physical effects of these adjacent land masses are expressed by the prevailing monsoon winds which reverse their directions seasonally, thereby causing drastic changes in the surface currents. The northeast monsoonal winds associated with NE monsoon develop during late October and continue through early March, gradually becoming more intermittent. Later in the year, typically in April, intermittent southwest monsoonal winds start to develop associated with the SW Monsoon and are at their maximum intensity from mid/late May through early October. Coastal and open ocean upwelling cells off Oman during SW monsoon increases the nutrient concentration in surface waters, which increases the surface water productivity, while sea-surface cooling leads to convection processes and injection of nutrients into the subsurface waters, and promotes high biological productivity during NE monsoon (Madhupratap, Kumar

et al. 1996). High eolian and fluvial input from the surrounding continents further enrich the subsurface waters of NE Arabian Sea and make it one of the most productive oceanic areas in the world characterized by phytoplankton blooms (Banse 1987). Oxygen is consumed in the process of biodegradation of this sinking biomass, which leads to the rise of oxygen starved regions at mid-water depth, known as Oxygen Minimum Zones (OMZ) (Helm, Bindoff and Church 2011; Keeling, Kortzinger and Gruber 2010; Wright, Konwar and Hallam 2012). Thermal stratification of the water column further intensifies OMZ. NE Arabian Sea harbours one of the most pronounced and intense OMZs (Naqvi 1987).

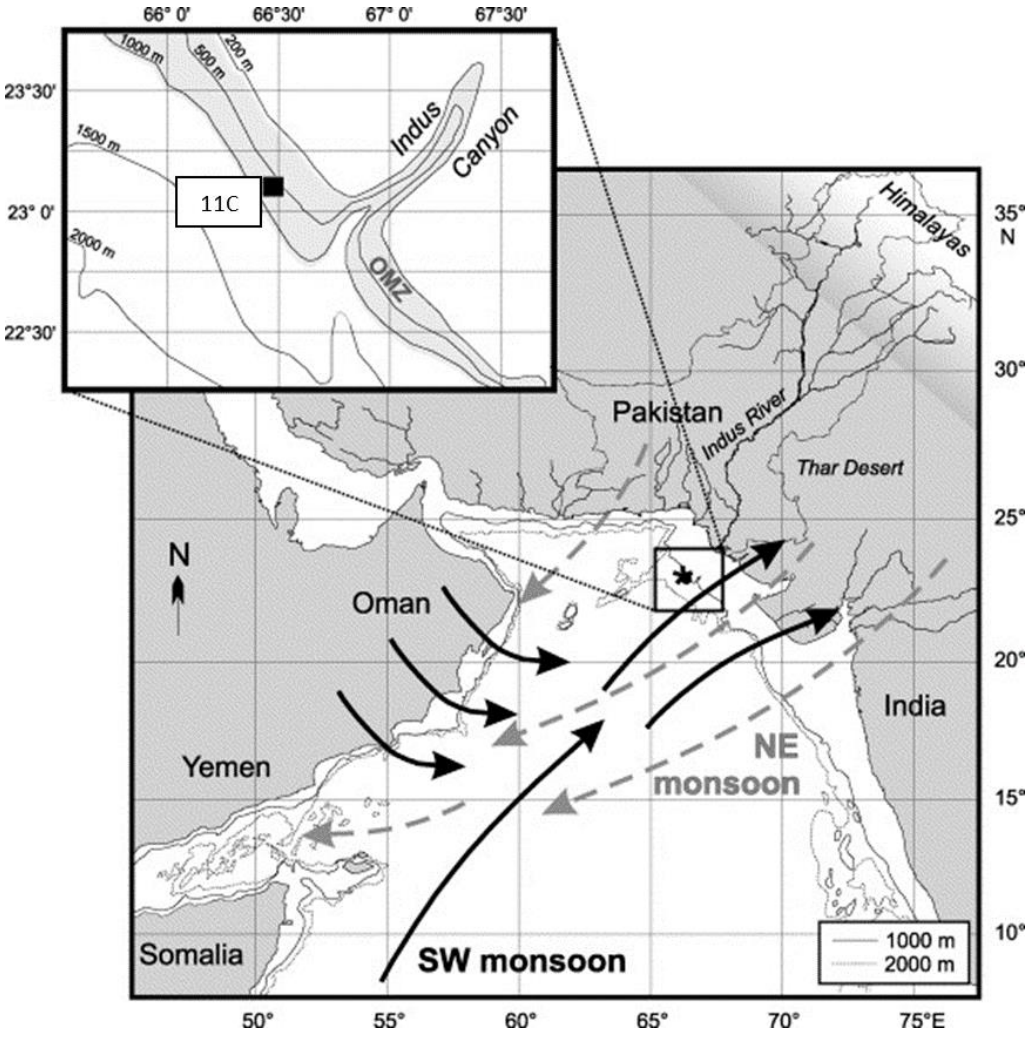

Figure 1.3 Sketch of the bathymetry and monsoonal wind patterns of the Arabian Sea modified after (Ansari and Vink, 2007). Inset shows the position of core 11C off the Indus Delta and in relation to the Indus Canyon and OMZ marked in light grey.

Today, an expanded, persistent OMZ can be observed in the entire northern Arabian Sea at intermediate water depths. In the NE Arabian Sea, a marked OMZ impinges the continental slope near the Indus canyon between 250 and 1000 m water depth. The intensity of the OMZ

conditions in the Arabian Sea is mainly controlled by surface-water productivity, which in turn, is influenced by monsoonal climate variations and respond to the intensity of Northern Hemisphere summer insolation (Altabet, Francois et al. 1995, Reichart, Lourens et al. 1998). The sediment record of the Arabian Sea provides a long-term time-series of past changes in OMZ expansion as a result of natural climate variability (Vonrad, Schulz et al. 1995, Schulz, Von Rad et al. 1996, Schulz, von Rad et al. 1998, von Rad, Schulz et al. 1999, Schulte and Muller 2001, Altabet, Higginson et al. 2002, Schulz, von Rad et al. 2002). For example, geochemical, sedimentological, and (micro)paleontological analyses using sediment cores from the classical continental slope coring location NW of the Indus Canyon, have implied strong SW-monsoon-controlled biological productivity, enhanced organic matter preservation, and upwelling conditions during the last 7,000 years. Stable OMZ conditions, reflected by laminated sediments also prevailed during warm interstadial Preboreal (9-10.3 ka BP) and Bølling/Allerød (B/A - ~13-14.5 ka BP) events, as well as during peak glacial times (17-22.5 ka cal BP) (von Rad et al, 1999). In contrast, the occurrence of bioturbated organic matter poor and carbonate-rich intervals representing the early Holocene (~7 to 10.5 ka), the cold Younger Dryas (YD) stadial (~11.7–13 ka), Heinrich events 1 (H1; 15-17 ka), and H2 (22.5-25 ka) suggests oxygen-rich bottom waters, extremely low organic matter (OM) accumulation rates, a high-diversity benthic fauna, and therefore lowered surface-water productivity. *Effects of the variable intensity of OMZ on the pelagic and benthic ecosystem is mostly available through recent modelling experiments (Blackford and Burkill 2002) and long-term effects of OMZ variability on the past marine ecosystems are largely unknown*.

1.3.2 The Black Sea

The Black Sea is an inland marine basin located north of Turkey. It is connected with the Mediterranean Sea by the Bosporus strait, the Sea of Marmara, and the Dardanelles. It is about 900 km long and 300 km wide with a 460 000 km^2 surface area and 534000 km^3 volume (Gross 1974). Tributary rivers such as Danube, Dnieper, Southern Bug, Dniester, Don, and the Rioni dilute salinity of surface waters of Black Sea to 17 ‰ which leads to low-salinity surface water export toward the Mediterranean (Aegean) through the narrow and shallow Straits of Bosporus, while denser water with salinity 38 ‰ from the Sea of Marmara flow as an undercurrent into the Black Sea. This process leads to the development of a halocline (Pross 2001). Furthermore, the deep waters do not mix with the upper oxic layers, which makes the permanently stratified Black Sea the largest anoxic basin in the world where a ~30-m-thick suboxic zone separates the sulfidic anoxic bottom waters from the upper ~100 m of oxygenated surface waters (Murray and Yakushev 2006). The Black Sea has experienced at

least eight marine flooding events in its history of 3 million years. The last marine flooding event was of the highest magnitude and occurred during the Pleistocene/Holocene transition (Ryan, Major et al. 2003). During the Last Glacial Maximum (LGM/Neoeuxinian epoch) minimum water levels were between 20 and 110 m below the present sea level (Kaplin and Selivanov 2004) and the Black Sea functioned as a giant lake with air temperatures and sea surface salinity (SSS) lower than today (Degens and Ross 1972).

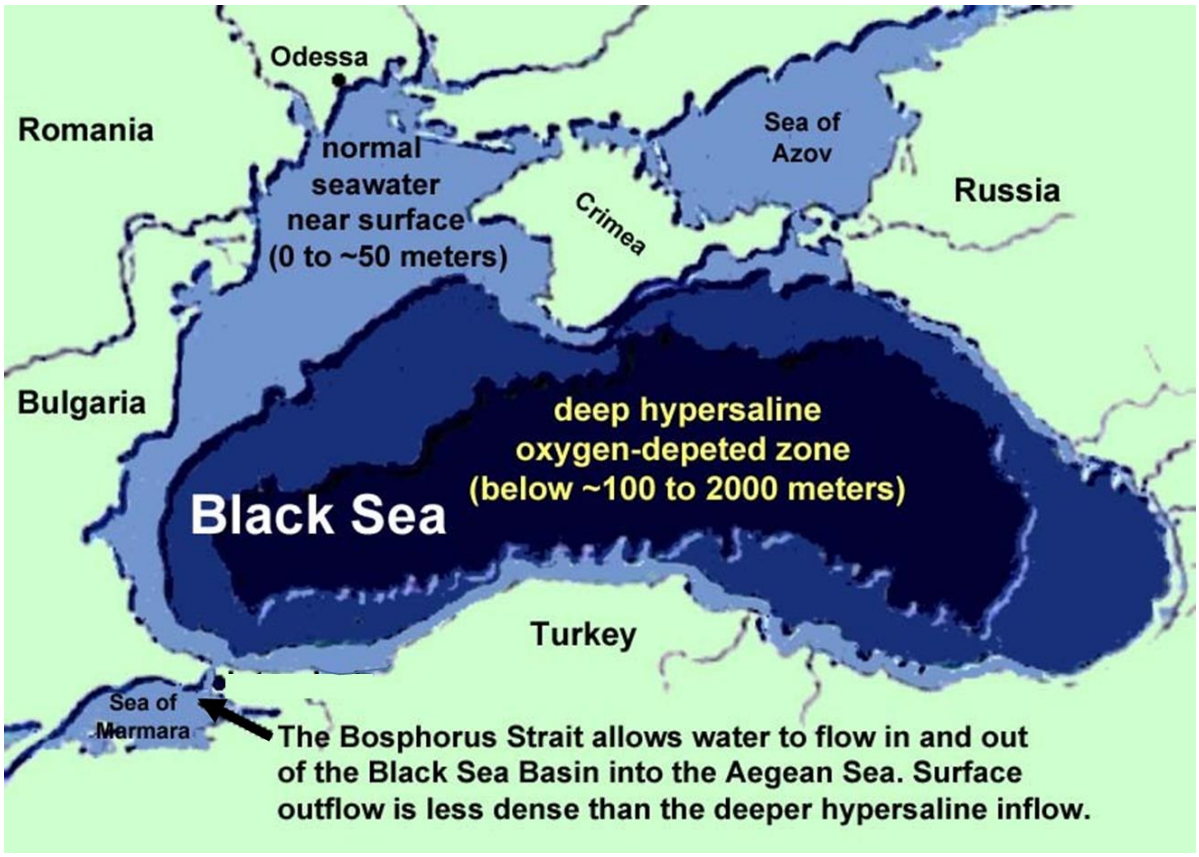

Figure 1.4 Bathymetry of Black Sea (Source: http://gotbooks.miracosta.edu/oceans/chapter9.html)

The debate exists over the recent marine reconnection of the Black Sea and two contrasting scenarios have been put forth to explain that transition from lacustrine to marine environment: a "catastrophic" postglacial flooding with Mediterranean waters (Ryan, Major et al. 2003, Giosan, Filip et al. 2009) and "progressive" marine reconnection (Ross, Degens et al. 1970, Hiscott, Aksu et al. 2007). Another debate exists over the salinity of the lacustrine Black Sea. The stable oxygen isotope ($\delta^{18}O$) composition and chloride content of sediment interstitial water indicate that the Late Glacial Black Sea was a freshwater lake (Soulet, Delaygue et al. 2010), while presence of the fossil dinocyst assemblage suggest brackish conditions [i.e., a salinity of ~7–12 parts per thousand (ppt)] (Marret, Mudie et al. 2009).

Furthermore, an increase in sea surface salinity during the Bølling-Allerød and Preboreal warm oscillations is implied by the oxygen isotopic composition of fossil *Dreissena* shells (Major, Ryan et al. 2002). During Holocene the Black Sea experienced four distinct climate stages: Preboreal (9 -11.5 ka BP), Holocene climate optimum (HCO, 5.4 to 9 ka BP), subboreal (2.5 to 5.2 ka BP) and subatlantic (2.5 ka BP onwards). The Preboreal was characterised by dry climate with sea level lowstands and the deposition of lacustrine sediments. The marine reconnection has been previously suggested to have occurred at the end of the Preboreal (~9 ka BP) (Soulet, Menot et al. 2011), but a recent ancient DNA study of the Black Sea sediments showed the arrival of marine fungi and the coccolithophorid haptophyte alga *Emiliania huxleyi* at 9.6 ka BP (Coolen et al. 2013), which is 600 years earlier. Sea surface salinity (SSS) continued to increase during the warm mid Holocene climate optimum and stratified and anoxic conditions prevailed since the onset of the deposition of the organic-rich laminated sapropel 7.2 ka BP. The establishment of modern-day salinity and environmental conditions at the start of dry and cooler subboreal (∼5.2 ka BP) is indicated by the arrival of marine copepod. Most notably *Calanus euxinus* (Coolen, Orsi et al. 2013) with a known minimum salinity tolerance of ∼17 ppt (Svetlichny, Hubareva et al. 2010). The Black Sea experienced a steep increase in the SSS from ∼17 ppt to a maximum of ∼32 ppt during this interval (Coolen, Orsi et al. 2013). With the onset of the Subatlantic climate, the Black Sea experienced a dramatic freshening throughout the entire basin (van der Meer, Sangiorgi et al. 2008, Giosan, Coolen et al. 2012) during which coccolith marls were deposited (Coolen, Orsi et al. 2013). *Since phytoplankton and zooplankton DNA was preserved in these sediments and microbial growth was stalled because the sediments were stored deeply frozen immediately after recovery, this Black Sea core was highly suitable to study to what extent the subseafloor microbiome also responded to above mentioned well-defined climate stages and their transitions.*

1.3.3 The Red Sea

The Red Sea's main water body (2000 x 335 km^2) (Rasul, Stewart et al. 2015) is bordered by six countries – Saudi Arabia and Yemen on the east and Egypt, Sudan, Eritrea and Djibouti on the west. In the north, the Sinai Peninsula divides the Red Sea into the Gulf of Aqaba and the Gulf of Suez. The part of the Red Sea that forms the central narrow axial trough is over 1,000 m deep and forms 15% of the total Red Sea, whereas 65 % of the Red Sea is shallow with depths less than 100 m. The Red Sea thanks its name to the release of the reddish brown pigment phycoerythrin during seasonal crashing of *Trichodesmium erythraeum* blooms. The Red Sea's salinity is highest 41 ‰ in the northern part and surface water mixing with the Gulf

of Aden water reduces the salinity to ~36 ‰ at the southern end. The entire Red Sea basin is influenced by an arid climate with annual rainfall of less than 20 mm in the north and 50–100 mm in the south (Pedgley 1974). Riverine input into the basin is negligible (Morcos 1970) with Baraka wadi in Sudan being the only major river delta, which is active only in autumn for a few months. Evaporation exceeds precipitation which results in a net annual water deficit of about 2m (Morcos 1970). Owing to its shallower depth profiles the Red Sea experienced dramatic changes in sea level throughout the global glacial-interglacial cycles and particularly in the last 500,000 yrs (Grant, Rohling et al. 2014). The Red Sea level was 80 to 120 m lower than today during peak glacials and 10 m higher than today interglacials (Grant, Rohling et al. 2014). A reduction in exchange flow of the Red Sea through Bab-el-Mandab led to extremely saline conditions (55‰) (Hemleben, Meischner et al. 1996) during times of sea level lowstands in the last and penultimate glacials (Rohling 1994, Fenton, Geiselhart et al. 2000). High salinity prevented benthic foraminifera from developing as evident from the absence of their microfossils which led to formation of a-planktonic intervals observed in the Red Sea sediments (Fenton, Geiselhart et al. 2000). One of the questions to be resolved is whether ancient DNA profiling could reveal past planktonic communities in this co-called a-planktonic interval.

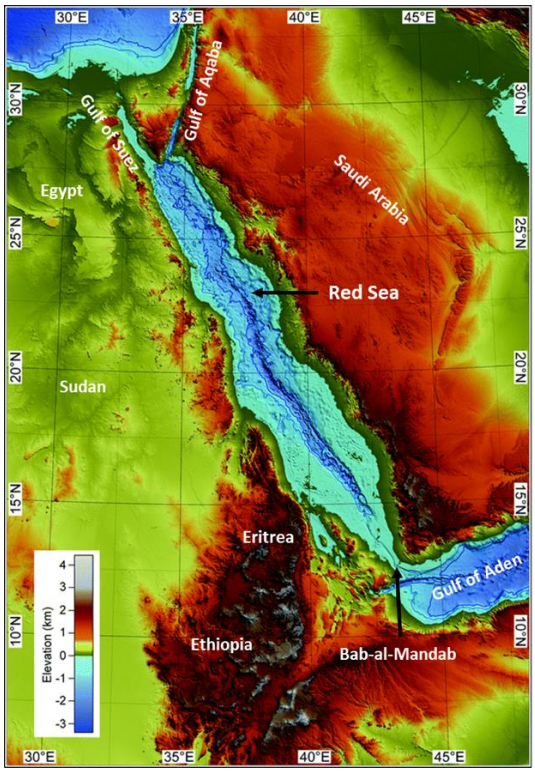

Figure 1.5 Topography and bathymetric map of the Red Sea. Bathymetric contours are at 500 m interval (modified after Rasul *et.al.* 2015).

Archaea contribute more than a quarter to the total subseafloor microbiome and yet, their diversity, abundance and role of paleodepositional environment in shaping sedimentary archaeal community composition is not well understood as compared to sedimentary bacteria. The Red Sea core provided an excellent opportunity to analyse if and how salinity and water level affected the sedimentary archaeal composition in the Red Sea during key climate stages of the last glacial-interglacial cycle (last 139,000 years).

1.4 AIMS

Despite significant ongoing research devoted to reconstructing paleoclimate-paleoecology dynamics using traditional approaches, the lack of species-specific approach impedes the efficacy of this process. The primary aim of this dissertation is to explore the potential of preserved sedimentary DNA as a novel proxy for paleoenvironmental change in combination with other paleo-oceanographic proxies. The thesis focusses on prokaryotic as well as eukaryotic ancient DNA in marine sediments and employs different paleogenomic techniques.

In Chapter 2, paired sedimentary 18S rDNA profiling and geochemical proxy analyses aimed to elucidate how long-term shifts in strong vs. weak OMZ conditions affected the distribution and relative abundance of protist communities and their survival strategies under low oxygen conditions in the Monsoon-impacted NE Arabian Sea during the last glacial-interglacial cycle.

In Chapter 3 the overarching aim was to study the response of subseafloor microbial communities in the Black Sea to Holocene hydrological changes inferred from shotgun metagenomics paired with the analysis of paleoceanographic proxies.

Chapter 4 uses 16S rDNA profiling paired with geochemical proxies to investigate how subseafloor archaeal communities were affected by dramatic changes in sea level and salinity during glacial lowstands vs. interglacial highstands in the Red Sea spanning the last 139,000 years.

1.5 REFERENCES

Altabet, M. A., R. Francois, D. W. Murray, and W. L. Prell. 1995. "Climate-Related Variations in Denitrification in the Arabian Sea from Sediment N-15/N-14 Ratios." *Nature* 373 (6514): 506-509.

Altabet, M. A., M. J. Higginson, and D. W. Murray. 2002. "The Effect of Millennial-Scale Changes in Arabian Sea Denitrification on Atmospheric CO_2." *Nature* 415 (6868): 159-162.

Banse, K. 1987. "Seasonality of Phytoplankton Chlorophyll in the Central and Northern Arabian Sea." *Deep-Sea Research Part a-Oceanographic Research Papers* 34 (5-6): 713-723.

Bemis, B. E., H. J. Spero, J. Bijma, and D. W. Lea. 1998. "Reevaluation of the Oxygen Isotopic Composition of Planktonic Foraminifera: Experimental Results and Revised Paleotemperature Equations." *Paleoceanography* 13 (2): 150-160.

Billups, K., and D. P. Schrag. 2002. "Paleotemperatures and Ice Volume of the Past 27 Myr Revisited with Paired Mg/Ca and O-18/O-16 Measurements on Benthic Foraminifera." *Paleoceanography* 17 (1).

Bissett, A., J. A. E. Gibson, S. N. Jarman, K. M. Swadling, and L. Cromer. 2005. "Isolation, Amplification, and Identification of Ancient Copepod DNA from Lake Sediments." *Limnology and Oceanography-Methods* 3: 533-542.

Blackford, J. C., and P. H. Burkill. 2002. "Planktonic Community Structure and Carbon Cycling in the Arabian Sea as a Result of Monsoonal Forcing: The Application of a Generic Model." *Journal of Marine Systems* 36 (3-4): 239-267.

Boere, A. C., B. Abbas, W. I. C. Rijpstra, G. J. M. Versteegh, J. K. Volkman, J. S. S. Damste, and M. J. L. Coolen. 2009. "Late-Holocene Succession of Dinoflagellates in an Antarctic Fjord Using a Multi-Proxy Approach: Paleoenvironmental Genomics, Lipid Biomarkers and Palynomorphs." *Geobiology* 7 (3): 265-281.

Bond, G., H. Heinrich, W. Broecker, L. Labeyrie, J. Mcmanus, J. Andrews, S. Huon et al. 1992. "Evidence for Massive Discharges of Icebergs into the North-Atlantic Ocean During the Last Glacial Period." *Nature* 360 (6401): 245-249.

Brassell, Simon C. 1993. "Applications of Biomarkers for Delineating Marine Paleoclimatic Fluctuations During the Pleistocene." In *Organic Geochemistry: Principles and Applications*, eds Michael H. Engel and Stephen A. Macko, 699-738. Boston, MA: Springer US.

Brocks, J. J., G. D. Love, R. E. Summons, A. H. Knoll, G. A. Logan, and S. A. Bowden. 2005. "Biomarker Evidence for Green and Purple Sulphur Bacteria in a Stratified Palaeoproterozoic Sea." *Nature* 437 (7060): 866-870.

Coolen, M. J. L. 2011. "7000 Years of Emiliania Huxleyi Viruses in the Black Sea." *Science* 333 (6041): 451-452.

Coolen, M. J. L., E. C. Hopmans, W. I. C. Rijpstra, G. Muyzer, S. Schouten, J. K. Volkman, and J. S. S. Damste. 2004. "Evolution of the Methane Cycle in Ace Lake (Antarctica) During the Holocene: Response of Methanogens and Methanotrophs to Environmental Change." *Organic Geochemistry* 35 (10): 1151-1167.

Coolen, M. J. L., W. D. Orsi, C. Balkema, C. Quince, K. Harris, S. P. Sylva, M. Filipova-Marinova, and L. Giosan. 2013. "Evolution of the Plankton Paleome in the Black Sea from the Deglacial to Anthropocene." *Proceedings of the National Academy of Sciences of the United States of America* 110 (21): 8609-8614.

Coolen, M. J. L., and J. Overmann. 2007. "217 000-Year-Old DNA Sequences of Green Sulfur Bacteria in Mediterranean Sapropels and Their Implications for the Reconstruction of the Paleoenvironment (Vol 9, Pg 238, 2007)." *Environmental Microbiology* 9 (4): 1099-1099.

Dabney, J., M. Knapp, I. Glocke, M. T. Gansauge, A. Weihmann, B. Nickel, C. Valdiosera et al. 2013. "Complete Mitochondrial Genome Sequence of a Middle Pleistocene Cave Bear Reconstructed from Ultrashort DNA Fragments." *Proceedings of the National Academy of Sciences of the United States of America* 110 (39): 15758-15763.

Damste, J. S. S., F. Kenig, M. P. Koopmans, J. Koster, S. Schouten, J. M. Hayes, and J. W. Deleeuw. 1995. "Evidence for Gammacerane as an Indicator of Water Column Stratification." *Geochimica Et Cosmochimica Acta* 59 (9): 1895-1900.

De Man, E., and S. Van Simaeys. 2004. "Late Oligocene Warming Event in the Southern North Sea Basin: Benthic Foraminifera as Paleotemperature Proxies." *Netherlands Journal of Geosciences-Geologie En Mijnbouw* 83 (3): 227-239.

Degens, Egon T., and David A. Ross. 1972. "Chronology of the Black Sea over the Last 25,000 Years." *Chemical Geology* 10 (1): 1-16. doi: https://doi.org/10.1016/0009-2541(72)90073-3.

Elderfield, H., and G. Ganssen. 2000. "Past Temperature and Delta O-18 of Surface Ocean Waters Inferred from Foraminiferal Mg/Ca Ratios." *Nature* 405 (6785): 442-445.

Fenton, M., S. Geiselhart, E. J. Rohling, and C. Hemleben. 2000. "Aplanktonic Zones in the Red Sea." *Marine Micropaleontology* 40 (3): 277-294.

Hayes, J.M., Freeman, K.H., Popp, B.N., Hoham, C.H. 1990. Compound-specific isotopic analyses: A novel tool for reconstruction of ancient biogeochemical processes. Organic Geochemistry 16 (4-6): 1115-1128.

Giosan, L., M. J. L. Coolen, J. O. Kaplan, S. Constantinescu, F. Filip, M. Filipova-Marinova, A. J. Kettner, and N. Thom. 2012. "Early Anthropogenic Transformation of the Danube-Black Sea System." *Scientific Reports* 2.

Giosan, L., F. Filip, and S. Constatinescu. 2009. "Was the Black Sea Catastrophically Flooded in the Early Holocene?" *Quaternary Science Reviews* 28 (1-2): 1-6.

Grant, K. M., E. J. Rohling, C. B. Ramsey, H. Cheng, R. L. Edwards, F. Florindo, D. Heslop et al. 2014. "Sea-Level Variability over Five Glacial Cycles." *Nature Communications* 5.

Grice, K., C. Q. Cao, G. D. Love, M. E. Bottcher, R. J. Twitchett, E. Grosjean, R. E. Summons, S. C. Turgeon, W. Dunning, and Y. G. Jin. 2005. "Photic Zone Euxinia During the Permian-Triassic Superanoxic Event." *Science* 307 (5710): 706-709.

Gross, M. Grant. 1974. "Degens, E. T., and D. A. Ross [Eds.]. 1974. The Black Sea—Geology, Chemistry, and Biology. American Association of Petroleum Geologists, Tulsa, Oklahoma, Ix + 633 P. $33.00." *Limnology and Oceanography* 19 (6): 1016-1017. doi: 10.4319/lo.1974.19.6.1016.

Hemleben, C., D. Meischner, R. Zahn, A. AlmogiLabin, H. Erlenkeuser, and B. Hiller. 1996. "Three Hundred Eighty Thousand Year Long Stable Isotope and Faunal Records from the Red Sea: Influence of Global Sea Level Change on Hydrography." *Paleoceanography* 11 (2): 147-156.

Hiscott, R. N., A. E. Aksu, P. J. Mudie, F. Marret, T. Abrajano, M. A. Kaminski, J. Evans, A. I. Cakiroglu, and D. Yasar. 2007. "A Gradual Drowning of the Southwestern Black Sea Shelf: Evidence for a Progressive Rather Than Abrupt Holocene Reconnection with the Eastern Mediterranean Sea through the Marmara Sea Gateway." *Quaternary International* 167: 19-34.

Hofreiter, M., D. Serre, H. N. Poinar, M. Kuch, and S. Paabo. 2001. "Ancient DNA." *Nature Reviews Genetics* 2 (5): 353-359.

Inagaki, F., H. Okada, A. I. Tsapin, and K. H. Nealson. 2005. "Microbial Survival - the Paleome: A Sedimentary Genetic Record of Past Microbial Communities." *Astrobiology* 5 (2): 141-153.

Jiang, H., M. S. Seidenkrantz, K. L. Knudsen, and J. Eiriksson. 2002. "Late-Holocene Summer Sea-Surface Temperatures Based on a Diatom Record from the North Icelandic Shelf." *Holocene* 12 (2): 137-147.

Johns, R. B. 1986. *Biological Markers in the Sedimentary Record*, *Methods in Geochemistry and Geophysics ;24*. Amsterdam ; New York : New York, NY: Elsevier ; Distributors for the United States and Canada, Elsevier Science Pub. Co.

Kaplin, Pavel A., and Andrei O. Selivanov. 2004. "Lateglacial and Holocene Sea Level Changes in Semi-Enclosed Seas of North Eurasia: Examples from the Contrasting Black and White Seas." *Palaeogeography, Palaeoclimatology, Palaeoecology* 209 (1): 19-36. doi: https://doi.org/10.1016/j.palaeo.2004.02.016.

Kirkpatrick, J. B., E. A. Walsh, and S. D'Hondt. 2016. "Fossil DNA Persistence and Decay in Marine Sediment over Hundred-Thousand-Year to Million-Year Time Scales." *Geology* 44 (8): 615-618.

Lear, C. H., H. Elderfield, and P. A. Wilson. 2000. "Cenozoic Deep-Sea Temperatures and Global Ice Volumes from Mg/Ca in Benthic Foraminiferal Calcite." *Science* 287 (5451): 269-272.

Lindahl, T. 1993. "Instability and Decay of the Primary Structure of DNA." *Nature* 362 (6422): 709-715.

Madhupratap, M., S. P. Kumar, P. M. A. Bhattathiri, M. D. Kumar, S. Raghukumar, K. K. C. Nair, and N. Ramaiah. 1996. "Mechanism of the Biological Response to Winter Cooling in the Northeastern Arabian Sea." *Nature* 384 (6609): 549-552.

Major, C., W. Ryan, G. Lericolais, and I. Hajdas. 2002. "Constraints on Black Sea Outflow to the Sea of Marmara During the Last Glacial-Interglacial Transition." *Marine Geology* 190 (1-2): 19-34.

Marcus, N. H. 1996. "Ecological and Evolutionary Significance of Resting Eggs in Marine Copepods: Past, Present, and Future Studies." *Hydrobiologia* 320 (1-3): 141-152.

Marlowe, I. T., J. C. Green, A. C. Neal, S. C. Brassell, G. Eglinton, and P. A. Course. 1984. "Long Chain (N-C37–C39) Alkenones in the Prymnesiophyceae. Distribution of Alkenones and Other Lipids and Their Taxonomic Significance." *British Phycological Journal* 19 (3): 203-216. doi: 10.1080/00071618400650221.

Marret, F., P. Mudie, A. Aksu, and R. N. Hiscott. 2009. "A Holocene Dinocyst Record of a Two-Step Transformation of the Neoeuxinian Brackish Water Lake into the Black Sea." *Quaternary International* 197: 72-86.

Morcos, S. A. 1970. "Physical and Chemical Oceanography of the Red Sea." *Oceanography and Marine Biology* 8: 73-202.

Murray, James W., and Evgeniy Yakushev. 2006. "The Suboxic Transition Zone in the Black Sea" *Past and Present Water Column Anoxia*, *Dordrecht*: Springer Netherlands.

Orlando, L., A. Ginolhac, G. J. Zhang, D. Froese, A. Albrechtsen, M. Stiller, M. Schubert et al. 2013. "Recalibrating Equus Evolution Using the Genome Sequence of an Early Middle Pleistocene Horse." *Nature* 499 (7456): 74

Orsi, William D., Marco J. L. Coolen, Cornelia Wuchter, Lijun He, Kuldeep D. More, Xabier Irigoien, Guillem Chust et al. 2017. "Climate Oscillations Reflected within the Microbiome of Arabian Sea Sediments." *Scientific Reports* 7 (1): 6040. doi: 10.1038/s41598-017-05590-9.

Parmesan, C. 2006. "Ecological and Evolutionary Responses to Recent Climate Change." *Annual Review of Ecology Evolution and Systematics* 37: 637-669.

Pedgley, D. E. . 1974. "An Outline of the Weather and Climate of the Red Sea" *Actes du Colloques*: Publications Centre National pour l'Exploitation des Oceans.

Poinar, H. N., M. Hoss, J. L. Bada, and S. Paabo. 1996. "Amino Acid Racemization and the Preservation of Ancient DNA." *Science* 272 (5263): 864-866.

Pross, J. 2001. "Paleo-Oxygenation in Tertiary Epeiric Seas: Evidence from Dinoflagellate Cysts." *Palaeogeography Palaeoclimatology Palaeoecology* 166 (3-4): 369-381.

Rammig, A., and M. D. Mahecha. 2015. "Ecology Ecosystem Responses to Climate Extremes." *Nature* 527 (7578): 315.

Rasul, Najeeb M. A., Ian C. F. Stewart, and Zohair A. Nawab. 2015. "Introduction to the Red Sea: Its Origin, Structure, and Environment." In *The Red Sea: The Formation, Morphology, Oceanography and Environment of a Young Ocean Basin*, eds Najeeb M. A. Rasul and Ian C. F. Stewart, 1-28. Berlin, Heidelberg: Springer Berlin Heidelberg.

Reichart, G. J., L. J. Lourens, and W. J. Zachariasse. 1998. "Temporal Variability in the Northern Arabian Sea Oxygen Minimum Zone (Omz) During the Last 225,000 Years." *Paleoceanography* 13 (6): 607-621.

Rohling, E. J. 1994. "Glacial Conditions in the Red-Sea." *Paleoceanography* 9 (5): 653-660.

Ross, David A., Egon T. Degens, and Joseph MacIlvaine. 1970. "Black Sea: Recent Sedimentary History." *Science* 170 (3954): 163-165. doi: 10.1126/science.170.3954.163.

Ryan, W. B. F., C. O. Major, G. Lericolais, and S. L. Goldstein. 2003. "Catastrophic Flooding of the Black Sea." *Annual Review of Earth and Planetary Sciences* 31: 525-554.

Sancetta, C., and S. Silvestri. 1986. "Pliocene-Pleistocene Evolution of the North Pacific Ocean-Atmosphere System, Interpreted from Fossil Diatoms." *Paleoceanography* 1 (2): 163-180.

Schulte, S., and P. J. Muller. 2001. "Variations of Sea Surface Temperature and Primary Productivity During Heinrich and Dansgaard-Oeschger Events in the Northeastern Arabian Sea." *Geo-Marine Letters* 21 (3): 168-175.

Schulz, H., U. Von Rad, and U. Von Stackelberg. 1996. "Laminated Sediments from the Oxygen-Minimum Zone of the Northeastern Arabian Sea." *Geological Society, London, Special Publications* 116 (1): 185-207. doi: 10.1144/gsl.sp.1996.116.01.16.

Schulz, Hartmut, Ulrich von Rad, Helmut Erlenkeuser, and Ulrich von Rad. 1998. "Correlation between Arabian Sea and Greenland Climate Oscillations of the Past 110,000 Years." *Nature* 393 (6680): 54-57.

Schulz, Hartmut, Ulrich von Rad, and Venugopalan Ittekkot. 2002. "Planktic Foraminifera, Particle Flux and Oceanic Productivity Off Pakistan, Ne Arabian Sea: Modern Analogues and Application to the Palaeoclimatic Record." *Geological Society, London, Special Publications* 195 (1): 499-516. doi: 10.1144/gsl.sp.2002.195.01.27.

Simoneit, B. R. T. 2004. "Biomarkers (Molecular Fossils) as Geochemical Indicators of Life." *Space Life Sciences: Search for Signatures of Life, and Space Flight Environmental Effects on the Nervous System* 33 (8): 1255-1261.

Sikes, E.L., Volkman, J.K. 1993. Calibration of alkenone unsaturation ratios ($U^{k'}_{37}$) for paleotemperature estimation in cold polar waters. Geochimica et Cosmochimica Acta 57 (8): 1883-1889.

Sluijs, A., J. Pross, and H. Brinkhuis. 2005. "From Greenhouse to Icehouse; Organic-Walled Dinoflagellate Cysts as Paleoenvironmental Indicators in the Paleogene." *Earth-Science Reviews* 68 (3-4): 281-315.

Song, Shuolin, Thomas Jarvie, and Masahira Hattori. 2013. "Chapter Three - Our Second Genome—Human Metagenome: How Next-Generation Sequencer Changes Our Life through Microbiology." In *Advances in Microbial Physiology*, ed. Robert K. Poole, 119-144. Academic Press.

Soulet, G., G. Delaygue, C. Vallet-Coulomb, M. E. Bottcher, C. Sonzogni, G. Lericolais, and E. Bard. 2010. "Glacial Hydrologic Conditions in the Black Sea Reconstructed Using Geochemical Pore Water Profiles." *Earth and Planetary Science Letters* 296 (1-2): 57-66.

Soulet, G., G. Menot, G. Lericolais, and E. Bard. 2011. "A Revised Calendar Age for the Last Reconnection of the Black Sea to the Global Ocean." *Quaternary Science Reviews* 30 (9-10): 1019-1026.

Summons, Roger E., and Trevor G. Powell. 1986. "Chlorobiaceae in Palaeozoic Seas Revealed by Biological Markers, Isotopes and Geology." *Nature* 319: 763. doi: 10.1038/319763a0.

Svetlichny, L., E. Hubareva, M. Isinibilir, A. Kideys, G. Belmonte, and E. Giangrande. 2010. "Salinity Tolerance of Calanus Euxinus in the Black and Marmara Seas." *Marine Ecology Progress Series* 404: 127-138.

Taylor, F. J. R. 1987. *The Biology of Dinoflagellates*. Edited by F. J. R. Taylor. Vol. 21. Oxford: Blackwell Scientific.

ten Haven, H. L., J. W. de Leeuw, J. S. Sinninghe Damsté, P. A. Schenck, S. E. Palmer, and J. E. Zumberge. 1988. "Application of Biological Markers in the Recognition of Palaeohypersaline Environments." *Geological Society, London, Special Publications* 40 (1): 123.

van der Meer, M. T. J., F. Sangiorgi, M. Baas, H. Brinkhuis, J. S. S. Damste, and S. Schouten. 2008. "Molecular Isotopic and Dinoflagellate Evidence for Late Holocene Freshening of the Black Sea." *Earth and Planetary Science Letters* 267 (3-4): 426-434.

Volkman, J.K. 1986. A review of sterol markers for marine and terrigenous organic matter. Organic Geochemistry 9(2): 83-89.

Volkman, J.K., Barrett, S.M., Dunstan, G.A., Jeffrey, S.W. 1993. Geochemical significance of the occurrence of dinosterol and other 4-methyl sterols in a marine diatom. Organic Geochemistry 20(1): 7-15.

von Rad, Ulrich, Hartmut Schulz, Volkher Riech, Maryke den Dulk, Ulrich Berner, and Frank Sirocko. 1999. "Multiple Monsoon-Controlled Breakdown of Oxygen-Minimum Conditions During the Past 30,000 Years Documented in Laminated Sediments Off Pakistan." *Palaeogeography, Palaeoclimatology, Palaeoecology* 152 (1–2): 129-161. doi: https://doi.org/10.1016/S0031-0182(99)00042-5.

Vonrad, U., H. Schulz, A. A. Khan, M. Ansari, U. Berner, P. Cepek, G. Cowie et al. 1995. "Sampling the Oxygen Minimum Zone Off Pakistan - Glacial Interglacial Variations of Anoxia and Productivity (Preliminary-Results, Sonne-90 Cruise)." *Marine Geology* 125 (1-2): 7-19.

Walther, G. R. 2010. "Community and Ecosystem Responses to Recent Climate Change." *Philosophical Transactions of the Royal Society B-Biological Sciences* 365 (1549): 2019-2024.

Walther, G. R., E. Post, P. Convey, A. Menzel, C. Parmesan, T. J. C. Beebee, J. M. Fromentin, O. Hoegh-Guldberg, and F. Bairlein. 2002. "Ecological Responses to Recent Climate Change." *Nature* 416 (6879): 389-395.

Willerslev, E., A. J. Hansen, and H. N. Poinar. 2004. "Isolation of Nucleic Acids and Cultures from Fossil Ice and Permafrost." *Trends in Ecology & Evolution* 19 (3): 141-147.

William, A. S. Sarjeant. 1986. "Sporopollenin Dinoflagellate Cysts. Their Morphology and Interpretation " Review of *Sporopollenin Dinoflagellate Cysts. Their Morphology and Interpretation, William R. Evitt*. *Micropaleontology* 32 (3): 282-285. doi: 10.2307/1485622.

Yun, S. M., T. Lee, S. W. Jung, J. S. Park, and J. H. Lee. 2017. "Fossil Diatom Assemblages as Paleoecological Indicators of Paleo-Water Environmental Change in the Ulleung Basin, East Sea, Republic of Korea." *Ocean Science Journal* 52 (3): 345-357.

Zonneveld, K. A. F., G. J. M. Versteegh, and G. J. deLange. 1997. "Preservation of Organic-Walled Dinoflagellate Cysts in Different Oxygen Regimes: A 10,000 Year Natural Experiment." *Marine Micropaleontology* 29 (3-4): 393-405.

CHAPTER 2

A 43 kyr record of protist communities and their response to Oxygen minimum zone variability in the Northeastern Arabian Sea

Kuldeep D. More, William Orsi, Valier Galy, Liviu Giosan, Lijun He, Kliti Grice and Marco Coolen

Earth and Planetary Science Letters, 496, 248-256 (2018)

https://doi.org/10.1016/j.epsl.2018.05.045

2.1 ABSTRACT

An extensive oxygen minimum zone (OMZ) occurs in the northeastern (NE) Arabian Sea where sedimentary records show evidence of alternating strong and weak OMZs that correlate with North Atlantic climate variability during the last glacial-interglacial cycle. OMZs are expanding world-wide, but information on long-term OMZ-ecosystem interactions is mainly limited to fossilised species, notably foraminifera. This chapter provides a first comprehensive ancient sedimentary DNA record of both fossilizing and non-fossilizing protists and their response to OMZ variability in the NE Arabian Sea over the last 43 ka. Protist communities changed significantly during strong vs. weak OMZ conditions coincident with interstadials and stadials respectively. Dinoflagellates were identified as significant indicator taxa for strong OMZs during glacial as well as interglacial interstadials, whereas diatoms were significant indicators for strong OMZs only during glacial interstadials. The chlorophyte *Chlorella* was found to be the main phototrophic protist in nutrient-depleted surface waters during glacial stadials. Notably, strong OMZ conditions shaped past protist communities by creating isolated habitats for those capable of sustaining oxygen depletion either by adapting a parasitic life cycle (e.g. apicomplexans) or by establishing mutualistic connections with others (e.g. radiolarians and mixotrophic dinoflagellates) or by forming cysts (e.g. colpodeans). Notably, a long-term increase in eutrophication and a decrease in the diatom/dinoflagellate ratio was observed during the late Holocene favoring the pelagic component of the marine food web. A similar scenario could be expected in the context of predicted worldwide expansion of coastal OMZs associated with global climate change.

2.2 INTRODUCTION

2.2.1 Oxygen minimum zone (OMZ)

Over geological timescales, recurring changes in the ocean oxygenation have resulted in multiple biotic crises with concomitant changes in marine ecosystems and climate balance (Wright et al., 2012). Over the last few decades, decline in oxygen concentrations has been observed throughout much of the world ocean's interior and is predicted to continue in the context of coastal eutrophication and global warming (Helm et al., 2011; Keeling et al., 2010). Upwelling of nutrients promote the formation of plankton blooms. Oxygen consumption through bacterial degradation of this sinking biomass and thermal stratification of the water column contribute to a decreased oxygen availability leading to the formation and expansion of oxygen minimum zones (OMZs) at mid-water depths (~150-1300m) (Schulz et al., 2002). Selective pressure under OMZ conditions has been observed in unicellular eukaryotes (protists), which are major components of the oceanic food chain and are important contributors to and consumers of pelagic productivity (Burkill et al., 1993; Strom and Welschmeyer, 1991; Worden et al., 2015). Photosynthetic protists are major primary producers inhabiting the photic zone, while bacterivorous and planktivorous heterotrophs bridge the prokaryotic component of the food web to higher trophic levels and follow the distribution of autotrophic protists. Mixotrophs being capable of autotrophy and phagotrophy, have a much wider distribution across the water column (Sherr and Sherr, 1994) and can be directly exposed to oxygen stress at intermediate depth (Jing et al., 2015). Shoaling of the upper boundaries of the OMZs can affect protist habitats and *vice versa*, changes in the distribution of primary producers and consumers can affect the oxygen demand and, hence the distribution of OMZs.

2.2.2 Modern observations: OMZ vs protists

The north-eastern Arabian Sea experiences semi-annual monsoonal wind reversals contributing to two periods of heightened surface productivity: during the southwest (SW) monsoon (June–September) and during the northeast (NE) monsoon (November–February) (Parab et al., 2006). Strong SW monsoonal winds lead to north-eastward drift of nutrient-rich surface waters from Oman to the Pakistan margin causing high primary productivity (Andruleit et al., 2000; Schulte and Muller, 2001; Schulz et al., 1996). While during NE monsoon, sea surface cooling activates the convection processes causing deep mixing of subsurface waters. This process leads to injection of nutrients to surface waters bolstering high winter pelagic productivity (Madhupratap et al., 1996). Microscopic cell counts and

pigment analysis revealed that during the SW monsoon when nitrate concentrations are high, diatoms become dominant along with prymnesiophytes (Parab et al., 2006). By the end of the SW monsoon, sinking biomass of decaying diatom blooms provides substrate for microbial degradation, which causes rapid oxygen consumption at intermediate depth and intensification of the OMZ (Parab et al., 2006; Schulz et al., 2002). During this period, nitrate concentrations become undetectable and a shift from diatoms and prymnesiophytes to dinoflagellates below the shallow pycnocline is observed (Parab et al., 2006). In the oxygenated surface waters, where nitrate is below detection limits, pico-cyanobacterial populations then become dominant (Parab et al., 2006). During the NE monsoon, low nitrate concentration causes the replacement of a mixed diatom-dinoflagellate population by the nitrogen-fixing cyanobacterium *Trichodesmium*. A combination of low phytoplankton biomass and high ammonium concentrations further suggest that active grazers prevent the establishment of diatom-dinoflagellate blooms in the eastern Arabian Sea during the NE Monsoon. In May, just prior to the start of the SW Monsoon, nutrient enrichment associated with the demise and decay of *Trichodesmium* blooms along with coastal upwelling of nitrates stimulate the growth of both diatoms and dinoflagellates (Parab et al., 2006).

Information on these OMZ-ecosystem interactions in the Arabian Sea and elsewhere is mainly based on such recent observations, modelling experiments, and fossilised foraminifera (Blackford and Burkill, 2002; Madhupratap et al., 1996; Parab et al., 2006; von Rad et al., 1999). A holistic overview of past OMZ-protist interactions is lacking world-wide since the majority of the above-mentioned protist taxa do not fossilize. However, even in the absence of microfossils, genetic signatures of past planktons were found to be preserved in the marine geological records and can be used to reconstruct marine ecosystem changes caused by environmental perturbations (Coolen et al., 2013; Inagaki et al., 2005; Lejzerowicz et al., 2013)

2.2.3 Coring location in North-eastern (NE) Arabian Sea

Records close to the Indus Canyon show that during the last glacial-interglacial cycle the NE Arabian Sea witnessed alternate strong and weak OMZs (Banakar et al., 2010; von Rad et al., 1995), which makes it an ideal location to study long-term protist-OMZ interactions. For this study, a highly resolved profiling of sedimentary protist 18S ribosomal RNA genes at centennial-scale resolution was used to reconstruct the interplay between past OMZ variability and protist community structures over the last glacial-interglacial cycle in the NE-Arabian Sea. The core used for this study was obtained from the centre of the OMZ on the

continental slope, NW of the Indus Canyon (Orsi et al., 2017). Geochemical analysis revealed a distinct pattern of laminated, organic carbon-rich intervals comparable to those present in previously studied cores, which were obtained in close vicinity and at comparable water depths within the OMZ (von Rad et al., 1995).

Here, integrated analysis of the sedimentary DNA and paleoceanographic proxy data revealed unprecedented details about long-term effects of OMZ conditions on protist communities. Similar approaches could potentially reveal insights about long-term OMZ-ecosystem interactions at important OMZ locations other than the Arabian Sea.

2.3 MATERIALS AND METHODS

2.3.1 Sample collection and storage

For this study, a 13-m-long Piston core 11C spanning 43 kyr of deposition was obtained during R/V Pelagia cruise 64PE300 from the center of the OMZ (566 m depth) on the continental slope NW of the Indus Canyon (23° N; 66° E). Subsamples (214 two-cm-thick intervals) for DNA and geochemical analysis were taken aseptically inside the ancient DNA-dedicated clean lab at the Woods Hole Oceanographic Institution (WHOI) as described in detail recently (Orsi et al., 2017). In that study, the same intervals of this core have been used to reveal to what extent the sub-seafloor microbiome was shaped by past OMZ conditions (Orsi et al., 2017).

2.3.2 Age model

Radiocarbon dates were obtained for the Holocene interval from mixed planktonic foraminifera or monospecific *Orbulina universa* samples (Orsi et al., 2017). Calibration was performed using Calib 7.1 with a reservoir age of 565±35 radiocarbon years (Stuiver and Reimer, 1993). For pre-Holocene sediments, the age model is based on correlative tie points from XRF-derived Br record in core 64PE300-11C to the high-resolution total organic carbon records of nearby core SO90-136KL (Schulz et al., 1998). Linear interpolation was used to determine ages for each individual sample.

2.3.3 Bulk Geochemistry

The intact archived core sections were scanned for bulk elemental composition using an ITRAXTM micro-XRF scanner with a molybdenum x-ray tube with a step-size of 200 µm for an exposure time of 10 s^{-1}. Bromine variability was used as proxy for organic matter (Ziegler et al., 2008). Total organic carbon (TOC), $\delta^{13}C$, $\delta^{15}N$, and C/N were analyzed using a Delta Plus

stable light isotope mass spectrometer from 214 freeze-dried and carbonate-free sediment samples spanning the entire core as described in detail elsewhere (Orsi et al., 2017).

2.3.4 Sedimentary DNA extraction and analysis

Inside the ancient DNA-dedicated lab at WHOI, genomic DNA was extracted and purified from 5-10 grams of wet weight sediment after Direito et al., 2012; with modifications described for this core in detail recently (Orsi et al., 2017). This protocol was repeated without the addition of sediment and the resulting extract was used as a control for contamination during extraction and purification of the sedimentary DNA. The recovered purified sedimentary DNA was quantified fluorometrically using Quant-iT PicoGreen™ double stranded DNA (dsDNA) Reagent (Invitrogen) and ~20 nanograms of each extract was used as template for PCR amplification of preserved planktonic 18S rRNA genes. The short ~130 bp long 18S rDNA-V9 region was amplified using the domain-specific primer combination 1380F (5'-CCC TGC CHT TTG TAC ACA C-3') and 1510R (5'CCT TCY GCA GGT TCA CCT AC-3') (Amaral-Zettler et al., 2009). Quantitative PCR (qPCR) was performed using a SYBR®Green I nucleic acid stain (Invitrogen) and using a Realplex qPCR system (Eppendorf, Hauppauge, NY). The annealing temperature was set to 66 °C and all reactions were stopped in the exponential phase after 35-42 cycles.

To generate template for subsequent Illumina MiSeq sequencing of PCR-amplified sedimentary 18S rRNA genes, the same qPCR conditions and region-specific primers were used, except for that the primers included the Illumina flowcell adapter sequences as well as the pad regions (Caporaso et al., 2012). The reverse primer now also included a unique 12 base Golay barcode sequence to support pooling of the samples. The quality of the PCR products was verified by agarose gel electrophoresis and equimolar amounts of the barcoded PCR products were pooled and purified using the AMPure®XP PCR purification kit (Agencourt Bioscience Corp., Beverly, MA). Four hundred nanograms of the mixed and purified barcoded amplicons were subjected to subsequent Illumina MiSeq sequencing using the facilities of the W.M. Keck Center for Comparative and Functional Genomics, University of Illinois at Urbana-Champaign, IL, USA. The sequenced 18S libraries resulted in approximately 12 million reads. QIIME was used for further processing of rRNA gene sequences (Caporaso et al., 2010). Reads were organized into Operational Taxonomic Units (OTUs) after passing quality control (95% sequence identity with UCLUST) and assigned to taxonomic groups through BLASTn searches against the SILVA database (Pruesse et al., 2007). OTU tables were rarified in QIIME using the single_rarefaction.py command to the sample and singletons as well as non-protist

reads were removed. Ecological statistics were calculated in R (https://www.r-project.org) using a Bray Curtis distance in the Vegan package (Oksanen, 2011). Analysis of Similarity (ANOSIM) was carried out using 999 permutations with a Bray Curtis distance (Clarke, 1993). Indicator Species Analysis (ISA) (Dufrene and Legendre, 1997) was performed in the Vegan package and significance was tested with a nonparametric procedure involving the Monte-Carlo permutation procedure with 999 permutations.

2.4. RESULTS

2.4.1 Chronology of the core and paleo-environment

The age model used to establish the timing of depositional and environmental changes is based on radiocarbon dating of foraminiferal carbonates and a comparison between XRF-derived bromine (Br) (Orsi et al., 2017) and TOC content (Fig. 2.1) to highly resolved TOC data from well-dated comparable cores from the same location (Schulz et al., 1998). Bromine, a biophilic halogen that binds to allochthonous marine organic matter (Ziegler et al., 2008) and TOC values correlate significantly ($r=0.65$ $P < 0.01$), which suggests a marine origin of the majority of organic matter over the last 43 Kyr. This is consistent with invariably low contributions of terrigenous OM from the Indus basin (Clift et al., 2010). Bulk sedimentary stable N isotope ($\delta^{15}N$) compositions above ~6.5 ‰ are indicative of strong paleo-denitrification and strong OMZ conditions. Since TOC preservation was enhanced when OMZ conditions penetrated the coring location, variations in sedimentary TOC content during enhanced preservation likely reflect changes in paleoproductivity. The TOC content correlates positively with bulk $\delta^{15}N$ values ($r = 0.37$, $P < 0.01$) (Orsi et al., 2017). Based on $\delta^{15}N$ and TOC content three depositional categories throughout the core were observed: 1) Sapropelic sediments (TOC>2 wt. %) with $\delta^{15}N$ values > 6.5 ‰ indicative of respectively high primary productivity and strong OMZ conditions; 2) Non-sapropelic sediments (TOC < 2 wt. %) and $\delta^{15}N$ values above 6.5 ‰ indicative of reduced primary productivity yet strong OMZ conditions; 3) non-sapropelic sediments with $\delta^{15}N$ <6.5‰ representing weak or no OMZ conditions. Since the surface sediments were likely to be oxygenated during weak OMZ conditions, it cannot be concluded whether reduced productivity or low preservation contributed to the lower TOC content in category 3 sediments.

During Oxygen Isotope stage (OIS) 2 and 3, the timing of deposition of Category 1 sapropelic sediments is coincident with North Atlantic millennial-scale Dansgaard-Oeschger (D/O) warm interstadials (Table 2.1). Category 1 sediments were also deposited during the Bølling/Allerød (BA) (~13-14.5 ka BP) and the Holocene (starting at ~ 10 Ka BP), when TOC content reached

a maximum of 4 wt%. Category 2 sediments were mainly deposited during the transitions between stadials and interstadials, while Category 3 bioturbated sediments coincided with the timing of stadials, notably Heinrich (H) events and the Younger Dryas (YD) (~ 11.4-13 ka BP) (Table 2.1).

2.4.2 Past protist diversity

The sequenced eukaryotic library resulted in 2863 OTUs in 13 protist phyla: Alveolata, Amoebozoa, Apuszoa, Centroheliozoa, Chlorophyta, Choanoflagellida, Cryptophyta, Euglenozoa, Haptophyta, Jakobida, Rhizaria, Rhodophyta and Stramenopiles. Changes in the relative abundance of the most abundant phyla and subgroups were compared with paleoenvironmental changes in the NE Arabian Sea during the last glacial interglacial cycle (Fig. 2.1 and Table 2.1)

Rhizaria is a supergroup of pelagic as well as benthic protists and comprise (a) Radiolaria, which are particle feeding or predatory zooplankton that can also form symbiotic relationships with e.g. dinoflagellates, (b) Cercozoa comprising various amoebae and flagellates, and (c) Foraminifera (Cavalier-Smith, 2002). Rhizaria represented 50-100% of the protistal reads in the majority of sediments deposited during strong OMZ conditions, notably during IS8, 7, 6, 3, 2, B/A, and the Holocene (Fig. 2.1). In contrast, a low relative abundance was observed especially during H1, H3, H4 and S11 (Fig. 2.1). Furthermore, a sharp decline in Rhizaria reads occurred between 8 to 8.5 kyrs, coinciding with the timing of the 8.2 ka cold event (Kobashi et al., 2007). The majority of Rhizaria belonged to the class Polycystinea (fossilizing radiolarians with silicate exoskeletons) (Fig. 2.2). Their relative abundance gradually increased over the course of the Holocene to reach 100% of Rhizaria reads (Fig. 2.2). Polycystines showed a sharp decline during H1 and H3. Polycystinea contains two major orders: Spumellaria and Nassellaria. Spumellarians were present during all climate stages (>25% of total Polycistinea reads) showing a general increasing trend after OIS2 (Fig. 2.3). Nassellarians were the most abundant Rhizaria during the LGM and H1 (Fig 2.3). Cercozoa were relatively abundant (up to 50% of total rhizarian reads) during late H4, IS6, IS4 and H1 (Fig. 2.2 and 2.3).

Alveolata comprised up to 50 to 90% of total reads after the OIS3 to OIS2 transition (Fig 2.1). This superphylum consist of protists with flattened vesicles known as alveoli and comprise dinoflagellates (Dinophyceae), ciliates (Ciliophora), and obligate parasites (Apicomplexa) (Cavalier-Smith, 1991) (Fig. 2.2). Dinoflagellate reads comprised more than 75% of the identified Alveolata during OIS2, except for a low relative abundance during H2 and YD-B/A

transition. They were furthermore consistently abundant during the Holocene, with the exception of a short decline at ~3.5 Ka BP (Fig. 2.2). The dinoflagellates identified in this core belonged to four major orders: (1) Blastodiniales, known parasites of zooplanktons (Coats, 1999), represented 25-65% of dinoflagellate reads during most of OIS2 (Fig. 2.3). (2) Mixotrophic Gymnodiniales, which lack an armored exterior, were mostly present during interstadials of OIS3 where they represented 90-100% of dinoflagellate reads. (3) Syndiniales, known endosymbionts or parasites of other dinoflagellates and zooplankton (Coats, 1999), were also found mainly during OIS3 (Fig. 2.3). (4) The less well-described Lophodiniales were mostly present during stadials S7, S6 (OIS3) and S3, H2 (OIS2).

A scattered predominance of ciliate reads was observed during OIS3 while they were consistently abundant alveolates during the B/A and YD (Fig. 2.2). They were dominated by the class Colpodea and Oligohymenophorea (Fig. 2.3). Colpodea, which are mainly freshwater ciliates, represented 80-95% of ciliate reads from H1 to Early Holocene. Oligohymenophorea (mostly microphagous ciliates) were the most abundant ciliate reads in interstadials like IS8, IS5, IS4, IS2 and Holocene with notable exception of the S6 stadial where they represented 90% of the ciliate reads (Fig. 2.3). Apicomplexa were sporadically present throughout the record (Fig. 2.2). More specifically, according to the detailed averaged dataset, reads related to the fish parasites Coccidia predominated the Apicomplexan reads during OIS2 and OIS1 (Fig. 2.3).

Unicellular Stramenopiles, consisting mainly of photosynthetic diatoms, were relatively abundant protists mainly during interstadials in OIS3. They were most consistently present in OIS2 sediments (~20% of the total protist reads) and were generally below 5% of total protist reads during most of the Holocene (Fig 2.1). However, diatoms showed cyclicity in abundance compared to other stramenopiles and represented up to 100% of stramenopile reads during interstadials of OIS3 as well as OIS2 and the early Holocene, while their relative abundance dropped during all stadials in OIS2 and OIS3 and at ~8.2 ka BP (Fig. 2.2). At the genus level, the primarily marine *Thalassiosira* was the most prominent diatom throughout the core, while coastal *Skeletonema* was the only diatom present during S11 and represented up to 80% of diatom reads during S3 (Fig. 2.3).

Green algae (Chlorophyta) identified in the Arabian Sea sediments comprised the unicellular pelagic families Trebouxiophyceae (exclusively the genus *Chlorella* in current record), Prasinophyceae, Chlorophyceae and Mamiellophyceae. Chlorophyta reads dominated the OIS 3 reaching up to 50% of total protists with a notable exception of their general absence

during long periods of strong denitrification and OMZ conditions such as during IS8 (Fig 2.1). *Chlorella* dominated the green algal population during stadials of OIS3 and H2 when denitrification and OMZ conditions were reduced (Fig. 2.2). *Chlorella* was also dominant during IS5 when denitrification was less extensive compared to other interstadials (Fig. 2.2). Chlorophyte DNA was no longer abundant after H2 (Fig. 2.1), but a sharp shift in the relative abundance towards eutrophic Prasinophyceae as the most abundant chlorophytes was observed mainly during interstadials of OIS2 and the Holocene (Figs. 2.2 and 2.3).

Centroheliozoans (amoeboid protists) were sporadically abundant (up to 50%) in glacial OIS3 sediments and generally below the detection limit in OIS2 and OIS1 (Fig 2.1). Reads of haptophyte algae were sporadically present throughout the core and comprised less than 5% of the reads notably during stadials such as H2 (Fig 2.1). Other protist groups (Amoebozoa, Apuszoa, Choanoflagellida, Cryptophyta, Euglenozoa, Jakobida and Rhodophyta) (Fig 2.1) were sporadically present and when combined, comprised less than 5% of the total protist sequences. The analysis below focusses exclusively on the most abundant protist groups that were not sporadically present and contributed more than 5% to the total protist reads.

2.4.3 Correlation between change in paleoenvironment and protist community structure

To investigate the effect of OMZ strength on protist community compositions, Non-Metric Multidimensional Scaling Analysis (NMDS; stress <0.05) was performed. Analysis of similarity (ANOSIM) revealed that the microbial communities were significantly different (P=0.001) in sediments of the three categories described above (Fig 2.4). In order to investigate which taxa were affected by strong vs. weak OMZ conditions and transitions, the indicator species analysis (ISA) was performed.

2.4.3 Indicator species analysis

ISA identified 52 significant ($p<0.05$) indicator taxa for category 1. Fig. 2.5 shows the specificity (A-value) vs. sensitivity (B-value) of each indicator species. In theory, an A-value of 1 indicates that the species in question occurs in only one indicator group, while an optimal B-value of 1 means that this species occurs in all samples of that category. Alveolata with 24 OTUs were the most abundant group of indicator species for Category 1. The majority of these indicator species were dinoflagellates (13 OTUs), followed by unnamed alveolata (4 OTUs), marine alveolate group 1 (5 OTUs), and parasitic ciliates (Scuticoliliates, 2 OTUs). Syndiniales were among the most closely related dinoflagellates, whereas the majority of the indicator dinoflagellates were related to environmental clones. Interestingly, two of the unclassified dinoflagellates (OTUs 52191 and 93979) showed 99% sequence similarity to

clones isolated from anoxic waters of respectively Cariaco Basin (Genbank accession number GU820545.1) (Edgcomb et al., 2011), and the east Pacific rise (KJ761327) (Lie et al., 2014). The next important group indicative of this category were Rhizarians (i.e., cercozoans and polycystines). Indicator cercozoans belonged to Cercomonadida (2 OTUs: 11339 and 38346), Thecofilosea (4 OTUs) Silicofilosea (1 OTU) and un-named cercozoans (2OTUs: Cercozoa 1 and Cercozoa 2). Polycystinea contained 2 nassellarian members and spumellarian families Actinommidae (1 OTU), Ethmosphaeridae (1 OTU), Sphaerozoidae (3 OTUs) and Spongodiscidae (1 OTU). Chlorophytes (Prasinophytes) with 4 OTUs were also important indicators for category 1 along with unnamed Stramenopiles and one Oomycete OTU.

Thirty-two indicator species (16 Rhizaria, 12 Alveolata, and 4 Stramenopiles) were identified for category 2 (Fig 2.6). Rhizarians belonging to the same polycystine families were found to be indicative of both categories 1 and 2. These involve spumellarian families Sphaerozoidae (3 OTUs), Actinommidae (1 OTU) and Ethmosphaeridae (1 OTU) plus 1 OTU of the nassellarian family Theoperidae. However, members of these families showed a generally stronger significance for category 1 (Fig. 2.6). Cercozoans, which were indicative of strong OMZ conditions and higher productivity were not indicative of less productive conditions during category 2.

Fewer and different dinoflagellates were found to be indicator species for category 2 (e.g. Blastodiniales) than for category 1. Category 2 also differed in the composition of indicator ciliates as it contained 4 OTUs of ciliates belonging to the class colpodea as opposed to scuticociliates indicative of category 1. Furthermore, apicomplexan parasites were indicators of category 2 as well as diatoms (Stramenopiles).

Only four important indicator species were identified for category 3 “weak OMZ conditions”: Chlorophyta (Chlorella), Centroheliozoa, and Rhizaria (Silicofilosea and an unnamed rhizarian) (Fig. 2.6).

2.5 DISCUSSION

2.5.1 Interplay between past OMZ conditions and phototrophic protists

In agreement with modern observations of plankton-OMZ interactions in the NE Arabian Sea (Parab et al., 2006), the paleogenomics record also revealed an increase in the relative abundance of diatoms and mixotrophic dinoflagellates during glacial interstadials when SW monsoon and OMZ conditions were strong. In contrast, a sharp decline in the relative abundance of diatom reads was observed during stadials including Heinrich events when SW

monsoon was weak (Deplazes et al., 2014). The data further showed a decline in the relative abundance of diatoms and a predominance of dinoflagellates during the mid to late Holocene, which is likely due to deepening of anoxia as this was reported to result in dinoflagellates replacing diatoms in the modern-day NE Arabian Sea (Parab et al., 2006). Indeed, the Diatom/Dinoflagellate ratio (Dia/Dino index) is being used as a proxy to assess the environmental status of oceans (e.g. Wasmund et al., 2017). When nutrients get depleted, rapid sinking of diatom blooms reduces the food stock for zooplankton (i.e., a high Dia/Dino Index), but avails food to zoobenthos. A high Dia/Dino index is typically considered an indicator of good environmental status. In contrast, a low Dia/Dino index is indicative of eutrophication since dinoflagellate blooms support pelagic components of the food web (e.g. Wasmund et al., 2017). Therefore, the lowering of the Dia/Dino index suggests an increase in eutrophication and stratified anoxic conditions during the late Holocene in the NE Arabian Sea. Similar long-term trends in eutrophication and a resulting lower Dia/Dino index may alter the higher trophic levels of the marine food web in the context of predicted expansion of costal OMZs associated with global climate change.

Data further revealed that *Chlorella* (Trebouxiophyceae) was an indicator species for weak OMZ conditions. *Chlorella* was relatively abundant in interstadial IS5, but otherwise predominated during the frequently occurring stadials of OIS3 and the H2 event in OIS2 (Fig. 2.2) when SW monsoon was weak and surface waters were likely to be depleted in key nutrients like nitrates (Deplazes et al., 2014). This abundance of *Chlorella* can be explained by the fact that under nitrogen stress it can survive by accumulation of fatty acids and carbohydrates in the cell membrane (Fan et al., 2014; Paes et al., 2016). Interestingly, Centroheliozoans also occurred during this period and were found to be a significant indicator species for weak OMZ conditions. Centroheliozoans as mentioned earlier are predatory amoeboid protists (Plotnikov and Ermolenko, 2015). However, they are also known to harbor endosymbiotic green algae such as *Chlorella* (Bubeck and Pfitzner, 2005), which would explain the co-occurrence of centroheliozoan reads with *Chlorella* in OIS3, and that both taxa were identified as significant indicator species for weak OMZs. Both *Chlorella* and Centroheliozoans were at or below detection limit during IS8 when according to the enriched $\delta^{15}N$ values, maximum denitrification and OMZ strength occurred, and when diatoms were the predominant primary producers instead (Fig. 2.2).

Chlorophytes as a group were no longer abundant protists after the OIS3-OIS2 transition, but *Chlorella* was succeeded by prasinophytes, which became the most abundant chlorophytes during the LGM and the Holocene (Figs. 2.1 and 2.2). Fossil pigments of prasinophytes

generally serve as a proxy for past stratified dysoxic to anoxic waters (Roncaglia and Kuijpers, 2006). In the present sedimentary 18S rDNA survey, prasinophytes were identified as important indicator taxa of strong OMZ with higher surface productivity. Deep mixing of nutrient-rich subsurface waters during SW monsoon brings nitrate into NE Arabian Sea surface waters (Madhupratap et al., 1996), which is required for the proliferation of prasinophytes (Prauss, 2007). Strengthening of the SW monsoon throughout and after the LGM (Schulz et al., 2002; von Rad et al., 1999) may have triggered the increased relative abundance of prasinophytes. In addition, elevated glacial sea surface salinity may have hindered prasinophytes from flourishing as they generally prefer brackish waters. An increased fluvial input from the Indus River, resulting into a reduced salinity after the LGM (Deplazes et al., 2014), may also have contributed to the growth of prasinophytes. Prasinophytes were absent or low in relative abundance during the cold stadials and the 8.2 ka event when weak monsoons resulted in reduced mixing (Singh et al., 2011; von Rad et al., 1995) and a scarcity of nutrients including nitrate must have prevailed. *Chlorella*, as a potential indicator for nutrient-limited conditions did not return as an abundant chlorophyte during the H1 and YD stadials. These events also experienced the continuous presence of dinoflagellates, which are significant indicators of strong OMZ conditions, suggesting that OMZ conditions were not entirely absent during these events.

2.5.2 Interplay between past OMZ conditions and non-phototrophic protists

According to paleogenomics survey presented here, Alveolata (i.e., mixotrophic dinoflagellates, ciliates, and apicomplexans) represented a predominant group of protists during strong OMZ conditions (Fig 2.1, 2.2 and 2.3). This is in agreement with current observations showing that during strong SW monsoons, dinoflagellates replace diatom blooms once anoxia starts to develop (Parab et al., 2006). The most abundant dinoflagellates were represented by members of the orders Blastodiniales, Gymnodiniales, and Syndiniales (Fig. 2.3). Blastodiniales are strictly parasitic dinoflagellates of zooplanktons and fish, while Syndiniales are either endosymbionts or parasites. Gymnodiniales are the least known groups of marine phytoplankton, but have been reported from suboxic interfaces and are known to form cysts as an adaptive strategy to survive adverse conditions such as low dissolved oxygen concentrations (Morquecho and Lechuga-Deveze, 2003). They are known ecto-parasites of zooplanktons (Coats, 1999). These dinoflagellates likely competed with a relatively large abundance of unclassified dinoflagellates with unknown growth requirements, notably during the entire Holocene (Fig. 2.3). It has been shown that stronger OMZs mainly occurred during interstadials after OIS3 when SW Monsoon intensified

(Deplazes et al., 2014; Schulz et al., 2002). DNA record is in agreement with this scenario since dinoflagellates fluctuated greatly in abundance between frequently alternating periods of strong vs. weak OMZ conditions during OIS3, but they became more continuously abundant during OIS2 and the Holocene, which experienced relatively long stretches of interstadials with increased SW monsoon intensity. Similar results with increased accumulation of dinoflagellates cysts during warm events of increased paleo-productivity such as the Holocene, B/A event and D/O interstadials has been witnessed in the anoxic Santa-Barbara basin (Pospelova et al., 2006). The second most abundant alveolates during strong OMZs were ciliates of the class Colpodea. Colpodeans are mostly freshwater ciliates that form cysts as a result of environmental stress. An increase in the relative abundance of Colpodea was observed during the B/A when high fluvial input from the Indus River was recorded in sediment cores obtained nearby (Deplazes et al., 2014). The next abundant ciliates were scuticociliates belonging to Oligohymenophorea, which contains endoparasites. Scuticociliates are obligate anaerobes that live in stratified low oxygen and anoxic marine waters in symbioses with sulfate reducing bacteria and methanogenic archaea and therefore serve as a proxy for OMZ conditions (Fenchel and Finlay, 1994). According to ISA, obligate endoparasitic pathogenic and spore-forming Apicomplexa (alveolata) were also significant indicators of strong OMZ conditions.

In addition to alveolata, rhizarians mainly represented by polycistine radiolarians and cercozoans (Fig 2.4), also dominated during periods of stronger OMZs. Cercozoans, which mostly represent heterotrophic protists, were abundant and significant indicator species for strong OMZ with high surface productivity, while polycystine radiolarians were significant indicators of strong OMZ irrespective of productivity. Polycystine radiolarians often form symbiotic relationships with mainly dinoflagellates, prymnesiophytes and prasinophytes (Steineck and Casey, 1990). In this case dinoflagellates are enclosed in a thin envelope of cytoplasm produced by the radiolarian host's rhizopodial system. This provides ammonium and carbon dioxide for the dinoflagellate symbionts, and in return the dinoflagellates provide their radiolarian host with a jelly-like layer that serves for protection and to capture prey (Steineck and Casey, 1990). A co-existence of polycystine radiolarians, dinoflagellates and prasinophytes was indeed observed in current paleogenomic record. Combined, these results show that OMZ conditions shaped the past protist community by creating isolated habitats for those capable of sustaining oxygen depletion either by adapting a parasitic life cycle or by establishing mutualistic connections with others or by cyst formation, which is in accordance with recent observations from other OMZ impacted sites (Jing et al., 2015).

2.6 CONCLUSIONS

Differences in genomic 18S rRNA gene copy numbers between eukaryotes (Hou and Lin, 2009), prevents the ability to provide absolute quantitative data on the past plankton. In addition, environmental DNA is prone to degradation. Nevertheless, this study show that stratigraphic analysis of sedimentary protist DNA can provide a useful long-term record of ecosystem responses to OMZ conditions including non-fossilizing taxa that traditionally escape microscopic identification in micro-paleontological studies. It is predicted that OMZs will continue to expand world-wide as a result of global warming and eutrophication (Helm et al., 2011; Keeling et al., 2010). Notably, protistal paleogenomic record suggests that long-term increase in eutrophication and a decrease in the Dia/Dino index, as has been the case in the NE Arabian Sea during the late Holocene, will likely favor the pelagic component of the marine food web in the context of predicted worldwide expansion of coastal OMZs associated with global climate change. Similar studies undertaken at other key locations with a history of persistent OMZs could provide a comprehensive window into past marine ecosystem changes and feedback mechanisms on OMZ expansion. If integrated with observations from modern time series, similar paleogenomic datasets could help towards forming a more comprehensive understanding and improved predictions of long-term OMZ expansion on coastal ecosystem interactions.

Acknowledgements

This work was primarily supported by NSF MGG Grant #1357017 to MJLC, VG, and LG. Additional financial support was provided via a C-DEBI grant #OCE-0939564 to WDO. This is C-DEBI contribution # 358. Core collection was supported by NSF OCE Grant #0634731 to LG. Kuldeep More thanks the co-chiefs Peter Clift and Tim Henstock as well as the scientific participants, captain and crew of the R/V Pelagia. Kuldeep More is also thankful to Dr. Cornelia Wuchter and Dr. Alisson Blyth for helpful discussions. Data has been deposited to SRA (Sequence Read Archive) NCBI under Bio project: PRJNA397489. Dr. Christopher Somes (GEOMAR Helmholtz Centre for Ocean Research) and two anonymous reviewers and Editor Prof. Derek Vance are thanked for their constructive feedback.

2.7 FIGURES

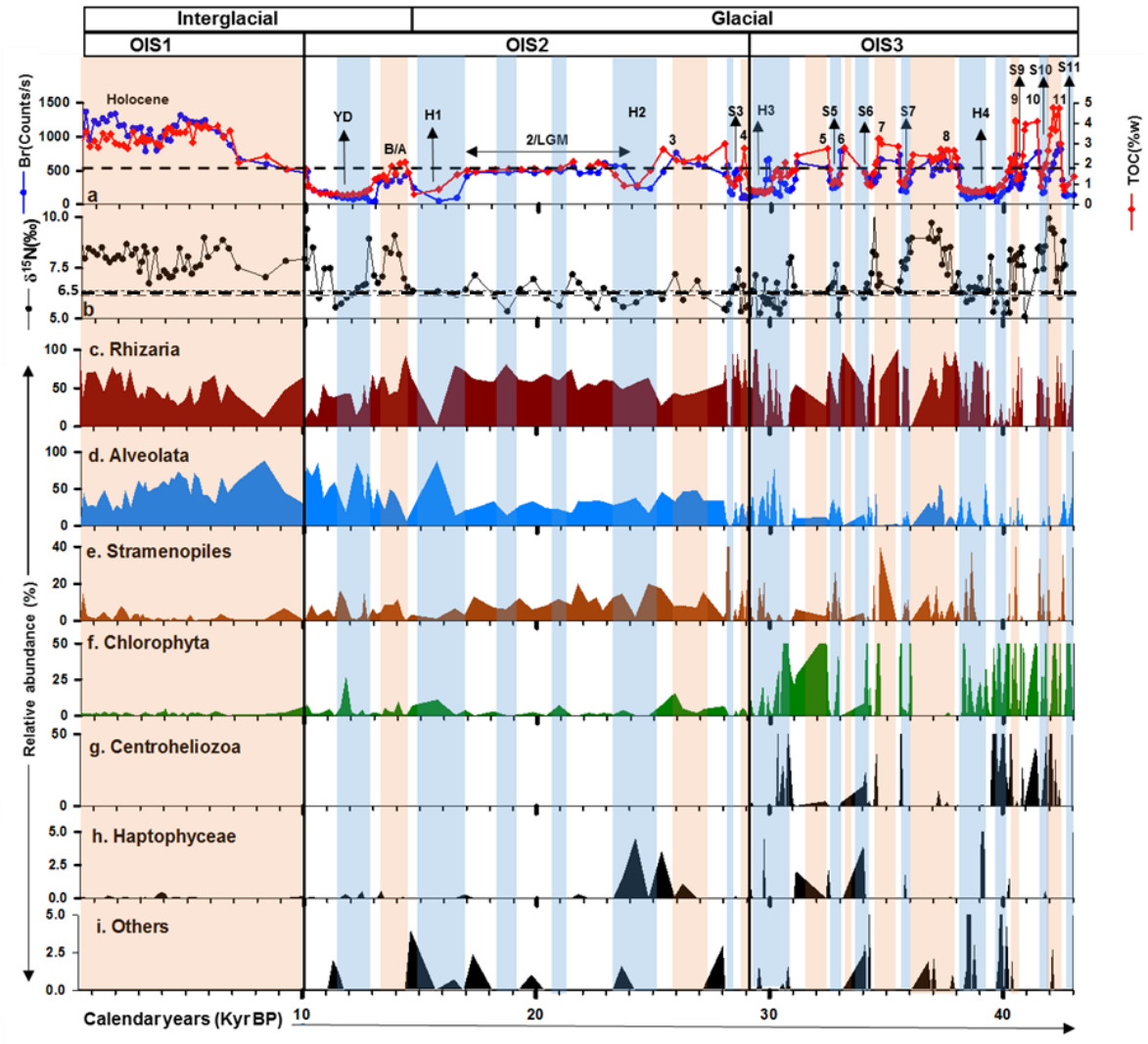

Figure 2.1 Overview of protist group abundance throughout the core. (a) Bromine XRF profile (blue) correlated with TOC content (red). (b) $\delta^{15}N$ record. Values above 6.5 (dotted line) represent higher denitrification rates. (c-i) Relative abundance (%) of key protist groups. (i) Includes the sum of Amoebozoa, Apusozoa, Choanoflagellida, Rhodophyta, Euglenozoa, Jakobida and Cryptophyta. Vertical black lines denote OIS transitions. Vertical pastel orange boxes indicate strong OMZ with high paleoproductivity, pastel blue boxes indicate weak OMZ and uncolored region indicates strong OMZ with low productivity. Interstadials are numbered on top of the TOC peaks while stadials are shown by arrows. Abbreviations: OIS (Oxygen Isotope Stage), YD (Younger Dryas), B/A (Bølling-Allerød), H (Heinrich event), IS (Interstadial), S (Stadial).

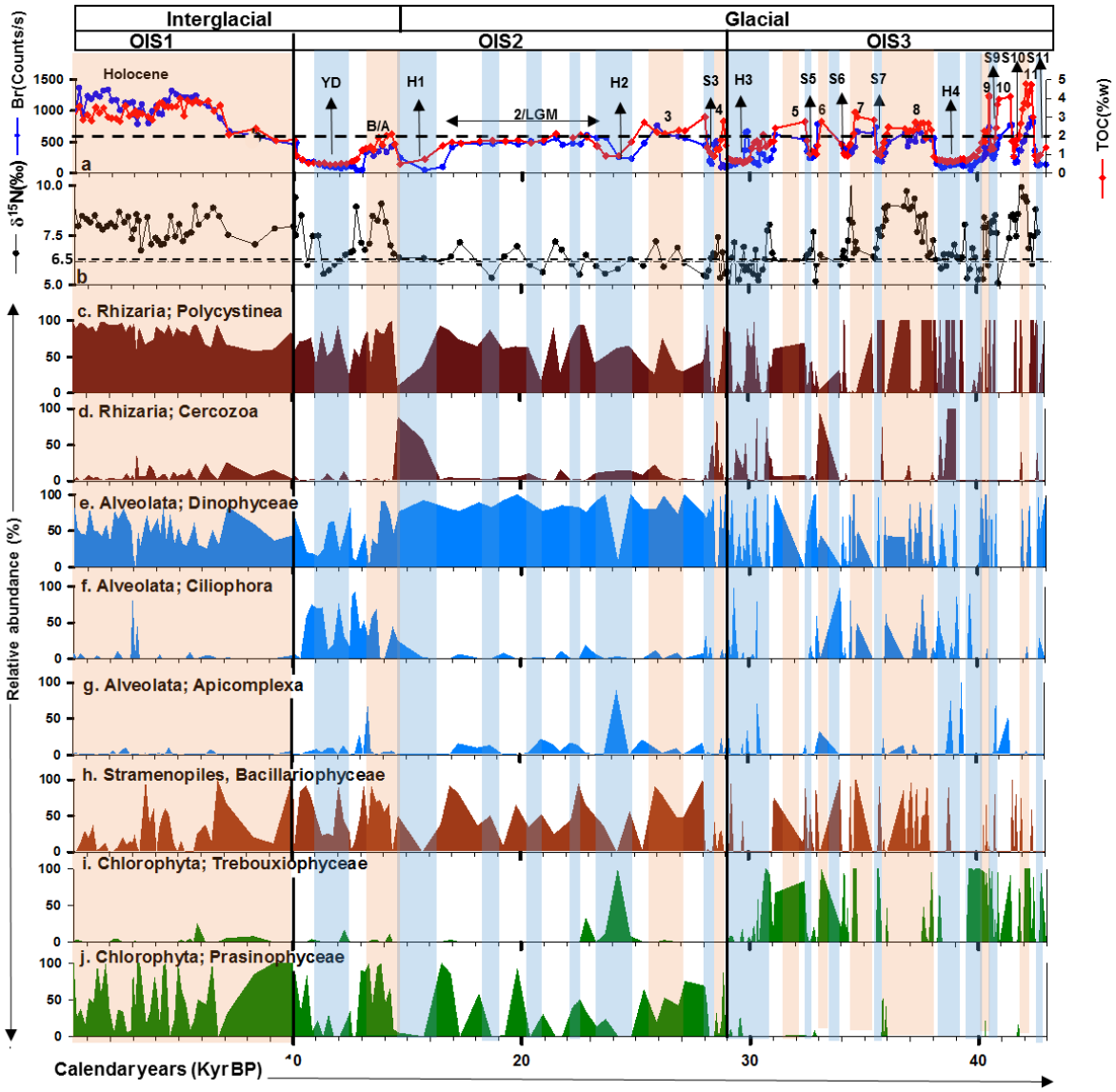

Figure 2.2 Relative abundance of protist subgroups.

(The same color coding and abbreviations as in Fig. 2.1)

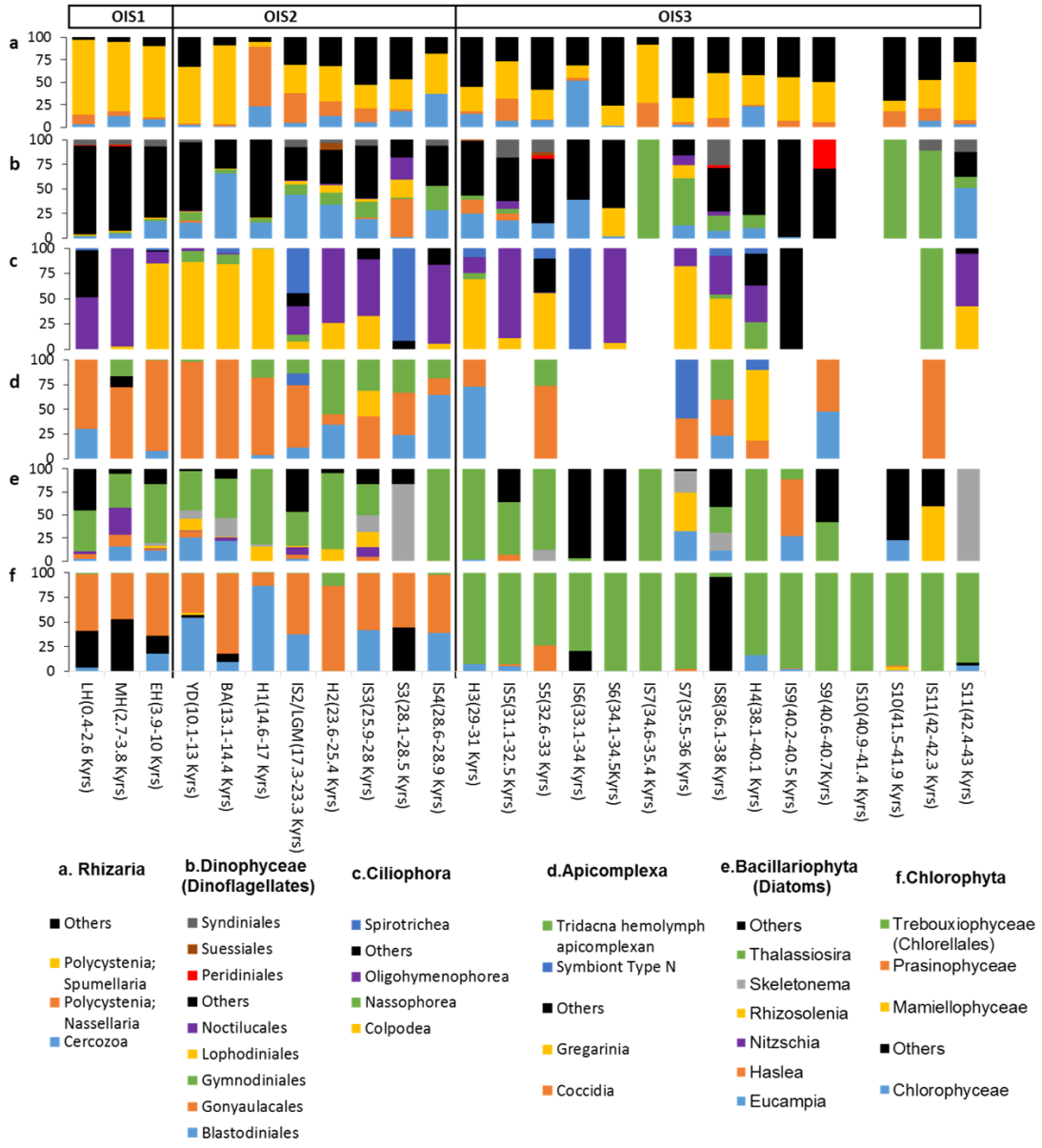

Figure 2.3 Detailed protist abundance overview. Averaged relative abundance of essential sub-groups within the most abundant supergroups in different climate intervals are represented in stacked histograms. The time span of each grouped climate stage is denoted below the figure. Abbreviations: OIS (Oxygen Isotope Stage), LH (Late Holocene), MH (Mid Holocene), EH (Early Holocene), YD (Younger Dryas), B/A (Bølling-Allerød), H (Heinrich event), IS (Interstadial), S (Stadial).

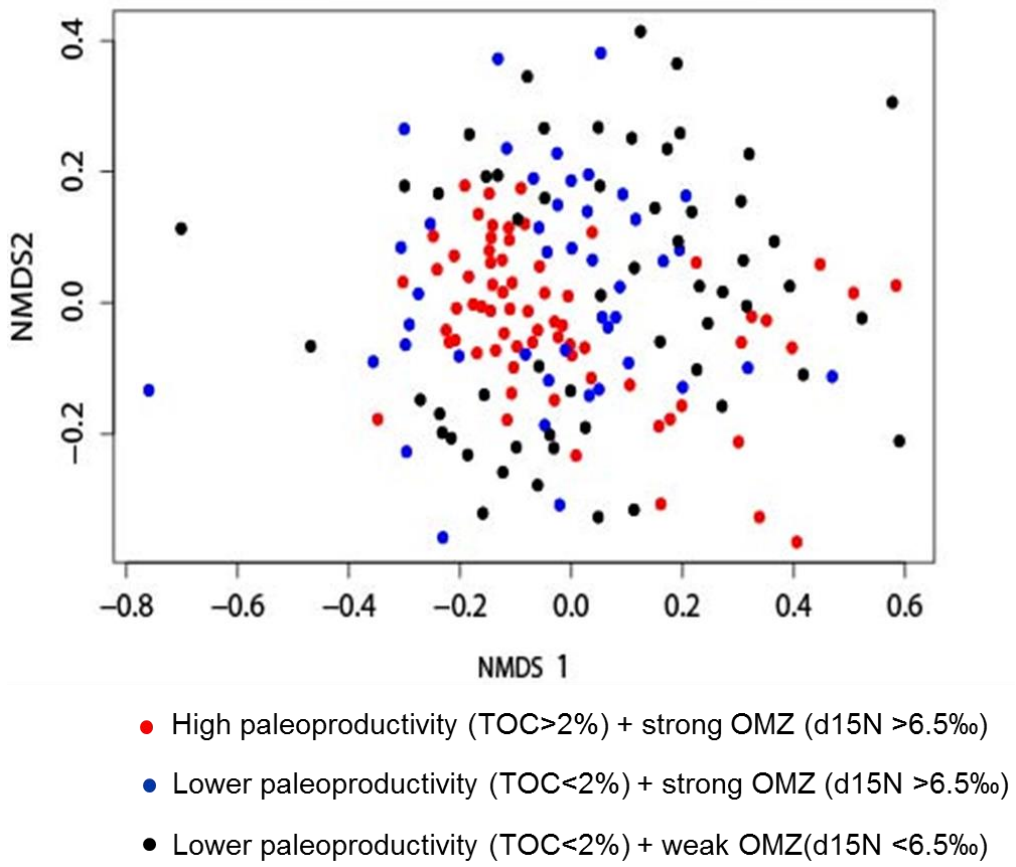

Figure 2.4 NMDS analysis of community composition using all protist OTUs (stress< 0.05). Analysis of similarity (ANOSIM) revealed that the overall protist community composition differed significantly between the three categories (P=0.001). Axes in NMDS are arbitrary.

Figure 2.5 Indicator species analysis. Horizontal bar diagrams of A and B values (X and Y axes respectively) of species indicative of Categories 1. “A” value denotes specificity (positive predictive value) while “B” value denotes the sensitivity (fidelity) of the species as indicator of the target site. Number of * indicate the significance value, 3 being the highest. Species names are written in the format “OTU number_Taxa; Subtaxa (r-value/ P-value and significance level*)”

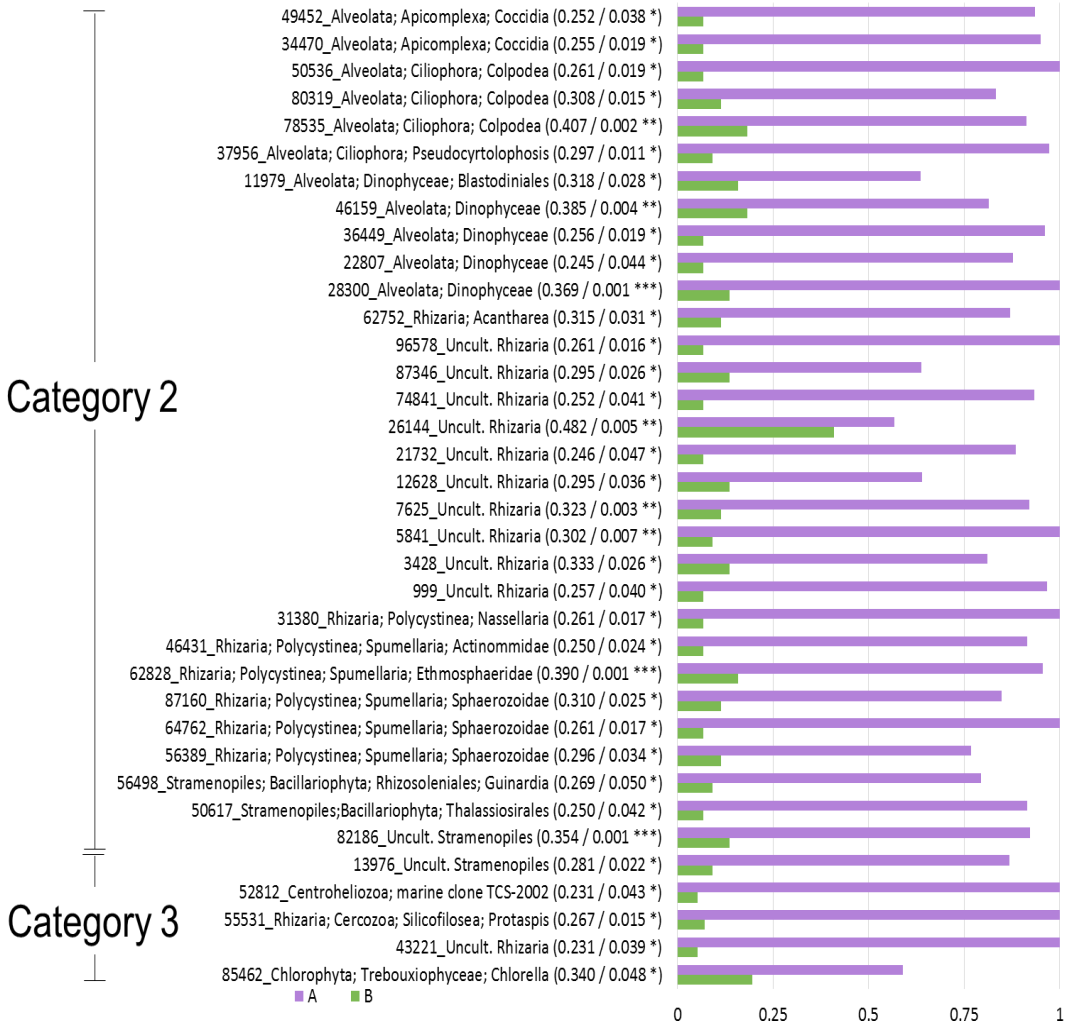

Figure 2.6 Indicator species analysis. Horizontal bar diagrams of A and B values (X and Y axes respectively) of species indicative of Categories 2 and 3.

2.8 TABLES

Table 2.1 Types of sediment categories deposited during different climate intervals.

Period	Age (Kyr)	Sediment category
Holocene	0.42-10	1
Younger-Dryas	10.2-11.3	2
	11.4-12.5	3
	12.6-13	2
Bolling-Allerod	13.1-13.5	2
	13.6-14.4	1
H1	14.6-16.9	3
IS2/LGM	17-18.15	2
	18.7-19.8	3
	20-20.4	2
	20.5-21	3
	21.1-22.23	2
	22.23-22.5	3
	22.6-23.3	3
H2	23.4-25	3
	25.1-25.6	2
IS3	25.9-28	1
S3	28-28.15	2
	28.15-28.5	3
IS4	28.6-29	1
H3	29-30.9	3
IS5	31-31.3	2
	31.1-32.4	1
S5	32.6-32.9	3
IS6	33-33.5	1
S6	33.6-34	3
	34.1-34.5	2
IS7	34.6-35.4	1
S7	35.5-36	2
IS8	36.1-38	1
H4	38.1-39.2	3
H4	39.2-39-5	2
H4	39.5-40	3

Period	Age (Kyr)	Sediment category
IS9	40.3-40.5	1
S9	40.6-40.8	2
IS10	40.8-41.3	2
S10	41.5-41.9	3
IS11	41.9-42.3	1
S11	42.4-43	3

2.9 REFERENCES

Amaral-Zettler, L.A., McCliment, E.A., Ducklow, H.W., Huse, S.M., 2009. A method for studying protistan diversity using massively parallel sequencing of v9 hypervariable regions of small-subunit ribosomal rna genes. Plos One 4, 6372.

Andruleit, H.A., von Rad, U., Bruns, A., Ittekkot, V., 2000. Coccolithophore fluxes from sediment traps in the northeastern Arabian Sea off Pakistan. Mar Micropaleontol 38, 285-308.

Banakar, V.K., Mahesh, B.S., Burr, G., Chodankar, A.R., 2010. Climatology of the Eastern Arabian Sea during the last glacial cycle reconstructed from paired measurement of foraminiferal δ18O and Mg/Ca. Quaternary Research 73, 535-540.

Blackford, J.C., Burkill, P.H., 2002. Planktonic community structure and carbon cycling in the Arabian Sea as a result of monsoonal forcing: the application of a generic model. J Marine Syst 36, 239-267.

Bubeck, J.A., Pfitzner, A.J.P., 2005. Isolation and characterization of a new type of chlorovirus that infects an endosymblotic Chlorella strain of the heliozoon Acanthocystis turfacea. J Gen Virol 86, 2871-2877.

Burkill, P.H., Edwards, E.S., John, A.W.G., Sleigh, M.A., 1993. Microzooplankton and their herbivorous activity in the Northeastern Atlantic-Ocean. Deep-Sea Res Pt Ii 40, 479-493.

Caporaso, J.G., Kuczynski, J., Stombaugh, J., Bittinger, K., Bushman, F.D., Costello, E.K., Fierer, N., Pena, A.G., Goodrich, J.K., Gordon, J.I., Huttley, G.A., Kelley, S.T., Knights, D., Koenig, J.E., Ley, R.E., Lozupone, C.A., McDonald, D., Muegge, B.D., Pirrung, M., Reeder, J., Sevinsky, J.R., Tumbaugh, P.J., Walters, W.A., Widmann, J., Yatsunenko, T., Zaneveld, J., Knight, R., 2010. QIIME allows analysis of high-throughput community sequencing data. Nat Methods 7, 335-336.

Caporaso, J.G., Lauber, C.L., Walters, W.A., Berg-Lyons, D., Huntley, J., Fierer, N., Owens, S.M., Betley, J., Fraser, L., Bauer, M., Gormley, N., Gilbert, J.A., Smith, G., Knight, R., 2012. Ultra-high-throughput microbial community analysis on the Illumina HiSeq and MiSeq platforms. Isme J 6, 1621-1624.

Cavalier-Smith, T., 1991. Cell diversification in heterotrophic flagellates, in: Patterson, D.J., Larsen, J. (Ed.), The biology of free-living heterotrophic flagellates. Oxford University Press, Oxford, pp. 113-131.

Cavalier-Smith, T., 2002. The phagotrophic origin of eukaryotes and phylogenetic classification of protozoa. Int J Syst Evol Micr 52, 297-354.

Clarke, K.R., 1993. Non-parametric multivariate analyses of changes in community structure. Australian Journal of Ecology 18, 117-143.

Clift, P.D., Giosan, L., Carter, A., Garzanti, E., Galy, V., Tabrez, A.R., Pringle, M., Campbell, I.H., France-Lanord, C., Blusztajn, J., Allen, C., Alizai, A., Lückge, A., Danish, M., Rabbani, M.M., 2010. Monsoon control over erosion patterns in the Western Himalaya: possible feed-back into the tectonic evolution. Geological Society, London, Special Publications 342, 185-218.

Coats, D.W., 1999. Parasitic life styles of marine dinoflagellates. J Eukaryot Microbiol 46, 402-409.

Coolen, M.J.L., Orsi, W.D., Balkema, C., Quince, C., Harris, K., Sylva, S.P., Filipova-Marinova, M., Giosan, L., 2013. Evolution of the plankton paleome in the Black Sea from the Deglacial to Anthropocene. P Natl Acad Sci USA 110, 8609-8614.

Deplazes, G., Luckge, A., Stuut, J.B.W., Patzold, J., Kuhlmann, H., Husson, D., Fant, M., Haug, G.H., 2014. Weakening and strengthening of the Indian monsoon during Heinrich events and Dansgaard- Oeschger oscillations. Paleoceanography 29, 99-114.

Dufrene, M., Legendre, P., 1997. Species assemblages and indicator species: The need for a flexible asymmetrical approach. Ecol Monogr 67, 345-366.

Edgcomb, V., Orsi, W., Bunge, J., Jeon, S., Christen, R., Leslin, C., Holder, M., Taylor, G.T., Suarez, P., Varela, R., Epstein, S., 2011. Protistan microbial observatory in the Cariaco Basin, Caribbean. I. Pyrosequencing vs Sanger insights into species richness. Isme J 5, 1344-1356.

Fan, J.H., Cui, Y.B., Wan, M.X., Wang, W.L., Li, Y.G., 2014. Lipid accumulation and biosynthesis genes response of the oleaginous Chlorella pyrenoidosa under three nutrition stressors. Biotechnol Biofuels 7.

Fenchel, T., Finlay, B.J., 1994. The Evolution of life without Oxygen. Am Sci 82, 22-29.

Helm, K.P., Bindoff, N.L., Church, J.A., 2011. Observed decreases in oxygen content of the global ocean. Geophys Res Lett 38, 23602.

Hou, Y.B., Lin, S.J., 2009. Distinct gene number-genome size relationships for eukaryotes and non-eukaryotes: gene content estimation for dinoflagellate genomes. Plos One 4, 6978.

Inagaki, F., Okada, H., Tsapin, A.I., Nealson, K.H., 2005. Microbial survival - The paleome: A sedimentary genetic record of past microbial communities. Astrobiology 5, 141-153.

Jing, H., Rocke, E., Kong, L., Xia, X., Liu, H., Landry, M.R., 2015. Protist communities in a marine oxygen minimum zone off Costa Rica by 454 pyrosequencing. Biogeosciences Discuss. 2015, 13483-13509.

Keeling, R.F., Kortzinger, A., Gruber, N., 2010. Ocean deoxygenation in a warming world. Annu Rev Mar Sci 2, 199-229.

Kobashi, T., Severinghaus, J.P., Brook, E.J., Barnola, J.M., Grachev, A.M., 2007. Precise timing and characterization of abrupt climate change 8200 years ago from air trapped in polar ice. Quaternary Sci Rev 26, 1212-1222.

Lejzerowicz, F., Esling, P., Majewski, W., Szczucinski, W., Decelle, J., Obadia, C., Arbizu, P.M., Pawlowski, J., 2013. Ancient DNA complements microfossil record in deep-sea subsurface sediments. Biol Letters 9, 0283.

Lie, A.A.Y., Liu, Z.F., Hu, S.K., Jones, A.C., Kim, D.Y., Countway, P.D., Amaral-Zettler, L.A., Cary, S.C., Sherr, E.B., Sherr, B.F., Gast, R.J., Caron, D.A., 2014. Investigating microbial eukaryotic diversity from a global census: insights from a comparison of pyrotag and full-length sequences of 18s rRNA genes. Appl Environ Microb 80, 4363-4373.

Madhupratap, M., Kumar, S.P., Bhattathiri, P.M.A., Kumar, M.D., Raghukumar, S., Nair, K.K.C., Ramaiah, N., 1996. Mechanism of the biological response to winter cooling in the northeastern Arabian Sea. Nature 384, 549-552.

Morquecho, L., Lechuga-Deveze, C.H., 2003. Dinoflagellate cysts in recent sediments from Bahia Concepcion Gulf of California. Bot Mar 46, 132-141.

Oksanen, J., 2011. Multivariate analysis of ecological communities in R: vegan tutorial, R package version 1.17-7 ed.

Orsi, W.D., Coolen, M.J.L., Wuchter, C., He, L., More, K.D., Irigoien, X., Chust, G., Johnson, C., Hemingway, J.D., Lee, M., Galy, V., Giosan, L., 2017. Climate oscillations reflected within the microbiome of Arabian Sea sediments. Scientific Reports 7, 6040.

Paes, C.R.P.S., Faria, G.R., Tinoco, N.A.B., Castro, D.J.F.A., Barbarino, E., Lourenco, S.O., 2016. Growth, nutrient uptake and chemical composition of Chlorella sp and Nannochloropsis oculata under nitrogen starvation. Lat Am J Aquat Res 44, 275-292.

Parab, S.G., Matondkar, S.G.P., Gomes, H.D., Goes, J.I., 2006. Monsoon driven changes in phytoplankton populations in the eastern Arabian Sea as revealed by microscopy and HPLC pigment analysis. Cont Shelf Res 26, 2538-2558.

Plotnikov, A.O., Ermolenko, E.A., 2015. Centrohelid heliozoa (Chromista, Hacrobia) of Southern Cis-Ural region. Biol Bull+ 42, 683-695.

Pospelova, V., Pedersen, T.F., de Vernal, A., 2006. Dinoflagellate cysts as indicators of climatic and oceanographic changes during the past 40 kyr in the Santa Barbara Basin, southern California. Paleoceanography 21, PA2010.

Prauss, M.L., 2007. Availability of reduced nitrogen chemospecies in photic-zone waters as the ultimate cause for fossil prasinophyte prosperity. PALAIOS 22, 489.

Pruesse, E., Quast, C., Knittel, K., Fuchs, B.M., Ludwig, W.G., Peplies, J., Glockner, F.O., 2007. SILVA: a comprehensive online resource for quality checked and aligned ribosomal RNA sequence data compatible with ARB. Nucleic Acids Research 35, 7188-7196.

Roncaglia, L., Kuijpers, A., 2006. Revision of the palynofacies model of Tyson (1993) based on recent high-latitude sediments from the North Atlantic. Facies 52, 19-39.

Schulte, S., Muller, P.J., 2001. Variations of sea surface temperature and primary productivity during Heinrich and Dansgaard-Oeschger events in the northeastern Arabian Sea. Geo-Mar Lett 21, 168-175.

Schulz, H., von Rad, U., Erlenkeuser, H., von Rad, U., 1998. Correlation between Arabian Sea and Greenland climate oscillations of the past 110,000 years. Nature 393, 54-57.

Schulz, H., von Rad, U., Ittekkot, V., 2002. Planktic foraminifera, particle flux and oceanic productivity off Pakistan, NE Arabian Sea: modern analogues and application to the palaeoclimatic record. Geological Society, London, Special Publications 195, 499-516.

Schulz, H., Von Rad, U., Von Stackelberg, U., 1996. Laminated sediments from the oxygen-minimum zone of the northeastern Arabian Sea. Geological Society, London, Special Publications 116, 185-207.

Sherr, E.B., Sherr, B.F., 1994. Bacterivory and herbivory - key roles of phagotrophic protists in pelagic food webs. Microbial Ecol 28, 223-235.

Singh, A.D., Jung, S.J.A., Darling, K., Ganeshram, R., Ivanochko, T., Kroon, D., 2011. Productivity collapses in the Arabian Sea during glacial cold phases. Paleoceanography 26, PA3210.

Steineck, P.L., Casey, R.E., 1990. Ecology and paleobiology of formainifera and radiolaria: Capriulo, G.M. (Ed.), Ecology of Marine Protozoa. Oxford University Press, Oxford.

Strom, S.L., Welschmeyer, N.A., 1991. Pigment-specific rates of phytoplankton growth and microzooplankton grazing in the open sub-arctic Pacific ocean. Limnol Oceanogr 36, 50-63.

von Rad, U., Schulz, H., Khan, A.A., Ansari, M., Berner, U., Cepek, P., Cowie, G., Dietrich, P., Erlenkeuser, H., Geyh, M., Jennerjahn, T., Luckge, A., Marchig, V., Riech, V., Rosch, H., Schafer, P., Schulte, S., Sirocko, F., Tahir, M., Weiss, W., 1995. Sampling the oxygen minimum zone off Pakistan - glacial interglacial variations of anoxia and productivity (preliminary-results, Sonne-90 cruise). Marine Geology 125, 7-19.

von Rad, U., Schulz, H., Riech, V., den Dulk, M., Berner, U., Sirocko, F., 1999. Multiple monsoon-controlled breakdown of oxygen-minimum conditions during the past 30,000 years documented in laminated sediments off Pakistan. Palaeogeography, Palaeoclimatology, Palaeoecology 152, 129-161.

Wasmund N., Kownacka J., Gobel J., Jaanus A., Johansen M., Jurgensone I., Lehtinen S., Powilleit M. 2017. The Diatom/Dinoflagellate index as an indicator of ecosystem changes in the Baltic sea1. Principle and handling instruction. Frontiers in Marine Science, 4, 22.

Worden, A.Z., Follows, M.J., Giovannoni, S.J., Wilken, S., Zimmerman, A.E., Keeling, P.J., 2015. Rethinking the marine carbon cycle: Factoring in the multifarious lifestyles of microbes. Science 347, 1257594.

Wright, J.J., Konwar, K.M., Hallam, S.J., 2012. Microbial ecology of expanding oxygen minimum zones. Nat Rev Microbiol 10, 381-394.

Ziegler, M., Jilbert, T., de Lange, G.J., Lourens, L.J., Reichart, G.J., 2008. Bromine counts from XRF scanning as an estimate of the marine organic carbon content of sediment cores. Geochem Geophy Geosy 9, Q05009.

CHAPTER 3

Holocene paleodepositional changes reflected in the sedimentary microbiome of the Black Sea

Kuldeep D. More, Liviu Giosan, Kliti Grice and Marco Coolen

Geobiology. https://doi.org/10.1111/gbi.12338.

3.1 ABSTRACT

Subsurface microbial communities are generally thought to be structured through *in situ* environmental conditions such as the availability of electron acceptors and donors and porosity, but recent studies suggest that the vertical distribution of a subset of subseafloor microbial taxa, which were present at the time of deposition, were selected by the paleo-depositional environment. However, additional highly resolved temporal records of subsurface microbiomes and paired paleoenvironmental reconstructions are needed to justify this claim. Here we performed a highly resolved shotgun metagenomics survey to study the taxonomic and functional diversity of the subsurface microbiome in Holocene sediments underlying the permanently stratified and anoxic Black Sea. Obligate aerobic bacteria made the largest contribution to the observed shifts in microbial communities associated with known Holocene climate stages and transitions. This suggests that the aerobic fraction of the subseafloor microbiome was seeded from the water column and did not undergo postdepositional selection. In contrast, obligate and facultative anaerobic bacteria showed the most significant response to the establishment of modern-day environmental conditions 5.2 ka ago that led to a major shift in planktonic communities and in the type of sequestered organic matter available for microbial degradation. No significant shift in the subseafloor microbiome was observed as a result of environmental changes that occurred shortly after the marine reconnection, 9 ka ago. This supports the general view that the marine reconnection was a gradual process. We conclude that a high-resolution analysis of downcore changes in the subseafloor microbiome can provide detailed insights into paleoenvironmental conditions and biogeochemical processes that occurred at the time of deposition.

3.2 INTRODUCTION

The subseafloor marine biosphere is estimated to harbor more than 10^{29} microbial cells, approximately equal to the number of open Ocean and soil microbiota (Kallmeyer, Pockalny et al. 2012). These sedimentary microbial communities mediate the carbon storage and contribute heavily to nitrogen and sulfur cycling (Orcutt, Sylvan et al. 2011). Such deep sub-surface microbial communities owe their genetic distinctness to selection faced after isolation from surface waters over long timescales (Starnawski, Bataillon et al. 2017). Subsurface microbial communities are generally thought to be structured through *in situ* environmental conditions such as the availability of electron acceptors and donors, porosity and sediment lithology (Parkes, Cragg et al. 2000, Rebata-Landa and Santamarina 2006, Kallmeyer, Pockalny et al. 2012, Orsi, Coolen et al. 2017). However, recent studies suggest that a subset of subseafloor microbial taxa were present at the time of deposition (Inagaki et al., 2015; Orsi et al., 2017) and form a genetic archive originally referred to as "the Paleome" (Inagaki, Okada et al. 2005). The paleoenvironmental conditions that prevailed at the time of deposition are partly reflected by concomitant shifts in the taxonomic and functional diversity of the subsurface microbial paleome (Inagaki, Hinrichs et al. 2015, Orsi, Coolen et al. 2017). For example, microbial life in 20 Ma-old coal-bearing sediments located up to 2.5 km below the ocean floor was found to resemble organotrophic bacterial communities typically found in forest soils (Inagaki, Hinrichs et al. 2015). Similarly, microbial communities likely of terrestrial origin were recovered from Mediterranean turbidites (Ciobanu, Rabineau et al. 2012). Downcore changes in microbial communities in radiocarbon-dated Baltic Sea sediments were shown to mirror temporal changes in sea surface salinity (Lyra, Sinkko et al. 2013). Most recently, highly resolved shotgun metagenomic profiling of north-eastern Arabian Sea sediments showed that up to 15% of the subsurface microbiome was explained by variations in past oxygen minimum zone (OMZ) strength over the last glacial-interglacial cycle (Orsi, Coolen et al. 2017). More specifically, the genomic potential for denitrification correlated with (isotopic) geochemical paleo-OMZ proxies independent of sediment depth and availability of nitrate and nitrite. The metagenomes also revealed fermentation pathways encoded by many of the same denitrifier groups indicating that fermentation could explain their long-term post-depositional survival. Thus, subsistence of bacteria that were seeded from the overlying water column may provide a mechanism for subseafloor microorganisms to provide a much longer genomic record of paleoenvironmental changes than sedimentary DNA from photic zone derived dead eukaryotic plankton, which is likely to be more prone to post-depositional degradation. However, additional highly resolved

temporal records of subsurface microbiomes and paired paleoenvironmental conditions are needed to justify this claim.

The Black Sea is the world's largest permanently stratified anoxic basin. Organic matter including DNA stemming from past plankton species has been shown to be well preserved in the underlying sediments. The pool of preserved plankton DNA forms a long-term archive of past ecosystem dynamics (Coolen, Orsi et al. 2013) resulting from known changes in past continental climate and concurrent hydrological changes in the basin (Ross, Degens et al. 1970, Major, Goldstein et al. 2006, Marret, Mudie et al. 2009, Soulet, Delaygue et al. 2010). For example, sedimentary ancient DNA recorded a major shift in the plankton composition to brackish taxa at 9 ka BP due to the postglacial reconnection of the lacustrine Black Sea with the Mediterranean Sea through the Bosphorus Strait. This timing agrees with strontium isotopic records (Major, Goldstein et al. 2006). In addition, sedimentary ancient DNA revealed the arrival of marine copepods at the onset of the dry Subboreal at ~5.2 ka BP, which marked the timing of the establishment of modern environmental conditions (Coolen et al., 2013). Most notably, this community comprised of the only marine calanoid copepod found in the Black Sea today: *Calanus euxinus* which has a minimum salinity tolerance of 17 ppt (Svetlichny, Hubareva et al. 2010). Paired deuterium isotopic analysis of *Emiliania huxleyi*-derived long chain alkenones also suggested that the sea surface salinity remained above the modern day 18 ppt since the last 5.2 kyrs (Coolen, Orsi et al. 2013).

Considering that the Black Sea's plankton paleome accurately reflected these paleoenvironmental changes, it is to be expected that a subset of the sedimentary microbial communities may also be seeded from the overlying water column and to mirror the variability of the paleodepositional conditions in the Black Sea. In order to test this hypothesis, we performed a metagenomic profiling of taxonomic and functional diversity of the subsurface bacteria in flash frozen intervals of the radiocarbon dated core GGC18. These intervals have been previously analysed for the above described ecosystem and environmental changes during key climate stages since the past 13,500 calendar years (Coolen, Saenz et al. 2009).

3.3 MATERIAL AND METHODS

3.3.1 Sampling

The sedimentary metagenomic and geochemical datasets presented in this study were generated from the upper 341 cm of Giant Gravity Core GGC18 (Coolen, Saenz et al. 2009, Coolen, Orsi et al. 2013). Briefly, GGC18 was recovered from a water depth of 971m in the

western basin of the Black Sea (42˚46.569”N:28˚40.647”E) during cruise AK06 on the R/V *Akademik* (Institute of Oceanology, Bulgarian Academy of Sciences; IOBAS) in September 2006. The obtained core was immediately split in half and subsamples were obtained aseptically at 1 cm resolution using sterile headless syringes. To prevent cross contamination, the upper 1 cm of exposed sediments was first scraped off with sterilized knives. Samples for DNA extraction were stored in liquid nitrogen during the cruise and shipped on dry ice to the Woods Hole Oceanographic Institution (WHOI). The remaining sampled and archived core halves were shipped refrigerated to WHOI and were used for organic and isotopic geochemical analysis. See Coolen et al. (2009) for more details.

3.3.2 Organic geochemistry

The weighted percentage of total organic carbon (TOC) was determined on acidified samples according to Eglinton et al. (2002) using a Carlo Erba EA 1108 elemental analyzer interfaced via a Finnigan-MAT Conflo-II open split device to a DeltaPlus isotope ratio monitoring mass spectrometer. Total lipids were extracted from ~ 2 g dry weight sediment by Accelerated Solvent Extraction (ASE) using 9:1 dichloromethane/methanol (100 °C, 1000 psi) and the neutral components including alkenones were further extracted as described in detail in Coolen et al. (2009). Alkenones were then analysed with GC-FID on a Hewlett Packard 5890 using a CPSil5-CB column (Chrompack, 30 m × 0.32 mm I.D.). Sedimentary alkenone δD as a proxy for salinity in the Black Sea (Van der Meer et al., 2008), was measured using an Agilent 6890 GC equipped with a DB-5MS column (60m length; 250 µm i.d.; 0.25µm film thickness; J&W, Folsom, CA, USA) coupled to a Delta^{Plus} XL (Bremen, Germany) isotope ratio mass spectrometer via a pyrolysis interface operated at 1440^{o}C (Burgoyne and Hayes 1998). The GC oven was initially set at 90^{o}C, held for 1 min, ramped at 15^{o}C min^{-1} to 220^{o}C, and finally ramped at 10^{o}C min^{-1} to 320^{o}C and held for 40 min. The H_3^+ factor was determined daily and was always below 5.1 ppm mV^{-1} (Sessions, Burgoyne et al. 2001). A suite of 16 normal alkanes was routinely analyzed to determine the normalization scale (Sessions et al., 2001) and to estimate instrument accuracy. The alkenones (an average of 37:2 and 37:3 due to chromatographic coelution) were compared to coinjected alkanes of known isotopic composition. All δD values are reported relative to V-SMOW in permil (‰) units and are normalized to the SMOW-SLAP scale. The precision of replicate analyses expressed as the pooled-standard-deviation was 2.9 ‰ for these data. The accuracy based on 14 external analyses of the suite of normal alkanes was 2.9 ‰.

3.3.3 Age model

Thirteen one cm intervals were selected from the marine section of the core (<9 ka BP) for ^{14}C AMS dating of bulk organic carbon at the National Ocean Sciences Accelerator Mass Spectrometry (NOSAMS) Facility at WHOI. A detrital carbon correction of 580 years (Jones and Gagnon 1994, Coolen, Saenz et al. 2009) was applied to our radiocarbon dates (Coolen et al., 2009). An age model for the core was then developed by calibrating the corrected radiocarbon dates to calendar years B.P. with Calib 5.0.1 (Stuiver and Reimer 1993) using INTCAL04 (Reimer, Baillie et al. 2004). Sedimentation rates in the marine interval are low, and hence, interpolation between the calibrated radiocarbon dates corresponding to these depths was used to derive age of each sample from that section of the core (Giosan et al., 2012). The age model was extended into the deglacial with two dates on micro-gastropod shells. These radiocarbon dates were calibrated using the marine reservoir age based on the latest information that between 8000 and 11,500 years BP the Black Sea-Lake reservoir age was between 300 and 500 years (Soulet et al., 2011). See Coolen et al., 2009; 2013; and Giosan et al., 2012 for further details.

3.3.4 Sedimentary DNA extraction and sequencing

For this study, total DNA was extracted from 8-10 gram of wet weight sediment from the 19 one cm intervals using the PowerMax™ Soil DNA Isolation Kit (Mobio, Carlsbad, CA) in the clean lab dedicated to ancient DNA analysis at WHOI (Coolen, Saenz et al. 2009) (Table 3.1). As a control for contamination during DNA extraction, one reagent mixture without sediment was subjected to the entire extraction and purification procedure (extraction control). Co-extracted PCR-inhibiting substances such as humic acids were efficiently removed using the OneStep PCR Inhibitor Removal Kit (Zymo Research, Irvine, CA, USA). See Coolen et al (2009) for further details.

3.3.5 Metagenome preparation

19 samples spanning 13.5 Ka of deposition were selected for metagenomic library preparations. Metagenomic libraries were prepared with 50 ng template DNA using the NEBNext® Ultra™ II DNA Library Prep Kit for Illumina® (New England BioLabs Inc.) according to manufacturer's instructions. The amplification involved 13-15 cycles. The resulting barcoded libraries (200-500 bp) were gel purified with the Monarch DNA Gel Extraction Kit (New England BioLabs Inc) and sent to the Australian Genomic Research Facility (AGRF) in Perth for final quality control and sequencing. At AGRF, the Illumina HiSeq2500 platform was used to generate 2 × 100-bp pair-end sequencing reads.

3.3.6 Processing of sequence data and bioinformatics

Approximately 200 million paired-end sequence reads were processed in CLC Genomics Workbench 7.0 (Qiagen, Hilden, Germany) which involved quality control using standard settings and de Novo paired-end assembly (Contig length = 200, Mismatch cost = 2, Insertion cost = 3, Deletion cost = 3). Assembled sequences were submitted to the MG-RAST server 4.0.3 (Meyer et al., 2008) for automated high-quality annotation of microbial reads in the metagenome using the SEED database (Overbeek et al., 2014). Only hits to reference proteins with at least 50% amino acid similarity over an alignment length of more than 50 amino acids were considered to be homologs and used for downstream analysis. Metagenomes were also prepared without the addition of template and from an extraction blank and were sequenced and analysed in parallel to the samples. Open reading frames (ORFs) that occurred in both samples and these controls for contamination were removed. Ecological statistics were calculated in R using a Bray Curtis distance in the Vegan package (https://cran.r-project.org/web/packages/vegan/index.html). Analysis of Similarity (ANOSIM) was carried out using 999 permutations using Bray Curtis dissimilarity. Indicator Species Analysis (ISA) (Dufrene & Legendre, 1997) was performed in the indicspecies package and significance was tested with a nonparametric procedure involving the Monte-Carlo permutation procedure with 999 permutations.

3.4 RESULTS

3.4.1 Downcore microbial distributions

After stringent removal of ORFs that also occurred in the sequenced controls, the metagenomic libraries of the sampled sediment intervals revealed 189 bacterial genera. Based on known metabolic properties of cultivated relatives (Whitman, 2015), the identified microbial populations were grouped into aerobes (71 genera), anaerobes (71 genera), facultative anaerobes (29 genera) and unknown mode of respiration (18 genera). Facultative anaerobes comprised 10-25% of the microbial populations throughout the core except for the youngest sample where they comprised half of the total bacteria (Fig. 3.1). Obligate anaerobes comprised up to 75% of total bacteria in sediments deposited before late HCO (>6 ka BP) after which obligate aerobes were found to dominate over anaerobes (Fig. 3.1 c).

3.4.2 Distribution of aerobes

Aerobes were further divided into photoautotrophs, those potentially involved in sulfur cycling and other chemo-organotrophs (Fig. 3.1d). Aerobic photoautotrophs showed highest

relative abundance (15-50% of total aerobic bacteria) in sediments deposited during the warmer deglacial and early Holocene climate stages (Allerød, Preboreal and HCO) and comprised up to 10% of aerobes in sediments younger than ~6 Kyr (Fig. 3.1d). Unicellular pelagic cyanobacteria (*Cyanothece, Prochlorococcus, Microcystis, Acacyochloris* and to a lesser extent *Cyanobium* and *Raphidiopsis*) comprised 60-75% of the aerobic photo-autotrophic community until the HCO-Subboreal transition. (Fig. 3.2a). Since the last 5.2 ka BP (e.g. spanning the Subboreal and Subatlantic), marine anoxygenic phototrophs (*Congregibacter, Dinoroseobacter*, and *Erythrobacter*) predominated over cyanobacteria (Fig. 3.2a).

Aerobic bacteria involved in sulfur cycling comprised up to 25 to 50 % of total aerobes during early and mid YD and up to 60% of total aerobes since 6 ka BP (Fig. 3.1d) The S oxidizer *Thiomicrospira* predominated this category with lower contributions of *Arcobacter, Sulfitobacter* and *Sulphurosprilillum* (Fig. 3.2b). Other aerobic chemoorganotrophs reads varied between 25 and 75% of total aerobic bacteria throughout the core. *Blastopirellula* represented a dominant chemo-organotrophic genus in all sediments deposited before the Subboreal (>5.2 Ka BP) where it co-occurred with the less abundant *Alkaliphilus*. In Subboreal and Subatlantic sediments, *Hyphomonas* along with *Sachharophagus*, *Cellvibrio* and putative manganese oxidizers (*Aurantimonas, Geodermatophilus* and *Fulvimarina*) predominated the chemo-organotrophic aerobic community (Fig. 3.2c). Other less abundant chemo-organotrophs such as *Bermanella* and *Idiomarina* maintained sporadic abundance throughout the core (Fig. 3.2c).

3.4.3 Distribution of anaerobic and facultative microbial communities

Anaerobes were divided into three groups - those involved in sulfur cycling, autotrophs and other chemoorganotrophs (Fig. 3.1e). Unlike aerobic bacteria, the relative abundance of these major groups did not vary much with sediment depth and age. Autotrophic anaerobes comprised 15% of the total anaerobic bacterial reads in the youngest analysed interval and less than 5% throughout the rest of the core. Chemo-organotrophs and anaerobes involved in sulfur cycling were equally abundant throughout the core. (Fig. 3.1e). Within the latter group, members of the sulfate-reducing genera *Desulfatibacillum, Desulfococcus*, and *Desulfatobacterium* predominated until late HCO after which *sulfur oxidising bacteria (Beggiatoa* and *Sulfurovum)* became more abundant (Fig. 3.3a). Less predominant sulfate reducing bacteria, which occurred in the majority of samples, involved *Desulfurivibrio*, *Dethiosulfovibrio*, *Desulfomicrobium, Desulfohalobium* and *Thermanaerovibrio* (Fig. 3.3a).

The next most abundant anaerobes represented chemo-organotrophs (Fig. 3.1e). The anaerobic chemoorganic community composition remained fairly constant until the late HCO and comprised of many genera such as saccharolytic *Alkaliphilus*, *Caldicellulosiruptor*, and syntrophic *Syntrophomonas* and *Syntrophothermus* (Fig. 3.3b). This composition changed drastically with the onset of the Subboreal at 5.2 ka BP with more contribution from *Puniceispirillum*, *Oceanicaulis* and nitrate reducing genera such as *Denitrivibrio*. Other genera (e.g. *Turicibacter, Trackia, Selenomas*) combined contributed up to 40 % of chemo-organotrophs in the majority of intervals (Fig. 3.3b). Autotrophic anaerobes were minor constituents of the total anaerobic community (Fig. 3.1e), but nevertheless revealed a shift in relative abundance at 5.2 ka BP from *Oscillochloris* to *Nitratiruptor* (Fig. 3.3c). *Planctomyces* and *Lactobacillus* were the most abundant facultative bacteria in sediments older than 5.2 ka BP after which *Kangiella* became more abundant (Fig. 3.3d). The sulfur oxidizing genera *Sulfurimonas* and *Sulfuricurvum* were abundant in the youngest analysed interval (Fig. 3.3d).

3.4.4 Metabolic functions

Functional metagenomic analysis revealed five major types of microbial energy metabolisms throughout the core (Fig. 3.1f). Glycolysis and fermentation contributed 50-60% of total energy yielding processes in all analysed intervals throughout the core. Methane metabolism was the second most dominant process in sediments older than 5.2 ka where it accounted for more than 25 to 40% of total metabolic processes. In contrast, nitrogen and sulfur metabolism combined accounted for respectively 25 to 40%% of the total energy metabolic processes in sediments younger than 5.2 ka. Dark carbon fixation accounted for 5-10% of total energy metabolism throughout the core.

3.4.5 Correlation between the paleodepositional environment and microbial communities

Changes in the subsurface microbial community composition associated with climate-triggered changes in the paleodepositional environment were investigated using Non-Metric Multidimensional Scaling Analysis (NMDS) and Analysis of Similarity (ANOSIM) (Clarke, 1993). It was analyzed whether significant changes occurred in the community structure between total bacteria, aerobes, anaerobes and facultative bacteria before and after the establishment of modern-day salinity at 5.2 ka (Category A); between known climate stages in the Black Sea (Category B); and before and after the marine reconnection at ~ 9 ka (Category C) (Fig. 3.4). NMDS (stress < 0.05) revealed that anaerobic bacteria showed the best correlation (ANOSIM; R=0.98; P=0.001) to Category A, significant but weak community

changes associated with Category B (R=0.28; P=0.009), and no significant response to Category C (R=0.026; P=0.26). The same pattern was also observed for facultative microbial communities. Aerobic communities revealed a significant response to categories A and B but not to Category C.

Total bacterial communities responded most significantly to depositional changes after the establishment of modern-day salinity (ANOSIM; R=0.88; P=0.001), (Fig. 3.4). NMDS and ANOSIM analysis using energy metabolism ORFs only showed the most significant response to Category A (R=0.8; P=0.001) followed by Category B (R=0.4, P=0.008) and the weakest response to Category C (R=0.181, P=0.05).

3.4.6 Indicator species analysis (ISA)

Since microbial communities were mostly affected by depositional changes before and after the establishment of modern-day salinity, ISA was only performed for Category A. In Category A, ISA based on the entire bacterial population (189 genera) revealed respectively 50 and 101 genera indicative for sediments younger vs. older than 5.2 ka BP (Table 3.2 and 3.3). *Kangiella, Hyphomonas, Puniceispirillum* and *Endoriftia* were the best indicator genera for sediments < 5.2 ka (subatlantic-subboreal period) with A>0.75. Marine aerobic bacteria were also among the strong indicators for < 5.2 ka of Category A, notably aerobic *Loktanella* (A=0.695 and B=1.000), known to be associated with the outbreak of harmful algal blooms (Bloh et al., 2016) as well as aerobic anoxygenic phototrophic bacteria such as *Erythrobacter, Congregibacter* and *Dinoroseobacter*. Other aerobic indicator taxa for sediments < 5.2 ka in Category A involved *Saccharophagus, Granulibacter, Maricaulis* and *Psychrobacter*. Best indicator genera for sediments >5.2 ka BP included *Pseudoramibacter*, syntrophic bacteria (*Syntrophomonas* and *Syntrophothermus*), anaerobic S-reducing genera such as *Dethiobacter, Dethiosulfovibrio, Desulfatibacillum, Desulfococcus, Desulfohalobium*, and *Desulfobacterium*. Anaerobic autotrophs *Methylacidiphilum* and *Oscillochloris* along with aerobic cyanobacteria *Acarychloris, Cyanobium, Cyanothece, Microcystis* and *Prochlorococcus* were also significant indicators of this group.

3.5 DISCUSSION

3.5.1 Putative indigenous vs. seeded subsurface microbial communities

The sediments underlying the permanently anoxic and sulfidic bottom waters of the Black Sea are expected to provide conditions that only favor facultative and obligate anaerobic microbial communities. It was observed that obligate and facultative anaerobic microbial

communities showed the most significant groupings before and after 5.2 ka (resp. R=0.98 and 0.91) (Fig. 3.4). The timing of this change in salinity was previously shown to have coincided with a major transition in the pelagic plankton community structure as the source of the sedimentary organic matter (Coolen et al., 2013). This would explain the concomitant shift in the diversity of the anaerobic bacterial communities, which are likely to be actively metabolizing the sedimentary organic matter as is further supported by the simultaneous shift in predominant energy metabolisms. Therefore, the indigenous anaerobic populations revealed an indirect response to environmental changes in the Black Sea.

In contrast, obligate aerobic communities are likely to be seeded from the oxygenated surface waters in the past (Orsi et al., 2017) and no longer to be metabolically active in the sediments. As a result, they are more likely to reveal a direct response to paleoenvironmental changes, such as the case for the observed shift in the predominance from photic-zone derived cyanobacteria to AAnPs after the establishment of a stable sulfidic chemocline. Furthermore, while anaerobic bacteria (R=0.98; P=0.001) contributed more to the total bacterial response (R=0.88; P=0.001) than aerobic bacteria (R=0.56; P=0.002) to the changes in organic matter sources before and after 5.2 ka BP, aerobic bacteria (R=0.32; P=0.019) contributed more to the response of total bacteria (R=0.37; P=0.011) than anaerobic bacteria (R=0.28; P=0.009) to the key climate stages and their transitions since the deglacial (Fig. 3.4). Bacterial communities showed no significant response to the marine reconnection at 9 ka BP (Fig. 3.4). This finding adds to the growing body of evidence that environmental conditions only changed gradually after the marine reconnection (Marret et al., 2009) with ample time for microbial communities to adapt.

3.5.2 Anaerobic communities and their putative functions

The most abundant anaerobic bacteria in sediments older than 5.2 ka BP include *Alkaliphilus, Heliobacterium, Caldicellulosiruptor*, and *Thermoanaerobacter* (Fig. 3.3b). *Alkaliphilus* was initially isolated from mine water containment dam at 3.2 km below ground in an ultra-deep gold mine in South Africa (Takai et al., 2001). Several *Alkaliphilus* spp. were shown to ferment organic compounds including proteinaceous substances and their growth was promoted in the presence of elemental sulfur or thiosulphate (Takai et al., 2001), which would explain their ability to thrive in the organic and sulfidic sediments of the Black Sea. *Heliobacterium* is a strictly anaerobic photoheterotrophic firmicute that can also grow in the absence of light by fermentation of pyruvate (Tang et al., 2010). *Caldicellulosiruptor* is cellulolytic and xylolytic (Huang et al., 1998) while *Thermoaenerobacter* is saccharolytic (Xue et al., 2001). In the same

sediment section, facultative *Spirochaeta* and *Planctomycetes* also dominated (Fig. 3.3d), both of which have been isolated from aquatic sediments and are known to degrade carbohydrates (Subhash & Lee, 2017; Jasmin et al., 2017). Syntrophic bacteria (*Syntrophomonas* and *Syntrophothermus*) were also abundant (Fig. 3.3b). Syntrophic bacteria are evolutionarily adapted for syntrophic growth with methanogens and other hydrogen-consuming microorganisms. *Syntrophomonas* has been found in co-culture with sulfate-reducing, non-fatty acid degrading bacteria like *Desulfovibrio* (Mcinerney et al., 1981). In the Black Sea sediments, syntrophic growth may exist between *Syntrophomonas*-*Syntrophothermus* and *Dethiosulfovibrio*. This sulfate reducer ferments peptides to isobutyrate and methylbutyrate, which are known substrates for *Syntrophomonas* as well as *Syntrophothermus*. Butyryl-CoA dehydrogenase plays a key role in this process. Both genera were the source of an ORF encoding this enzyme in this section of the core. These bacterial genera were the source of ORFs encoding for butyryl and hydroxybutyryl CoA dehydrogenases respectively, which play a key role in this process (Fig. 3.6).

In sediments younger than 5.2 ka BP, *Puniceispirillum* was a predominant anaerobe (Fig. 3.3b). The only known species in this genus has been shown to possess genes for metabolism of C1 compounds such as methanol, formaldehyde, formate, formamide, and methanesulfonate along with genes for Entner-Doudoroff pathway used for Glucose metabolism (Oh et al. 2010). Facultative *Kangiella* with proteolytic metabolism was also dominant in this section of the core. This interval also revealed a relatively high abundance of ORFs derived from nitrate reducing *Denitrivibrio* and *Nitratiruptor* (Fig. 3.3c). Molecular hydrogen produced by syntrophic bacteria may be used by *Nitratiruptor* to reduce nitrate with H2 to molecular nitrogen (Nakagawa et al., 2005). Acetate and fumarate produced by chemoorganotrophy may be used by *Denitrivibrio* spp., which reduces nitrate to ammonia (Myhr & Torsvik, 2000). ORFs encoding periplasmic nitrate reductase and nitrate reductase from both species were found in the functional metagenomes in sediments younger than 5.2 ka (Fig. 3.6). The verrucomicrobial methanotroph *Methylacidiphilum* is capable of using both dark carbon fixation and nitrogen fixation and can store glycogen as a reserved energy store when carbon is in excess and nitrogen supply is limited (Khadem et al., 2012).

The metagenomic survey implies that anaerobic chemo-organotrophy is an important ongoing degradation process in the Holocene Black Sea sediments spanning the entire analyzed record. However, genes involved in methane metabolism predominated in sediments older than 5.2 ka BP (before the subboreal), while both nitrogen and sulfur metabolisms increased in relative abundance after 5.2 ka BP. These observation imply that

this depth marks the sulfate-methane transition zone (SMTZ) and that the concomitant shift in these microbial communities indirectly reflects paleoenvironmental changes that caused a shift in past plankton communities (Coolen et al., 2013) and thus changes in organic matter input that coincided with the establishment of modern environmental conditions (Coolen et al., 2013).

3.5.3 Pelagic phototrophic bacteria

The relative abundance of pelagic unicellular cyanobacteria (*Prochlorococcus, Microcystis*, and *Cyanothece*) was highest among the total phototrophic bacteria in sediments older than 5.2 ka BP (Fig. 3.2a) when sea surface salinity was lower than in the Black Sea today (Coolen et al., 2013). They represent past photic zone dwelling photosynthetic communities since they are unlikely to currently thrive in the dark, anoxic sediments below. Namely, only low irradiance-adapted strains of *Prochlorococcus* have been shown to assimilate glucose, but only in the presence of oxygen (Gomez-Baena et al., 2008). *Microcystis* are nitrogen-fixing cyanobacteria found to form blooms in eutrophic (P and N-rich) freshwater environments and have also been reported to form blooms near river deltas in coastal waters (Atkins et al., 2001). *Microcystis* can also ferment glycogen under anoxic dark conditions (Moezelaar & Stal, 1997; Vanderoost et al., 1989). *Cyanothece* are marine nitrogen-fixing cyanobacteria, which are also capable of fermenting sugars anaerobically in the dark (van der Oost et al., 1989). However, if cyanobacterial anaerobic fermentation was an active ongoing sedimentary process, one would expect an increase in their relative abundance after 5.2 ka BP since younger sediments should have a higher content of easily degradable organic matter. Instead their higher relative abundances in the older sediments suggests that they were derived from the past photic zone and less capable to adapt in the Black Sea after salinity increased to modern levels or higher. The presence of cyanobacteria as main nitrogen-fixing phytoplankton in the Black sea during early to mid-Holocene has been also postulated based on $\delta^{15}N$ signals (Fulton et al., 2012).

After 5.2 ka BP, aerobic anoxygenic phototrophs (AAnP) *Congregibacter*, *Dinoroseobacter* and *Erythrobacter* became the most abundant aerobic phototrophic taxa (Fig. 3.2a). AAnP are photoheterotrophs that need oxygen for respiration and use their photosynthetic apparatus to generate energy in order to survive starvation when light is available (Hanada et al., 2016). *Erythrobacter* was the first AAnP to be discovered (Shiba & Simidu, 1982) and species of this genus are known to oxidize thiosulfate to tetrathionate in presence of an organic carbon source and oxygen. None of the *Erythrobacter* species were shown to be able

to use nitrate as an electron acceptor and are unable to live in anaerobic conditions (Okamura et al., 1985). *Dinoroseobacter* is capable of reducing nitrate and was isolated from marine dinoflagellates as an endosymbiont. Anaerobic growth is not observed, either on acetate in the light or by fermentation of glucose in the dark (Biebl et al., 2005). *Congregibacter* has recently been discovered and is a potential sulfur oxidizer based on the presence of sulfur-oxidizing (SoX) genes and has not been shown to survive under anaerobic conditions (Spring, 2014). AAnPs contain bacteriochlorophyll a (Bchl a) and typically occur at the oxic/anoxic interface of the upper sulfidic chemocline where both oxygen required for respiration and light for anoxic photosynthesis is available (Blankenship et al., 1995). The total amount of Bacteriochlorophyll in the sulfidic part of the photic chemocline of the modern Black Sea surpasses the amount of planktonic Chlorophyll a in the oxygenated surface waters (Repeta & Simpson, 1991). Anoxygenic photosynthesis, however, has been attributed to green sulfur bacteria (GSB) (Repeta et al., 1989) in spite of their low abundance in the deep sulfidic chemocline (Overmann & Manske, 2006). However, our sedimentary metagenome profiling suggests that the biomass of AAnPs may have exceeded that of GSB and that they possibly contributed substantially to anoxygenic photosynthesis in the stratified Black Sea especially since the last ~5200 years.

3.5.4 Bacteria involved in sulfur cycling

In the current Black Sea, microbial cycling of sulfur takes place at depths at and below the sulfidic chemocline (~100 m) (Neretin et al., 2006) (Pimenov & Neretin, 2006). In this core, ORFs of both aerobic and anaerobic bacteria involved in sulfur cycling were found (Fig. 3.2 and 3.3). Aerobes involved in S cycling were present in all analysed intervals since the marine reconnection and were especially abundant since the last ~6 Ka BP. The aerobic S-oxidizing genera *Thiomicrospira* was most abundant, followed by *Arcobacter* and *Sulfitobacter* (Fig. 3.2b). Previous 16S rRNA gene profiling revealed that *Thiomicrospira* is abundant at the oxic/anoxic interface of sulfidic chemocline in the modern Black Sea (Vetriani et al., 2003). The predominance of *Thiomicrospira* as along with the above discussed AAnPs suggests the presence of permanent stratified conditions and a persistent sulfidic chemocline after ~ 6 Kcal BP. *Thiomicrospira* also dominated the aerobic bacterial fraction in the sediments deposited during the dry YD (Fig. 3.2b). At this time bottom waters were most likely oxygenated, while *Thiomicrospira* could have been part of a microbial mat overlying anaerobic sediments (Brinkhoff and Muyzer 1997). An increasing abundance of obligate aerobic *Aurantimonas, Geodermatophilus* and *Fulvimarina* was also observed in sediments younger than 5.2 ka (Fig. 3.2c). Species of these genera are known to oxidise Mn(II) to Mn(III)

(Anderson et al., 2009; Kang et al., 2010), which most likely took place in the upper boundaries of the suboxic zone, where manganese concentrations are found to be elevated in the modern Black Sea (Murray et al., 1999). Mn (III) has high oxidizing potential. According to the latter study, this microbially produced Mn (III) led to sulfide oxidation and sedimentary DNA of aerobic bacteria directly and indirectly involved in S-cycling was derived from cells that were seeded from the past water column (Orsi et al., 2017).

Sulfate reducing bacteria (SRB) were the most abundant anaerobes throughout the core (Fig. 3.3a). *Desulfatibacillum, Thermosipho* and *Thermanaerovibrio* reduce elemental sulfur. *Desulfococcus, Desulfotalea, Desulfomicrobium* and *Desulphohalobium* reduce sulfate and *Dethiosulfovibrio* reduces thiosulphate to H_2S. These SRB most likely represent indigenous and active sedimentary populations since their overall relative abundance did not vary substantially throughout the analysed record. This would explain why the highest concentrations of H_2S is being observed in the surface sediments (Pimenov & Neretin, 2006). The sedimentary metagenomes revealed the presence of genes encoding for sulphate adenylyltransferase (ATP sulfurylase), adenyl-sulphate reductase (APS reductase) and dissimilatory sulfite reductase (Fig. 3.7), which are the enzymes involved in dissimilatory sulphate reduction (Bradley et al., 2011). Pyruvate ferredoxin oxidoreductase (PFOR), carbon monoxide dehydrogenase and acetyl-CoA synthase encoding genes, which are involved in acetogenesis through the Wood-Ljungdahl pathway were also detected (Fig. 3.7) (Ragsdale, 2008). This suggests that acetone serves as one of the key electron donors for the reduction of sulfate to sulfide in the Black Sea sediments.

Based on these observations, current study proposes the major players in the biological sulfur cycle in the Black Sea as shown in Fig. 3.5. In summary, in the anoxic sediments and bottom waters sulfate is reduced to sulfide by anaerobic sulfate reducers like *Desulfatibacillum, Desulfomicrobium* and *Desulfococcus*. This sulfide diffuses upwards to the sulfidic chemocline where obligate anaerobic photoautotrophic green sulfur bacteria oxidize sulfide back to sulfate. Low amounts of sulfide passing the sulfidic chemocline is then oxidized in the ~30 m thick suboxic zone by aerobes like *Thiomicrospira*, together with anoxygenic phototrophs like *Congregibacter* and *Erythrobacter*. Mn oxidizers located in the suboxic zone oxidize Mn (II) to Mn (III), which further contributes to oxidation of sulfide back to sulfate.

3.5.5 Aerobic chemo-organotrophs

The majority of aerobic chemo organotrophs were indicator species of sediments younger than 5.2 ka. By way of exception, *Blastopirellula* is the dominant aerobic chemo-organotroph indicative of sediments older than 5.2 ka BP after which it was succeeded by mainly *Hyphomonas, Saccharophagus, Idiomarina, Cellvibrio* and *Endoriftia* (Fig. 3.2c). *Blastopirellula* grows optimally at neutral pH (Lee et al., 2013) while *Hyphomonas* is alkaliphilic (Weiner, 2015). The shift towards a predominance of akaliphilic *Hyphomonas* agrees with the timing of the Black Sea becoming more alkaline (Bahr et al., 2008). *Endoriftia* is predicted to perform sulfide oxidation via a reverse sulfate reduction pathway, involving the enzymes APS reductase and ATP sulfurylase (Robidart et al., 2008). *Endoriftia*, as for the source of these genes, was identified in metagenomes as old as 7,200 years when the Black Sea became stratified along with the deposition of the sapropel, but their relative abundance increased substantially after 5.2 ka (Fig. 2) when the Black Sea chemocline deepened (Huang et al., 2000). Furthermore, the presence of cellulolytic *Cellvibrio* at 8 ka BP and after 5.4 ka BP coincides with that of ancient DNA originating from terrestrial vegetation and fungi (Coolen et al., 2013), and therefore points towards an increased discharge and sedimentation of terrigenous cellulose. Several genera of aerobic chemo-organotrophic bacteria are only known from the marine environment such as *Blastopirellula, Idiomarina*. ORFs from these genera were present even in sediments deposited prior to the suggested marine reconnection at 9.0 ka BP. These results are in accordance with the fossil dinocyst assemblage implying non-fresh water conditions even before marine reconnection (Marret et al., 2009).

3.6 Conclusion

In summary, this study provides first insights into how marine microbial communities responded to changing oceanographic conditions at centennial timescale resolution in the Black Sea. Obligate anaerobic bacteria showed the most drastic response to the establishment of modern conditions at 5.2 ka BP, which coincides with a shift in the plankton community composition as the source of sedimentary organic matter. The functional metagenomic dataset suggests that these communities most likely are still actively involved in the sulfur and methane cycling as this timing also corresponds to the sediment depth where the SMTZ occurs. In contrast, aerobic microbial communities are likely to be seeded from the past water column with little to no postburial selection. This shows that a subset of past as well as potentially still active subseafloor microbial communities respectively provide direct and indirect insights into the paleodepositional environment.

Acknowledgements

This study was supported by National Science Foundation Grants OCE 0602423 (to M.J.L.C.), OCE 0825020 (to M.J.L.C.), and EAR 0952146 (to L.G.) and by the Woods Hole Oceanographic Institution. Kuldeep More also thanks the Curtin Office for Research and Development (ORD) for funding a PhD stipend. Authors thank Dr. Valier Galy from Woods Hole Oceanographic Institution for his valuable feedback on the manuscript. Metagenomes are in MG-RAST under project "Black Sea Metagenomes".

3.7 FIGURES

Figure 3.1 Geochemical proxies (Coolen et al., 2013) and downcore distributions of microbial communities (this work). (a) C/N ratio (blue) and TOC content (orange), (b) δD values of long-chain alkenones (i.e., C37 mK and C36:2 eK), relative abundance of (c) major microbial categories, (d) major aerobic groups, (e) major anaerobic groups, and (f) total energy metabolisms.

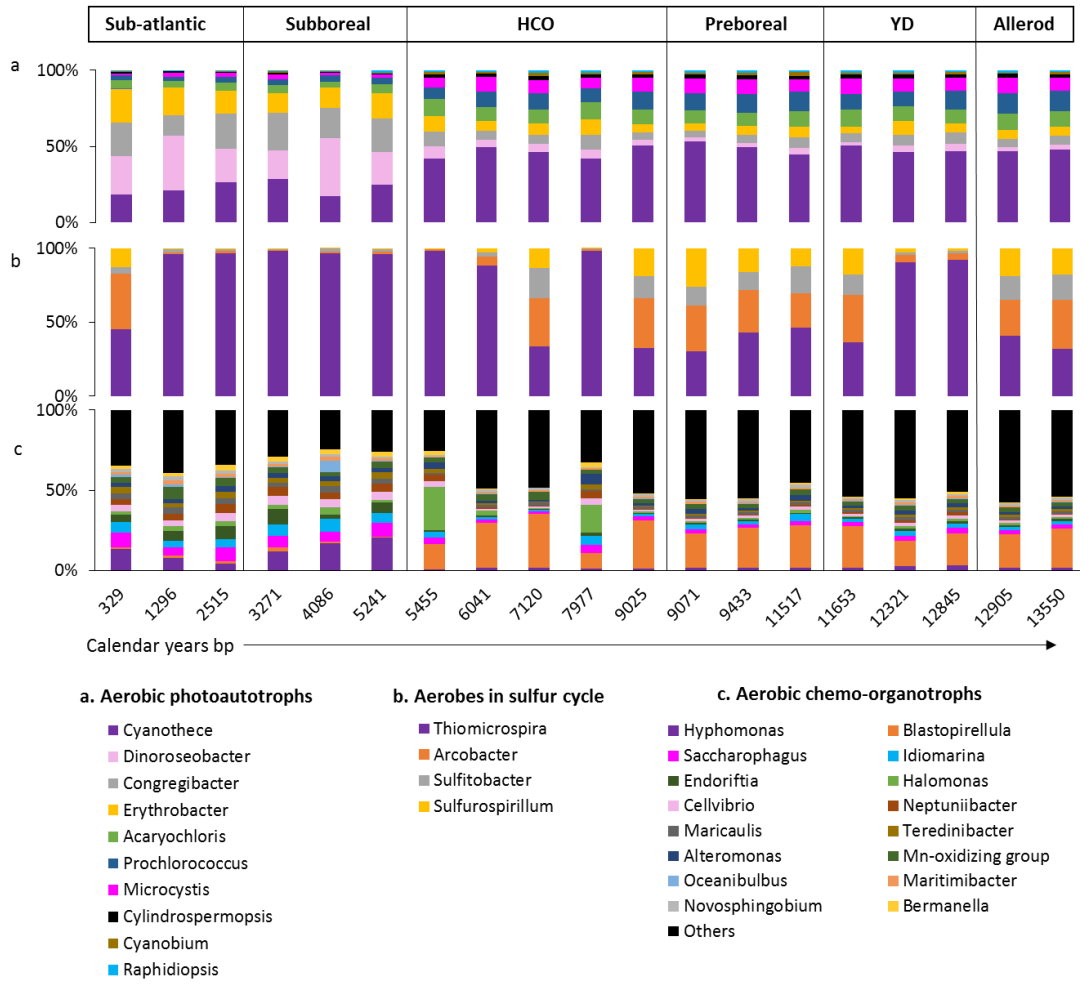

Figure 3.2 Distribution of obligate aerobes. Averaged relative abundance of major groups in aerobes (a) photo-autotrophic aerobes, (b) aerobes involved in S-cycling and (c) other chemo-organotrophic aerobes.

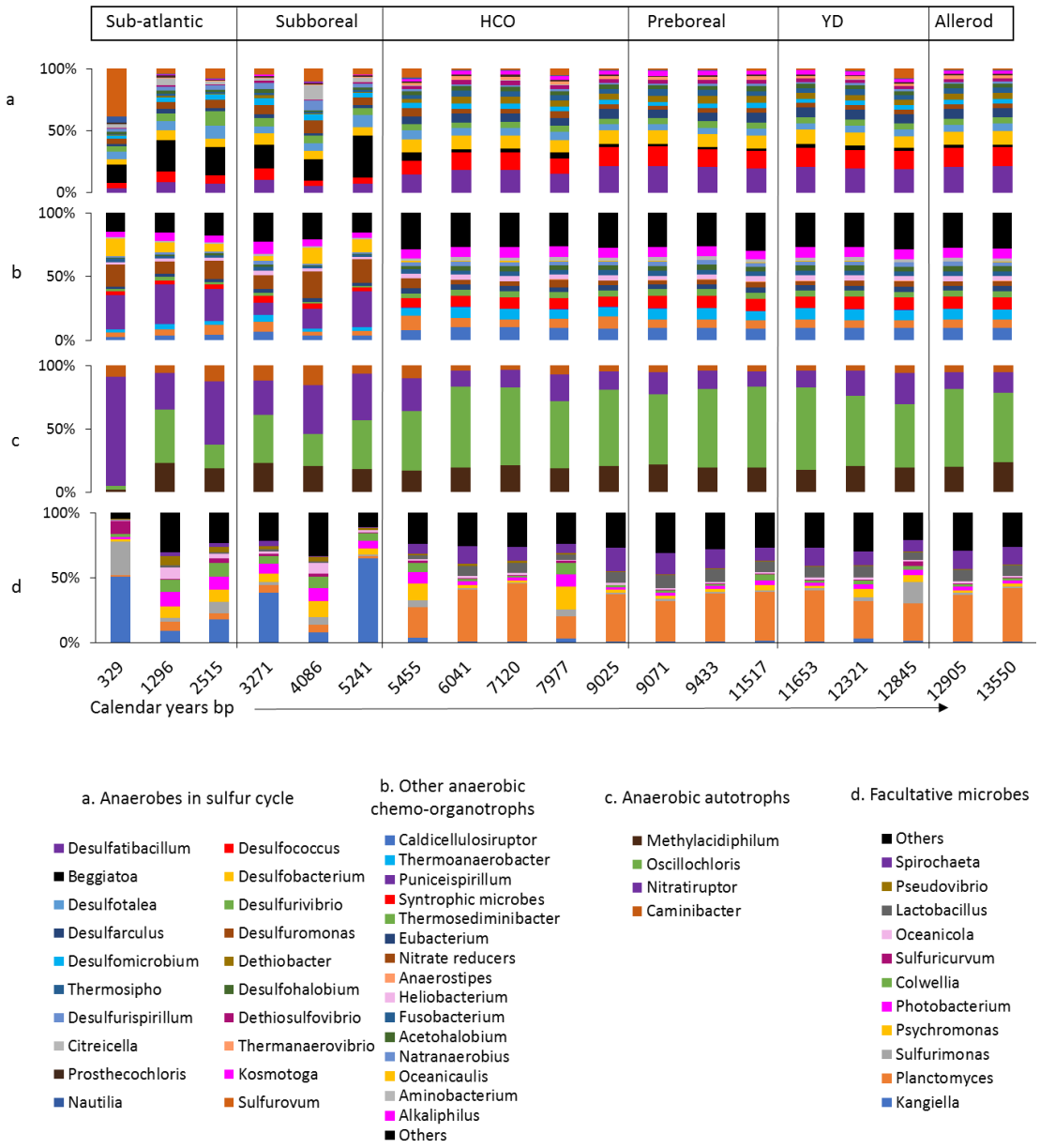

Figure 3.3 Distribution of obligate anaerobes. Averaged relative abundance of major groups in anaerobes (a) anaerobes involved in S-cycling, (b) other chemo-organotrophic anaerobes and (c) autotrophic anaerobes.

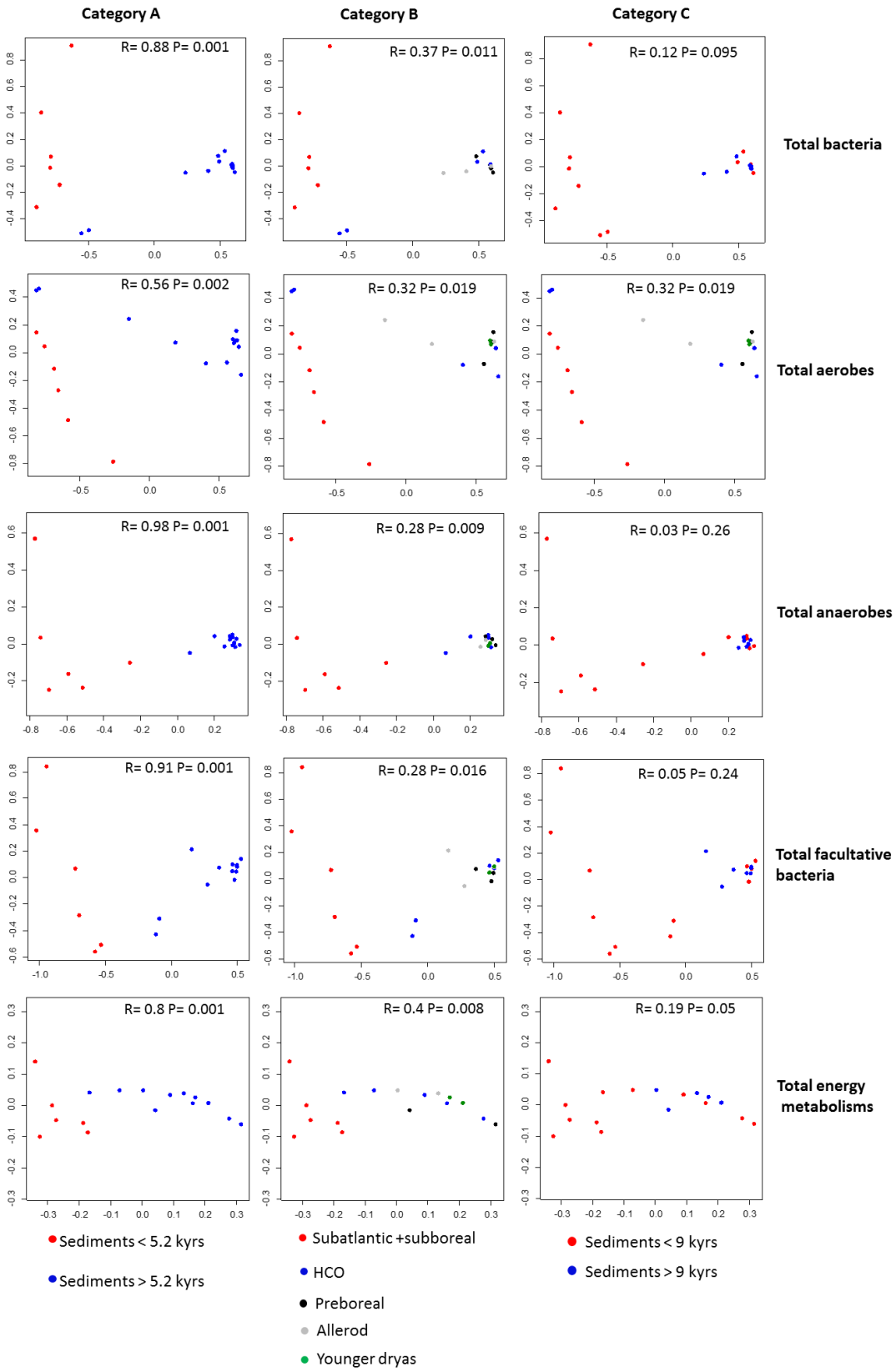

Figure 3.4 NMDS analysis of community compositions of total microbes and energy metabolism in three categories. NMDS stress was < 0.05 in all the analyses. R value and P value of each NMDS analysis are indicated at upper right corner. P value indicates significance

levels, while R value denotes the strength of the analysed factors on the samples. R value close to 1 indicates high separation between treatment samples, while R value close to 0 indicates no separation. Axes in NMDS are arbitrary.

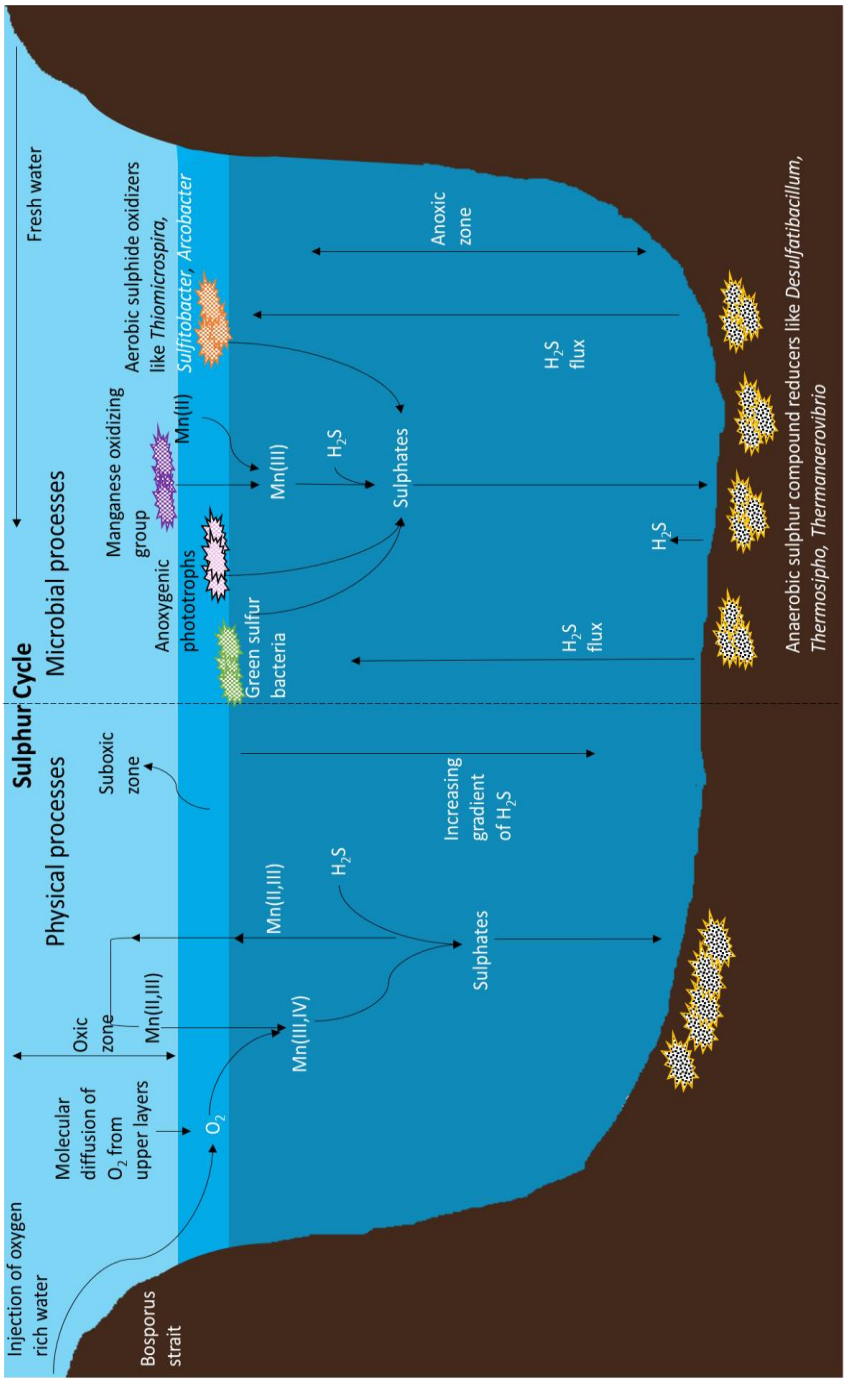

Figure 3.5 The Sulfur cycle in the Black Sea basin as inferred from the sedimentary metagenomic survey. Dotted line separates physical vs. microbial processes involved in S-cycling.

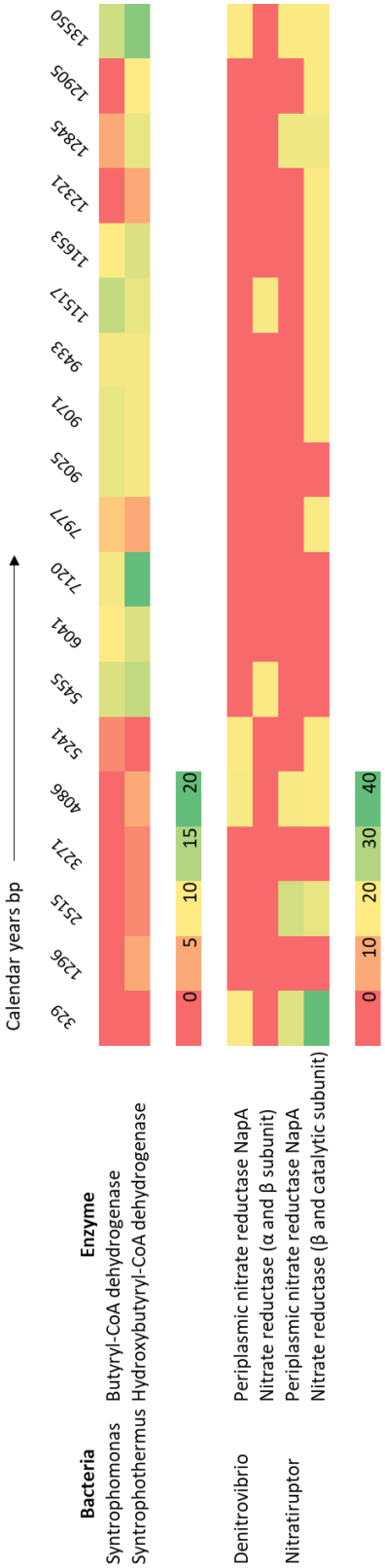

Figure 3.6. Heat maps showing the abundance of ORFs encoding enzymes of interest from syntrophic and denitrifying bacterial genera. The color key shows the number of ORFs in each sample**.**

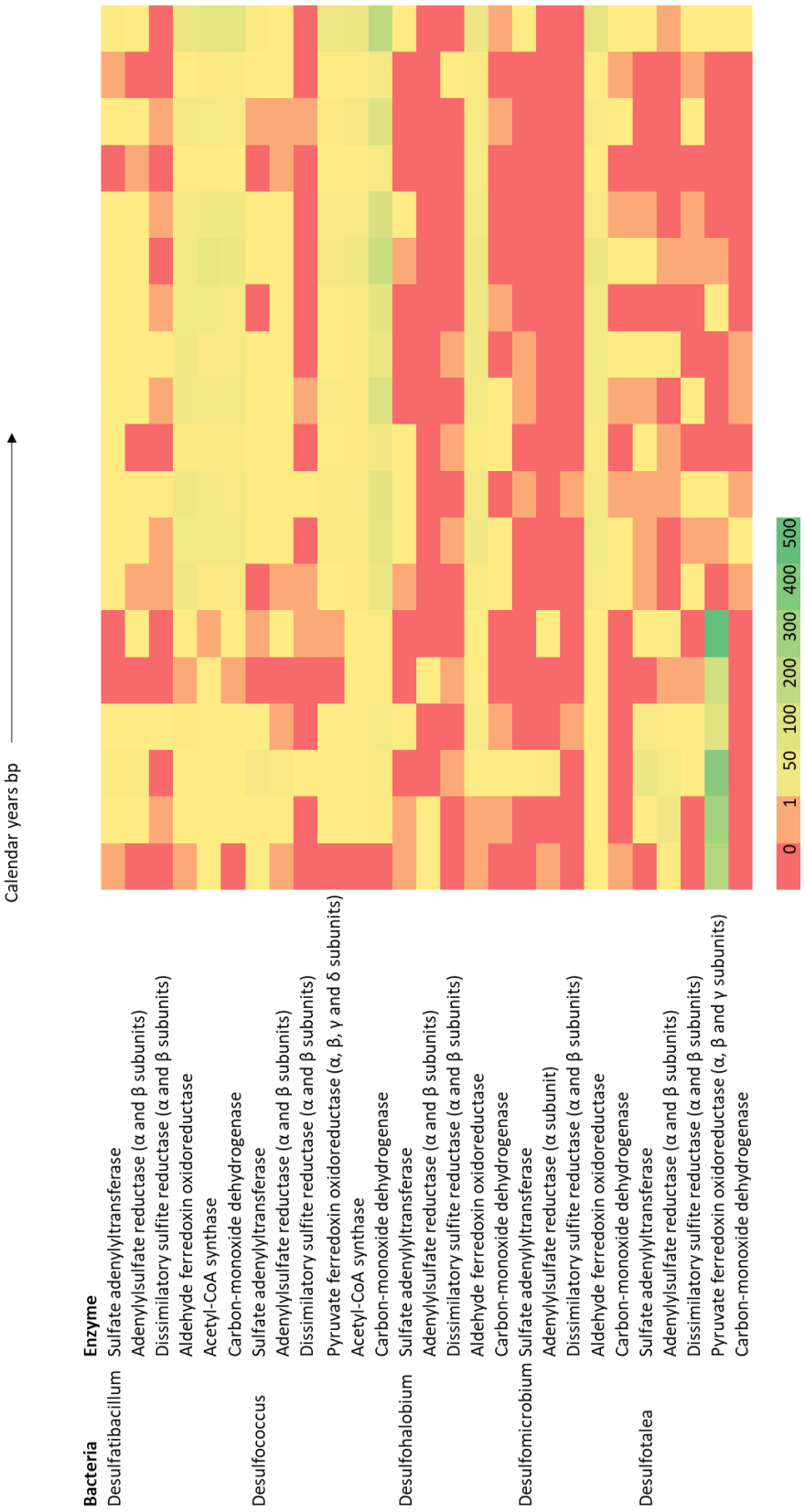

Figure 3.7. Heat map showing abundance of ORFs encoding key enzymes involved in sulphur metabolism from and their source bacterial genera. The color key shows the number of ORFs in each sample.

3.8 TABLES

Table 3.1 General information of sediment intervals used for shotgun metagenomic analysis and metagenome accession numbers.

Metagenome name	Depth (mbsf)	Age (yrs)	Sediment Lithology (Coolen et al., 2013)	Climate stage	MG-RAST id
BS19_R	8	329	Unit I	subatlantic	mgm4805918.3
BS18_R	30	1296	Unit I	subatlantic	mgm4807276.3
BS17_R	53.5	2515	Unit I	subatlantic	mgm4805917.3
BS16_R	66.5	3271	Unit II	subboreal	mgm4805910.3
BS15_R	79.5	4086	Unit II	subboreal	mgm4805896.3
BS14_R	96.5	5241	Unit II	subboreal	mgm4805899.3
BS13_R	99.5	5455	Unit II	HCO	mgm4805892.3
BS12_R	107.5	6041	Unit II	HCO	mgm4805893.3
BS11_R	121.5	7120	Unit II	HCO	mgm4805894.3
BS10_R	125.5	7977	Unit III-T	HCO	mgm4805891.3
BS9_R	128	9025	Unit III-T	HCO	mgm4805890.3
BS8_R	129	9071	Unit III-T	Preboreal	mgm4805889.3
BS7_R	137	9433	Unit III-C1	Preboreal	mgm4805888.3
BS6_R	195	11517	Unit III-C1	Preboreal	mgm4810150.3
BS5_R	200	11653	Glacial type	YD	mgm4805885.3
BS4_R	230.5	12321	Glacial type	YD	mgm4805886.3
BS3_R	274.5	12845	Glacial type	YD	mgm4805887.3
BS2_R	295	12905	C2	Allerod	mgm4807275.3
BS1_R	349	13550	C2	Allerod	mgm4805884.3
Negative control	_	_	_	_	mgm4805920.3
Extraction control	_	_	_	_	mgm4805919.3

Table 3.2 Indicator species for sediments deposited after the establishment of modern-day salinity at 5.2 ka with specificity (A-value) vs. sensitivity (B-value) of each indicator species.

Genus (r-value)	A	B
Acetobacter (0.791)	0.626	1
Actinobacillus (0.748)	0.559	1
Ahrensia (0.833)	0.694	1
Aurantimonas (0.816)	0.666	1
Basfia (0.761)	0.579	1
Bermanella (0.84)	0.706	1
Cardiobacterium (0.771)	0.594	1
Cellvibrio (0.824)	0.679	1
Citreicella (0.828)	0.686	1
Congregibacter (0.79)	0.624	1
Dinoroseobacter (0.839)	0.705	1
Endoriftia (0.871)	0.758	1
Erwinia (0.767)	0.589	1
Erythrobacter (0.768)	0.589	1
Ferrimonas (0.815)	0.664	1
Francisella (0.753)	0.567	1
Fulvimarina (0.806)	0.649	1
Gluconobacter (0.81)	0.656	1
Granulibacter (0.82)	0.673	1
Hirschia (0.842)	0.710	1
Hoeflea (0.827)	0.684	1
Hyphomonas (0.883)	0.780	1
Idiomarina (0.819)	0.670	1
Kangiella (0.918)	0.842	1
Ketogulonicigenium (0.769)	0.591	1
Loktanella (0.834)	0.695	1
Maricaulis (0.818)	0.669	1

Mariprofundus (0.815)	0.664	1
Maritimibacter (0.801)	0.641	1
Neptuniibacter (0.847)	0.717	1
Novosphingobium (0.778)	0.605	1
Oceanibulbus (0.863)	0.745	1
Oceanicola (0.789)	0.622	1
Octadecabacter (0.783)	0.612	1
Parvularcula (0.8)	0.640	1
Pelagibaca (0.797)	0.635	1
Phaeobacter (0.822)	0.676	1
Photobacterium (0.783)	0.613	1
Photorhabdus (0.764)	0.583	1
Pseudovibrio (0.827)	0.684	1
Puniceispirillum (0.876)	0.767	1
Reinekea (0.82)	0.672	1
Roseibium (0.806)	0.649	1
Saccharophagus (0.828)	0.685	1
Sagittula (0.831)	0.690	1
Sodalis (0.761)	0.579	1
Sulfitobacter (0.805)	0.648	1
Teredinibacter (0.825)	0.680	1
Thalassobium (0.811)	0.658	1
Oceanicaulis (0.811)	0.658	1

Table 3.3 Indicator species for sediments deposited before the establishment of modern-day salinity at 5.2 ka with specificity (A-value) vs. sensitivity (B-value) of each indicator species.

Genus (r-value)	A	B
Acaryochloris (0.778)	0.6057	1
Acetivibrio (0.851)	0.7236	1
Acetohalobium (0.899)	0.8074	1
Acidaminococcus (0.878)	0.7706	1
Acidimicrobium (0.859)	0.7372	1
Actinosynnema (0.801)	0.641	1
Aeromicrobium (0.818)	0.6685	1
Akkermansia (0.81)	0.6562	1
Alkaliphilus (0.852)	0.7251	1
Aminobacterium (0.881)	0.7763	1
Aminomonas (0.878)	0.7703	1
Anaerococcus (0.854)	0.7293	1
Anaerofustis (0.863)	0.745	1
Anaerostipes (0.862)	0.7432	1
Anaerotruncus (0.873)	0.7613	1
Bdellovibrio (0.77)	0.5927	1
Bifidobacterium (0.855)	0.7318	1
Blastopirellula (0.874)	0.7642	1
Brevibacterium (0.805)	0.6473	1
Butyrivibrio (0.853)	0.7271	1
Caldicellulosiruptor (0.884)	0.781	1
Carnobacterium (0.835)	0.697	1
Catenulispora (0.824)	0.6784	1
Cellulomonas (0.814)	0.6618	1
Cellulosilyticum (0.845)	0.7145	1
Clavibacter (0.834)	0.6958	1
Collinsella (0.859)	0.7371	1

Conexibacter (0.839)	0.7034	1
Coprothermobacter (0.898)	0.8071	1
Crocosphaera (0.799)	0.6378	1
Cyanobium (0.78)	0.609	1
Cyanothece (0.783)	0.6135	1
Cylindrospermopsis (0.82)	0.6721	1
Xylanimonas (0.817)	0.6674	1
Denitrovibrio (0.824)	0.6794	1
Dermacoccus (0.811)	0.657	1
Desulfarculus (0.866)	0.7496	1
Desulfatibacillum (0.861)	0.7421	1
Desulfobacterium (0.827)	0.684	1
Desulfococcus (0.853)	0.7279	1
Desulfohalobium (0.836)	0.6987	1
Desulfomicrobium (0.793)	0.6283	1
Desulfuromonas (0.754)	0.5691	1
Dethiobacter (0.89)	0.7923	1
Dethiosulfovibrio (0.869)	0.7545	1
Dorea (0.864)	0.7467	1
Eggerthella (0.866)	0.7506	1
Ethanoligenens (0.858)	0.7363	1
Eubacterium (0.863)	0.7445	1
Exiguobacterium (0.805)	0.6475	1
Fervidobacterium (0.861)	0.7408	1
Fusobacterium (0.865)	0.7482	1
Geodermatophilus (0.794)	0.6303	1
Heliobacterium (0.868)	0.7529	1
Holdemania (0.854)	0.7301	1
Ilyobacter (0.844)	0.712	1
Janibacter (0.791)	0.6253	1
Kineococcus (0.791)	0.6252	1

Kosmotoga (0.895)	0.8019	1
Kribbella (0.8)	0.6407	1
Lactobacillus (0.849)	0.7208	1
Lactococcus (0.825)	0.6811	1
Lawsonia (0.854)	0.7289	1
Leptotrichia (0.849)	0.7211	1
Megasphaera (0.892)	0.7962	1
Methylacidiphilum (0.848)	0.7191	1
Microcystis (0.828)	0.6851	1
Victivallis (0.882)	0.7784	1
Mitsuokella (0.878)	0.7717	1
Mycoplasma (0.864)	0.7457	1
Natranaerobius (0.873)	0.7625	1
Nocardiopsis (0.779)	0.6066	1
Oscillochloris (0.885)	0.7824	1
Parachlamydia (0.872)	0.7595	1
Peptoniphilus (0.88)	0.7746	1
Planctomyces (0.853)	0.728	1
Prochlorococcus (0.811)	0.6581	1
Prosthecochloris (0.796)	0.6338	1
Pseudoramibacter (0.903)	0.8153	1
Raphidiopsis (0.792)	0.6272	1
Ruminococcus (0.872)	0.7611	1
Saccharomonospora (0.796)	0.633	1
Sebaldella (0.841)	0.7066	1
Selenomonas (0.864)	0.7464	1
Slackia (0.866)	0.7491	1
Spirochaeta (0.853)	0.727	1
Stackebrandtia (0.798)	0.637	1
Staphylococcus (0.825)	0.6809	1
Streptococcus (0.845)	0.7144	1

Syntrophomonas (0.872)	0.7603	1
Syntrophothermus (0.903)	0.8147	1
Thermanaerovibrio (0.885)	0.7825	1
Thermoanaerobacter (0.882)	0.778	1
Thermobifida (0.811)	0.6573	1
Thermobispora (0.826)	0.6815	1
Thermomonospora (0.798)	0.6374	1
Thermosediminibacter (0.886)	0.7856	1
Thermosipho (0.871)	0.7589	1
Turicibacter (0.83)	0.6894	1
Veillonella (0.866)	0.75	1
Verrucomicrobium (0.816)	0.6659	1

3.9 REFERENCES

Anderson CR, Dick GJ, Chu ML, Cho JC, Davis RE, Brauer SL, Tebo BM (2009) Aurantimonas manganoxydans, sp nov and Aurantimonas litoralis, sp nov.: Mn(II) Oxidizing Representatives of a Globally Distributed Clade of alpha-Proteobacteria from the Order Rhizobiales. Geomicrobiol J, 26, 189-198.

Atkins R, Rose T, Brown RS, Robb M (2001) The Microcystis cyanobacteria bloom in the Swan River - February 2000. Water Sci Technol, 43, 107-114.

Bahr A, Lamy F, Arz HW, Major C, Kwiecien O, Wefer G (2008) Abrupt changes of temperature and water chemistry in the late Pleistocene and early Holocene Black Sea. Geochem Geophy Geosy, 9. Q01004, doi:10.1029/2007GC001683.

Bieble, H.m Allgaier, M., Tindall, B.J., Koblizek, M., Lunsdorf, H., Pukall, R., Wagner-Dobler, I. (2005) *Dinoroseobacter shibae* gen. nov., sp. nov., a new aerobic phototrophic bacterium isolated from dinoflagellates. International Journal of Systematic and Evolutionary Microbiology, 55: 1089-1096, doi: 10.1099/ijs.0.63511-0.

Blankenship RE, Madigan MT, Bauer CE (1995) Anoxygenic Photosynthetic Bacteria, Springer Netherlands.

Bloh AH, Usup G, Ahmad A (2016) Loktanella spp. Gb03 as an algicidal bacterium, isolated from the culture of Dinoflagellate Gambierdiscus belizeanus. Veterinary World, 9, 142-146.

Bradley AS, Leavitt WD, Johnston DT (2011) Revisiting the dissimilatory sulfate reduction pathway. Geobiology, 9, 446-457.

Ciobanu MC, Rabineau M, Droz L, Revillon S, Ghiglione JF, Dennielou B, Jorry SJ, Kallmeyer J, Etoubleau J, Pignet P, Crassous P, Vandenabeele-Trambouze O, Laugier J, Guegan M, Godfroy A, Alain K (2012) Sedimentological imprint on subseafloor microbial communities in Western Mediterranean Sea Quaternary sediments. Biogeosciences, 9, 3491-3512.

Clarke KR (1993) Non-parametric multivariate analyses of changes in community structure. Australian Journal of Ecology, 18, 117-143.

Coolen MJL, Orsi WD, Balkema C, Quince C, Harris K, Sylva SP, Filipova-Marinova M, Giosan L (2013) Evolution of the plankton paleome in the Black Sea from the Deglacial to Anthropocene. P Natl Acad Sci USA, 110, 8609-8614.

Coolen MJL, Saenz JP, Giosan L, Trowbridge NY, Dimitrov P, Dimitrov D, Eglinton TI (2009) DNA and lipid molecular stratigraphic records of haptophyte succession in the Black Sea during the Holocene. Earth Planet Sc Lett, 284, 610-621.

Dufrene M, Legendre P (1997) Species assemblages and indicator species: The need for a flexible asymmetrical approach. Ecol Monogr, 67, 345-366.

Eglinton, T. I., G. Eglinton, L. Dupont, E. R. Sholkovitz, D. Montluc¸on, and C. M. Reddy (2002), Composition, age, and provenance of organic matter in NW African dust over the Atlantic Ocean, Geochemistry, Geophysics, Geosystems, 3(8), 1050, doi:10.1029/2001GC000269.

Fulton JM, Arthur MA, Freeman KH (2012) Black Sea nitrogen cycling and the preservation of phytoplankton delta N-15 signals during the Holocene. Global Biogeochem Cy, 26. GB2030, doi:10.1029/2011GB004196.

Giosan, L., Coolen, M.J.L., Kaplan, J.O., Constantinescu, S., Filip, F., Filipova-Marinova, M., Kettner, J. and N. Thom (2012) Early anthropogenic transformation of the Danube-Black Sea system. Scientific Reports, 2: 10.1038/srep00582

Gomez-Baena G, Lopez-Lozano A, Gil-Martinez J, Lucena JM, Diez J, Candau P, Garcia-Fernandez JM (2008) Glucose Uptake and Its Effect on Gene Expression in Prochlorococcus. Plos One, 3.

Hanada, S. (2016) Anoxygenic Photosynthesis -A Photochemical Reaction That Does Not Contribute to Oxygen Reproduction. Microbes and environments, 31(1), 1-3.

Huang CY, Patel BK, Mah RA, Baresi L (1998) Caldicellulosiruptor owensensis sp. nov., an anaerobic, extremely thermophilic, xylanolytic bacterium. Int J Syst Bacteriol, 48, 91-97.

Huang YS, Freeman KH, Wilkin RT, Arthur MA, Jones AD (2000) Black Sea chemocline oscillations during the Holocene: molecular and isotopic studies of marginal sediments. Org Geochem, 31, 1525-1531.

Inagaki F, Hinrichs KU, Kubo Y, Bowles MW, Heuer VB, Hong WL, Hoshino T, Ijiri A, Imachi H, Ito M, Kaneko M, Lever MA, Lin YS, Methe BA, Morita S, Morono Y, Tanikawa W, Bihan M, Bowden SA, Elvert M, Glombitza C, Gross D, Harrington GJ, Hori T, Li K, Limmer D, Liu CH, Murayama M, Ohkouchi N, Ono S, Park YS, Phillips SC, Prieto-Mollar X, Purkey M, Riedinger N, Sanada Y, Sauvage J, Snyder G, Susilawati R, Takano Y, Tasumi E, Terada

T, Tomaru H, Trembath-Reichert E, Wang DT, Yamada Y (2015) Exploring deep microbial life in coal-bearing sediment down to similar to 2.5 km below the ocean floor. Science, 349, 420-424.

Inagaki F, Okada H, Tsapin AI, Nealson KH (2005) Microbial survival - The paleome: A sedimentary genetic record of past microbial communities. Astrobiology, 5, 141-153.

Jasmin C, Anas A, Tharakan B, Jaleel A, Puthiyaveettil V, Narayanane S, Lincy J, Nair S (2017) Diversity of sediment-associated Planctomycetes in the Arabian Sea oxygen minimum zone. J Basic Microb, 57, 1010-1017.

Kallmeyer J, Pockalny R, Adhikari RR, Smith DC, D'hondt S (2012) Global distribution of microbial abundance and biomass in subseafloor sediment. P Natl Acad Sci USA, 109, 16213-16216.

Kang I, Oh HM, Lim SI, Ferriera S, Giovannoni SJ, Cho JC (2010) Genome Sequence of Fulvimarina pelagi HTCC2506(T), a Mn(II)-Oxidizing Alphaproteobacterium Possessing an Aerobic Anoxygenic Photosynthetic Gene Cluster and Xanthorhodopsin. J Bacteriol, 192, 4798-4799.

Khadem AF, Van Teeseling MCF, Van Niftrik L, Jetten MSM, Den Camp HJMO, Pol A (2012) Genomic and physiological analysis of carbon storage in the verrucomicrobial methanotroph "Ca. Methylacidiphilum funnariolicunn" SolV. Front Microbiol, 3. https://doi.org/10.3389/fmicb.2012.00345/full.

Lee HW, Roh SW, Shin NR, Lee J, Whon TW, Jung MJ, Yun JH, Kim MS, Hyun DW, Kim D, Bae JW (2013) Blastopirellula cremea sp nov., isolated from a dead ark clam. Int J Syst Evol Micr, 63, 2314-2319.

Lyra C, Sinkko H, Rantanen M, Paulin L, Kotilainen A (2013) Sediment Bacterial Communities Reflect the History of a Sea Basin. Plos One, 8.

Major CO, Goldstein SL, Ryan WBF, Lericolais G, Piotrowski AM, Hajdas I (2006) The co-evolution of Black Sea level and composition through the last deglaciation and its paleoclimatic significance. Quaternary Sci Rev, 25, 2031-2047.

Marret F, Mudie P, Aksu A, Hiscott RN (2009) A Holocene dinocyst record of a two-step transformation of the Neoeuxinian brackish water lake into the Black Sea. Quatern Int, 197, 72-86.

Mcinerney MJ, Bryant MP, Hespell RB, Costerton JW (1981) Syntrophomonas-Wolfei Gen-Nov Sp-Nov, an Anaerobic, Syntrophic, Fatty-Acid Oxidizing Bacterium. Appl Environ Microb, 41, 1029-1039.

Meyer F, Paarmann D, D'souza M, Olson R, Glass EM, Kubal M, Paczian T, Rodriguez A, Stevens R, Wilke A, Wilkening J, Edwards RA (2008) The metagenomics RAST server - a public resource for the automatic phylogenetic and functional analysis of metagenomes. Bmc Bioinformatics, 9.

Moezelaar R, Stal LJ (1997) A comparison of fermentation in the cyanobacterium Microcystis PCC7806 grown under a light/dark cycle and continuous light. Eur J Phycol, 32, 373-378.

Murray JW, Lee B-S, Bullister J, Luther GW (1999) The Suboxic Zone of the Black Sea. In: Environmental Degradation of the Black Sea: Challenges and Remedies (eds Beşiktepe ST, Ünlüata Ü, Bologa AS). Springer Netherlands, Dordrecht, pp. 75-91.

Myhr S, Torsvik T (2000) Denitrovibrio acetiphilus, a novel genus and species of dissimilatory nitrate-reducing bacterium isolated from an oil reservoir model column. Int J Syst Evol Micr, 50, 1611-1619.

Nakagawa S, Takai K, Inagaki F, Horikoshi K, Sako Y (2005) Nitratiruptor tergarcus gen. nov., sp. nov. and Nitratifractor salsuginis gen. nov., sp. nov., nitrate-reducing chemolithoautotrophs of the epsilon-Proteobacteria isolated from a deep-sea hydrothermal system in the Mid-Okinawa Trough (vol 55, pg 925, 2005). Int J Syst Evol Micr, 55, 2233-2233.

Neretin LN, Volkov II, Rozanov AG, Demidova TP, Falina AS (2006) Biogeochemistry of the Black Sea anoxic zone with a reference to sulphur cycle. In: Neretin, L. (eds) Past and Present Water Column Anoxia. Nato Science Series: IV: Earth and Environmental Sciences, 64, 67-104. Springer, Dordrecht. https://doi.org/10.1007/1-4020-4297-3_04Oh, H., Kwon, K., Kang, I., Kang, S., Lee, J., Kim, S., Cho, J. (2010) Complete Genome Sequence of "*Candidatus* Puniceispirillum marinum" IMCC1322, a Representative of the SAR116 Clade in the *Alphaproteobacteria*. Journal of Bacteriology, 192 (12) 3240-3241; DOI: 10.1128/JB.00347-10.

Okamura K, Takamiya K, Nishimura M (1985) Photosynthetic Electron-Transfer System Is Inoperative in Anaerobic Cells of Erythrobacter Species Strain Och-114. Arch Microbiol, 142, 12-17.

Orcutt BN, Sylvan JB, Knab NJ, Edwards KJ (2011) Microbial Ecology of the Dark Ocean above, at, and below the Seafloor. Microbiol Mol Biol R, 75, 361-422.

Orsi WD, Coolen MJL, Wuchter C, He L, More KD, Irigoien X, Chust G, Johnson C, Hemingway JD, Lee M, Galy V, Giosan L (2017) Climate oscillations reflected within the microbiome of Arabian Sea sediments. Scientific Reports, 7, 6040.

Overbeek R, Olson R, Pusch GD, Olsen GJ, Davis JJ, Disz T, Edwards RA, Gerdes S, Parrello B, Shukla M, Vonstein V, Wattam AR, Xia FF, Stevens R (2014) The SEED and the Rapid Annotation of microbial genomes using Subsystems Technology (RAST). Nucleic Acids Res, 42, D206-D214.

Overmann J, Manske AK (2006) Anoxygenic phototrophic bacteria in the Black Sea chemocline. In: Neretin L. (eds) Past and Present Water Column Anoxia. Nato Science Series: IV: Earth and Environmental Sciences, vol 64, 523-541. Springer, Dordrecht.

Parkes RJ, Cragg BA, Wellsbury P (2000) Recent studies on bacterial populations and processes in subseafloor sediments: A review. Hydrogeol J, 8, 11-28.

Pimenov NV, Neretin LN (2006) Composition and activities of microbial communities involved in carbon, sulfur, nitrogen and manganese cycling in the oxic/anoxic interface of the Black Sea. Nato Sci S Ss Iv Ear, 64, 501-521.

Ragsdale SW (2008) Enzymology of the Wood-Ljungdahl pathway of acetogenesis. Ann Ny Acad Sci, 1125, 129-136.

Rebata-Landa, V., & Santamarina, J. C. (2006). Mechanical limits to microbial activity in deep sediments. *Geochemistry, Geophysics, Geosystems*, *7*,

Q11006, doi:10.1029/2006GC001355.

Reimer, P. J., Baillie, M. G. L., Bard, E., Bayliss, A., Beck, J. W., Bertrand, C. J. H., Weyhenmeyer, C. E. (2004). IntCal04 terrestrial radiocarbon age calibration, 0-26 cal kyr BP. *Radiocarbon*, *46*, 1029–1058. https://doi.org/10.1017/S0033822200032999

Repeta DJ, Simpson DJ (1991) The Distribution and Recycling of Chlorophyll, Bacteriochlorophyll and Carotenoids in the Black-Sea. Deep-Sea Res, 38, S969-S984.

Repeta DJ, Simpson DJ, Jorgensen BB, Jannasch HW (1989) Evidence for Anoxygenic Photosynthesis from the Distribution of Bacteriochlorophylls in the Black-Sea. Nature, 342, 69-72.

Robidart JC, Bench SR, Feldman RA, Novoradovsky A, Podell SB, Gaasterland T, Allen EE, Felbeck H (2008) Metabolic versatility of the Riftia pachyptila endosymbiont revealed through metagenomics. Environ Microbiol, 10, 727-737.

Ross DA, Degens ET, Macilvaine J (1970) Black Sea: Recent Sedimentary History. Science, 170, 163-165.

Shiba T, Simidu U (1982) Erythrobacter-Longus Gen-Nov, Sp-Nov, an Aerobic Bacterium Which Contains Bacteriochlorophyll-A. Int J Syst Bacteriol, 32, 211-217.

Soulet, G., Menot, G., Garreta, V., Rostek, F., Zaragosi, S., Lericolais, G., Bard, E. (2011) Black Sea "lake" reservoir age evolution since the Last Glacial: Hydrologic and climatic implications. Earth and Planetary Science Letters, 308(1-2):245–258.

Spring S (2014) Function and Evolution of the Sox Multienzyme Complex in the Marine Gammaproteobacterium *Congregibacter litoralis.* ISRN Microbiology 2014, Article ID 597418. https://doi.org/10.1155/2014/597418.

Starnawski P, Bataillon T, Ettema TJG, Jochum LM, Schreiber L, Chen X, Lever MA, Polz MF, Jorgensen BB, Schramm A, Kjeldsen KU (2017) Microbial community assembly and evolution in subseafloor sediment. P Natl Acad Sci USA, 114, 2940-2945.

Subhash Y, Lee SS (2017) Description of *Oceanispirochaeta sediminicola* gen. nov., sp nov., an obligately anaerobic bacterium isolated from coastal marine sediments, and reclassification of *Spirochaeta litoralis* as *Oceanispirochaeta litoralis* comb. nov. Int J Syst Evol Micr, 67, 3403-3409.

Svetlichny L, Hubareva E, Isinibilir M, Kideys A, Belmonte G, Giangrande E (2010) Salinity tolerance of *Calanus euxinus* in the Black and Marmara Seas. Mar Ecol Prog Ser, 404, 127-138.

Takai K, Moser DP, Onstott TC, Spoelstra N, Pfiffner SM, Dohnalkova A, Fredrickson JK (2001) *Alkaliphilus transvaalensis* gen. nov., sp nov., an extremely alkaliphilic bacterium isolated from a deep South African gold mine. Int J Syst Evol Micr, 51, 1245-1256.

Tang KH, Yue H, Blankenship RE (2010) Energy metabolism of *Heliobacterium modesticaldum* during phototrophic and chemotrophic growth. Bmc Microbiol, 10.

Van der Meer, M.T.J., Sangiorgi, F., Baas, M., Brinkhuis, H., Sinninghe-Damste, J.S., Schouten, S. (2008) Molecular isotopic and dinoflagellate evidence for late Holocene freshening of the Black Sea. Earth and Planetary Science Letters, 267:426–434.

Van Der Oost J, Bulthuis BA, Feitz S, Krab K, Kraayenhof R (1989) Fermentation Metabolism of the Unicellular Cyanobacterium *Cyanothece* Pcc-7822. Arch Microbiol, 152, 415-419.

Vetriani C, Tran HV, Kerkhof LJ (2003) Fingerprinting microbial assemblages from the oxic/anoxic chemocline of the Black Sea. Appl Environ Microb, 69, 6481-6488.

Weiner RM (2015) Hyphomonas. In: Bergey's Manual of Systematics of Archaea and Bacteria. Ed. Whitman W.B. RF, Kämpfer P., Trujillo M., Chun J., Devos P., Hedlund B., Dedysh S. Bergey's Manual Trust, American Society for Microbiology, Online ISBN: 9781118960608. doi:10.1002/9781118960608.gbm00855.

Whitman WB (2015) Bergey's manual of systematics of archaea and bacteria. Bergey's Manual Trust, American Society for Microbiology, Online ISBN: 9781118960608.

DOI: 10.1002/9781118960608.

Xue YF, Xu Y, Liu Y, Ma YH, Zhou PJ (2001) *Thermoanaerobacter tengcongensis* sp nov., a novel anaerobic, saccharolytic, thermophilic bacterium isolated from a hot spring in Tengcong, China. Int J Syst Evol Micr, 51, 1335-1341.

CHAPTER 4

Subseafloor archaea reflect 139 kyr of paleo-depositional changes in the Northern Red Sea

Kuldeep D. More, Xabier Irigoien, Jessica Tierney, Liviu Giosan and Marco J.L. Coolen

4.1 ABSTRACT

The vertical zonation of subseafloor archaeal communities is thought to be primarily controlled by *in situ* environmental conditions such as the availability of electron donors and sediment lithology. Yet recent studies suggest that a subset of sedimentary archaea reflect changes in paleoenvironmental conditions. However, highly resolved temporal records of subsurface Archaea and paired paleoenvironmental reconstructions are needed to substantiate this claim. Here a highly resolved 16S profiling of subseafloor archaeal communities was performed in up to 139 kyr-old sediments of the northern Red Sea covering the last six Marine Isotope Stages (MIS) when alternating glacial low stands and interglacial highstands caused drastic changes in sea level and salinity in the Red Sea. The results revealed a strong significant response of subseafloor archaeal communities to changes in paleodepositional conditions associated with MIS stages and their transitions and only a moderately significant response to changes in sediment lithology. Even at phylum level it appeared that Crenarchaeota predominated in sediments deposited during glacial periods (MIS6, MIS4, MIS3 and MIS2) while Euryarchaeota predominated during major interglacials (Eemian and the Holocene). This shows that a substantial part of the subseafloor archaeal communities would have been present at the time of deposition and therefore their vertical distribution revealed a strong correlation with paleoceanographic changes.

4.2 INTRODUCTION

Subseafloor sediments sediments host ~2.9×10^{29} prokaryotic cells, equivalent to 0.18–3.6% of the total living biomass on the planet (Kallmeyer, Pockalny et al. 2012) with Archaea accounting for 37.3% of that population (Hoshino and Inagaki 2018). These subsurface microbial communities are generally structured through in situ environmental conditions such as the availability of electron acceptors and donors, porosity and sediment lithology (Cragg et.al., 2000; Kallmeyer et al. 2012; Parkes et.al., 2014; Orsi et al. 2017). Archaea are considered active members of subseafloor communities and to play key roles in carbon assimilation, mineralization, and precipitation (Berg et al., 2010; Offre et al., 2013), as well as in nitrogen- (Cabello et al., 2004; Wuchter et al., 2006), and sulfur cycling (Offre et al., 2013). Yet, recent studies have shown that a subset of subseafloor microbial communities were present at the time of deposition and formed a genetic archive originally referred to as "the Paleome" and reflect the paleo-depositional environment (Inagaki et al. 2005). For example, two very different geohydrological settings (grayish pelagic clays and volcanic ash layers) in coastal sediments of the Sea of Okhotsk (Japan) contained drastically different archaeal communities and that the differences persisted through a series of layers spanning approximately 100,000 years. It was concluded that the coastal subseafloor sediments acted as a reservoir of microbial diversity and that these reservoirs maintain their genetic properties over long periods of time although it remained speculative if these communities were alive or represented dead relicts (Inagaki et al., 2003). A recent high sampling resolution metagenomic survey revealed that a fraction of subseafloor bacterial communities in the northeastern Arabian Sea subsisted through fermentation but originated from the overlying water column during the last glacial interglacial cycle where they were involved in denitrification during periods of strong oxygen minimum zone conditions (Orsi et al., 2017). It was concluded that this fraction of the subseafloor microbiome underwent weak postburial selection and therefore formed a living long-term genomic record of the paleodepositional environment. A similar scenario may explain why subseafloor archaeal communities may also form a long-term genomic record of past environmental changes. Other examples of archaeal paleomes include Holocene variations in archaeal community composition as a result of changes in lake water temperature and duration of lake ice cover in late glacial lake sediments of Hässeldala Port (Sweden) (Ahmed, Parducci et al. 2018), and sedimentary archaea from lacustrine deposits of Laguna Potrok Aike, Argentina reflecting paleoenvironmental changes during the last glacial-interglacial cycle since 51 ka BP (Vuillemin, Ariztegui et al. 2016). Furthermore, some of the sedimentary archaeal DNA can

be used to analyse for the indications of paleoenvironmental variations as demonstrated by the recent archaeal amoA gene survey that reflects historic nutrient level and salinity fluctuations in Qinghai Lake, Tibetan Plateau (Yang, Jiang et al. 2015)

To further explore the global potential of sedimentary archaea to record changes in the paleodepositional environment, a highly-resolved 16S rDNA survey of subseafloor archaeal communities was performed in the northern the Red Sea sediments paired with paleoenvironmental proxies.

The Red Sea is a semi-enclosed, elongated warm body of water. Its northern end is bifurcated into the Gulf of Aqaba and the Gulf of Suez while at southern end it is connected via the Bab-el-Mandeb strait to the Gulf of Aden, which connects to the Indian Ocean (Rasul et al., 2015). Strong excess of evaporation over freshwater input into the Red Sea results in a net annual water deficit of ~2m (Morcos 1970). The Red Sea has experienced dramatic changes in sea level throughout the last and penultimate glacials. Sea level highstands occurred during the marine isotope stage 5 (MIS5e: last interglacial or Eemian), which started with the termination of the penultimate glacial maximum (MIS6) (Grant et al., 2014) and during the Holocene (MIS1). Limited exchange of the Red Sea with the open ocean led to extremely saline conditions during times of sea level lowstands in the last and penultimate glacials (Rohling, 1994; Fenton et al., 2000). During MIS6 and MIS2 (last glacial maximum; LGM) the Red Sea levels reached its minimum at 135 and 20 ka BP respectively (Grant et al., 2014), which caused the reduction in exchange flow through the Bab-el-Mandab strait raising salinities to 55 psu (Hemleben et al., 1996). This high salinity prevented foraminifera from growing and reproducing as evident from the absence of their microfossils in the so-called a-planktonic intervals observed in the Red Sea sediments (Fenton et al., 2000). These drastic paleoceanographic changes make the Red Sea an ideal setting to study associated temporal changes in subseafloor archaeal communities.

4.3 MATERIALS AND METHODS

4.3.1 Sample collection and storage

A 4.4-m-long gravity core spanning 139 kyr of deposition was obtained during the *RV Aegaeo* cruise in 2014 from the Northern Red Sea (26.96 N, 34.89 E) at 1200m depth. On board, the core sections were split in half and 91 one-cm-intervals were sub-sampled aseptically to prevent (cross) contamination with foreign DNA (Coolen, Saenz et al. 2009). Samples for DNA extraction were stored in liquid nitrogen during the cruise and shipped on dry ice to the Woods Hole Oceanographic Institution (WHOI). The remaining sampled and archived core

halves were shipped refrigerated to WHOI. From the sampled core the remainder of the 87 corresponding intervals were sub-sampled and transferred into pre-combusted glass jars and freeze-dried for TEX_{86} paleothermometry, and for geochemical analysis on bulk organic matter and on foraminiferal microfossils. The intact archived half was used for XRF analysis.

4.3.2 Age model

Ten one-cm-intervals were selected for 14C AMS dating on foraminifera shells or from bulk organic matter from the a-planktonic intervals at the National Ocean Sciences Accelerator Mass Spectrometry (NOSAMS) Facility at WHOI. An age model for the core was then developed by calibrating the radiocarbon dates to calendar years B.P. (1950) with Calib 5.0.1 (Stuiver and Reimer 1993) using the INTCAL04 calibration curve (Reimer, Baillie et al. 2004).

4.3.3 Geochemistry

Titanium and calcium content was measured with an ITRAX^{TM} micro-XRF scanner, using a molybdenum x-ray tube at an exposure time of 10 s per measurement and a step-size of 200 µm to allow for high resolution analysis of bulk chemistry (Coolen, Saenz et al. 2009). The downcore variability in Ti/Ca served as a proxy for terrestrial vs. marine input. Total organic carbon, $\delta^{13}C$, $\delta^{15}N$, and C/N were analyzed from freeze-dried subsamples from the same 91 one-cm-thick sediment intervals used for DNA analysis using a Carlo Erba/Fisons 1108 flash elemental analyzer equipped with a Costech "ZeroBlank" air-excluding carousel and conditions described previously (Orsi, Coolen et al. 2017).

4.3.4 TEX_{86} paleothermometry

Total lipids were extracted using a Dionex Accelerated Solvent Extractor (ASE 350) in 9:1 (dichloromethane: methanol, v/v) and then separated into neutral (eluent: 2:1 dichloromethane: isopropanol, v/v) and acid (eluent: 4% acetic acid in DCM) fractions over NH2 gel. The neutral fraction was further partitioned into hydrocarbon (eluent: hexane), ketone (eluent: dichloromethane), and polar (eluent: methanol) fractions over silica gel. The polar fractions containing the GDGTs were then analyzed by high performance liquid chromatography-mass spectroscopy (HPLC-MS) on an Agilent 1260 HPLC/6120 MSD at the Woods Hole Oceanographic Institution (WHOI) according to the method of Schouten et al., (2007), which uses a Prevail Cyano column (150 x 2.1 mm, 3 um) to separate the GDGTs and analyzes the compounds in single ion monitoring mode. A synthetic C_{46} GDGT standard (Huguet et al., 2006) was added to each sample in order to quantify the concentrations of GDGTs. All samples were analyzed in duplicate and average laboratory precision was 0.002

TEX_{86} units (1δ). TEX_{86} values were converted to SST using the BAYSPAR SST calibration (Tierney and Tingley 2014; Tierney and Tingley 2015).

4.3.5 DNA extraction

Sediment samples 2 cm thick were sampled aseptically and DNA was extracted inside the clean lab at WHOI as described previously (Coolen, Orsi et al. 2013). Co-extracted PCR-inhibiting humic acids and other contaminants were efficiently removed from the concentrated extract using the PowerClean® Pro DNA Clean-up Kit (MoBio). Genomic DNA extracted from all 100 sediment intervals spanning the last 139,000 years of deposition served as template for subsequent PCR amplification of archaeal 16S rDNA and Illumina MiSeq sequencing. The exact same procedures were performed in triplicate without the addition of sediment as a control for contamination during extraction and purification of the sedimentary DNA. Aliquots of these "extraction blanks" were treated the same way as samples in further processes.

4.3.6 rRNA gene amplification, quantification, and bioinformatic analysis

DNA was quantified fluorometrically using Quant-iT PicoGreen dsDNA Reagent (Invitrogen). Archaeal 16S rRNA genes were amplified using the Domain-specific primers Arch21F (5'-TTC CGG TTG ATC CYG CC-3') (Delong 1992) and Arch915r (5'-GTG CTC CCC CGC CAA TTC-3') (Stahl 1991) and then re-amplified (nested PCR) prior to sequencing using the universal primers for the V4 region after (Caporaso, Lauber et al. 2012). qPCR was performed using a SYBR®Green I nucleic acid stain (Invitrogen) and using a Realplex quantitative PCR system (Eppendorf, Hauppauge, NY). The annealing temperature was set to 63.5 °C and reactions were stopped in the exponential phase. These libraries were sequenced on an Illumina MiSeq sequencing using the facilities of the W.M. Keck Center for Comparative and Functional Genomics, University of Illinois at Urbana-Champaign, IL, USA. Archaeal libraries resulted in 30 million OTUs. These sequences were processed in QIIME (Caporaso, Kuczynski et al. 2010, Orsi, Coolen et al. 2017) and a resulting OTU table was obtained using settings as described elsewhere (Orsi, Coolen et al. 2017). Singletons were removed from the dataset. Ecological statistics were calculated in R using a Bray Curtis distance in the Vegan package (https://cran.r-project.org/web/packages/vegan/index.html). Analysis of Similarity (ANOSIM) was carried out using 999 permutations with a Bray Curtis distance (Clarke 1993). Indicator Species Analysis (ISA) (Dufrene & Legendre 1997) was performed in the indicspecies package (De Caceres, Legendre et al. 2012) and significance was tested with a nonparametric procedure involving the Monte-Carlo permutation procedure with 999 permutations.

4.4 RESULTS

4.4.1 Chronology of the core and paleo-environment

The age model used to establish the timing of depositional and environmental changes is based on radiocarbon dating of foraminiferal carbonates. The core spans 139 kyr of deposition spanning the Holocene (MIS1; last 10 ka), the deglacial and last glacial maximum (LGM) (MIS2; ~10-29 ka), the glacial MIS3 (~29-53 ka BP) and MIS4 (~53-72 ka BP), the alternate warmer and cooler climates of MIS5 (~72-127 ka BP) including the previous interglacial MIS5e (Eemian; 120-127 ka BP), and part of the previous glacial (MIS6; ~127-139 ka BP)(Fig. 1). XRF-Ca counts/s were above 40000 throughout the core except during the most recent a-planktonic phase that started during mid-MIS3 at 40 ka BP and lasted until the onset of the Holocene at 10 ka BP (Fig. 4.1). Foraminifera tests were absent from this a-planktonic phases as well as during the previous a-planktonic interval at the end of MIS6, which explains the absence of $\delta^{18}O$ data from foraminifera. Foraminiferal $\delta^{18}O$ values were most depleted during the Holocene and most enriched during MIS6 (Fig. 4.1). XRF Titanium used as a proxy for terrestrial input reached its maxima (3000 counts/s) during the recent a-planktonic phase but remained below 1000 counts/s in the remainder of the core. The total organic carbon (TOC) content and %N co-varied throughout the core with maximum values during the most recent a-planktonic (%TOC=1.5, %N = 0.15) and the short a-planktonic interval during MIS 6 (TOC=0.7, %N = 0.07) (Fig. 4.1). TOC and %N values were only ~0.15% and 0.01% in the remainder of the record. TEX_{86} derived SST were lowest (below $16^{O}C$) during the glacial maxima of MIS2 and MIS6. SST increased to 22 ^{O}C with the onset of the Eemian (MIS5e- penultimate interglacial) at 130 kaBP and reached modern day levels (~$26^{O}C$) during the peak Eemian at 123 to 119 kaBP. SST were also elevated (respectively 24 ^{O}C and 26 ^{O}C) during MIS5c (~96 ka BP) and MIS5a (~82 ka BP) and remained above 20 ^{O}C until MIS3 with the exception of short-term temperature declines to 18 ^{O}C and 17 ^{O}C at ~ 64 and 49 kaBP which correspond to the timing of Heinrich events H6 and H5a (Rashid, Hesse et al. 2003). During MIS3 a temperature drop occurred at ~38 kaBP which coincides with the timing of the H4 event (Schulz, von Rad et al. 1998). SST increased to 25 ^{O}C at ~ 31 kaBP and dropped drastically with onset of MIS2 to 16 ^{O}C and remained below 20 ^{O}C until ~17 kaBP, which marks the last glacial maximum (LGM). SST reached modern day levels with the onset of the Holocene at ~ 10 ka BP. $\delta^{13}C$ values of bulk organic matter were most depleted (~21 ‰) during the a-planktonic intervals. Total DNA content is expressed as pg $(g\ sediment)^{-1}$ and ng $(g\ TOC)^{-1}$) showing an exponential decline of over four orders of magnitude during the first 40 kyrs but remained relatively constant in sediments older than 40 ka (Fig. 4.1).

4.4.2 Down-core archaeal distribution

After stringent removal of OTUs that also occurred in the sequenced controls, the genomic libraries of the sampled sediment intervals revealed a total of 4675 archaeal OTUs, mostly belonging to Crenarchaeota (3867 OTUs) and to a lesser extent Euryarchaeota (808 OTUs). Crenarchaeota comprised less than 40% of the total archaeal OTUs in sediments deposited during warm climate stages (Eemian, MIS5C, MIS5C, and the entire Holocene) and reached 90-100% of total archaeal OTUs in glacial sediments. Crenarchaeotal OTUs belonged to 6 main classes: Marine Benthic Group A (MBGA, 98 OTUs), Marine Benthic Group B (MBGB, 607 OTUs), Miscellaneous Crenarchaeota group (MCG, 2633 OTUs), Marine Hydrothermal Vent Group (MHVG, 14 OTUs), Thaumarchaeota (452 OTUs) and Terrestrial Hot Spring Crenarchaeota Group (THSCG, 3 OTUs). MBGA contributed up to 4% to total crenarchaeotal abundance mainly in the Holocene sediments (Fig. 4.2). MBGB comprised >70% of Crenarchaeota during MIS6, MIS4, most of MIS3 and early MIS2 and less than 30% in MIS5. MBGB showed a distinct drop in abundance during H4 event at 39 ka BP. Their contribution was lowest in sediments spanning the LGM and deglacial and were not detected in the Holocene sediments (Fig. 4.2). The relative abundance of MCG followed the opposite trend of MBGB except for the early MIS5 including the Eemian and the Holocene where total crenarchaeota remained low. The majority of MCG were unclassified, except those belonging to the uncultivated orders B10 and pGrf_C26, which were especially abundant during glacial maxima (respectively up to 40% of MCG during MIS2 and up to 10% of MCG during MIS6) (Fig. 4.2). MHVG OTUs were only present during peak LGM at 24 ka BP and contributed up to 2% to the total crenarchaeotal OTUs. Marine Thaumarchaeota were sporadically relatively abundant in sediments younger than 80 kyr (Fig. 4.2).

Euryarchaeota represented 90 to 100% of total archaeal OTUs in sediments deposited during the warm intervals of MIS5 (Eemian, MIS5c, MIS5a) as well as in Holocene sediments. Euryarchaeotal OTUs belonged to mainly three classes – Thermoplasmata (465 OTUs), Methanobacteria (280 OTUs) and Deep Sea Euryarchaeotal Group (DSEG, 44 OTUs). Methanobacteria and Thermoplasmata were the most abundant Euryarchaeota in MIS5 substages and the Holocene respectively. DSEG OTUs were only present during MIS2 and contributed less than 10% to total Euryarchaeota (Fig. 4.2).

Figure 4.3 shows the relative abundance of classified Thermoplasmata at the family level. Methanomassilicoccaceae comprised between 70 to 100% of total Thermoplasmata in Holocene sediments. Deep Hydrothermal Vent Euryarchaeota Group 1 (DHVEG1) were the

most abundant classified Thermoplamata in MIS2 and with sporadic high relative abundance in MIS5 sediments. The Terrestrial Miscellaneous Euryarchaeota Group (TMEG) and 20c-4 were only detected in MIS2 sediments where they comprised less than 0.2% of the total Thermoplasmata. Surface water Marine Group II OTUs were only detected (less than 0.3% of total Thermoplasmata) in Holocene sediments, while deep water Marine Group III OTUs maintained very low but continuous presence (max 0.01% of the total Thermoplasmata) throughout the core.

4.4.3 Correlation between the paleodepositional environment and archaeal communities

To characterize which factors influenced the changes in the subsurface archaeal community composition Non-Metric Multidimensional Scaling Analysis (NMDS) and Analysis of Similarity (ANOSIM) (Clarke 1993) was performed (Fig. 4.4). This analysis showed a moderate, but significant response of the sedimentary archaeal communities to changes in sediment lithology (R=0.48; P=0.001) and a strong significant response to changes in paleodepositional conditions associated with MIS stages and their transitions (ANOSIM; R=0.73; P=0.001) (Fig. 4). Based on this outcome, an indicator species analysis (ISA) was then performed to identify which OTUs were significant indicators of individual MIS.

Canonical Correspondence Analysis (CCA) (Fig. 4.5) further revealed that variations in archaeal species abundance in sediments deposited during the Holocene was influenced strongly with SST and δ13C. In sediments deposited during the aplanktonic interval-2 (12 - 27 ka BP), nitrogen and TOC contents revealed a strong correlation while terrigenous titanium content revealed a weaker but significant ($p<0.05$) correlation with archaeal species abundance. Calcium content was the key influential factor in Eemian sediments.

4.4.4 Indicator species analysis (ISA)

ISA revealed a total of 278 indicator species for all MIS combined. These OTU indicators are enlisted in tables 4.1 to 4.6 along with their specificity (A) and sensitivity (B) values. A-value of 1 implies that the indicator species occurs in only one sample category, while a B-value of 1 indicates that this species occurs in all samples of that category. The Holocene (MIS1) yielded total of 85 indicator OTUs with 44 crenarchaeotal OTUs and 41 euryarchaeotal OTUs. These mainly comprised of MBGA and Thaumarchaeota (Crenarchaeota with A values > 0.9 and B values > 0.5) and euryarchaeotal Thermoplasmata (37 OTUs with A and B >0.9) and methanobacteria (4 OTUs with A values > 0.9 and B=1) (Table 4.1). The largest number of indicator species were identified in MIS2 sediments: 129 crenarchaeotal OTUs

(predominantly MCG) and 18 euryarchaeotal OTUs (predominantly Thermoplasmata). All indicator OTUs of MIS2 had A values > 0.65 and B values > 0.5 (Table 4.2).

MIS3 and MIS4 revealed 3 and 10 indicator OTUS respectively all belonging to crenarchaeotal MBGB group with A values > 0.8 and B values > 0.55 (Table 4.3, 4.4). 23 OTUs with A and B values > 0.6 were indicative of MIS5. Methanobacteria solely dominated these indicator OTUs with 18 OTUs, followed by 3 OTUs of MBGB and 2 OTUs of MCG (Table 4.5). MIS6 revealed 10 indicator OTUs belonging mainly to MBGB (8 OTUs) (Table 4.6).

4.5 DISCUSSION

4.5.1 Archaeal distribution pattern

MCG were among the most abundant group of Archaea in the sapropel interval deposited during MIS2. This interval differs from the carbon-lean MCG-rich deeper sediments by the relatively high abundance of the uncultivated B10 group. Inferring metabolic properties based on 16S-inferred taxonomic relationships is highly speculative, but it is possible that these MCG are involved in the degradation of labile organic matter in the MIS2 sapropelic interval. For example, single cell sequencing of MCG in marine sediments revealed the presence of genes encoding extracellular protein-degrading enzymes such as gingipain and clostripain (Lloyd, Schreiber et al. 2013). The Thermoplasmata group DHVEG-1, commonly found in hydrothermal vent systems, was also abundant in the MIS2 sapropel. Members of this group are known to be able to degrade detrital proteins in marine sediments using extracellular protein degrading enzymes (Lloyd, Schreiber et al. 2013). The presence of easily biodegradable organic matter has previously been reported from late-Pleistocene Mediterranean sapropels (Coolen et al., 2002). The timing of the sapropel coincides with the glacial lowstand, and the subsequent increased salinity that resulted in the deposition of the a-planktonic interval. The simultaneous increase in Titanium indicates an increased terrigenous input at that time, which is also reflected by the distinct presence of the terrestrial miscellaneous Euryarchaeota group (TMEG).

MBGB followed the opposite trend of MCG except for the sediments deposited early during MIS5 including the Eemian and the Holocene. MBGB have been found to be abundant at the Sulfate Methane Transition Zone (SMTZ) in other sediment records (Sorensen and Teske 2006), but in the Red Sea sediments this group shows multiple relative abundance maxima in intervals older than MIS2. They have been shown to prefer eutrophic subsurface sediments (Durbin and Teske 2012) whereas in our core, their abundance does not correlate with TOC content (R= 0.17; P= 0.145). Furthermore, MCG and MBGB deposited during the aplanktonic

interval (12.3-27.8ka) were influenced by nitrogen content and increased total organic carbon as shown in Fig. 4.5 which is explained by organic matter degrading activity of both these groups as described above. Crenarchaeotal MBGA have been found in oxygen minimum zone (OMZ) located sediments (Xia, Guo et al. 2017). In the Red Sea core they comprised up to 4% of total archaea and only occurred in the Holocene interval. The continuous dominant co-presence of strictly anaerobic methanogenic archaea (Thermoplasmata; Methanomassiliicoccaceae) in the Holocene sediments suggests a completely anaerobic lifestyle of the MBGA. Members of Methanomassiliicoccaceae produce methane in a distinct way: They use H_2 as electron donor but are not able to reduce CO_2 directly to CH_4 (Dridi, Fardeau et al. 2012). Instead, H_2 is used to reduce methanol and methylamines for methanogenesis (Lang, Schuldes et al. 2015) and they may form a syntrophic relation with bacteria (Offre, Spang et al. 2013) in the Red Sea subsurface sediments that produce molecular hydrogen and fermentative by-products. MBGA could be essential partners in this syntrophic relationship. Hydrogenotrophic methanogenic Methanobacteria prevailed in the majority of MIS5 sediments. These methanogens are likely to be vertically separated from Methanomassiliicoccaceae since Methanobacteria can reduce CO_2 directly to methane or reduce formate in the absence of CO_2 to methane. The MCG that prevailed in this organic-lean section of the core are likely to differ in their metabolic capabilities from the phylogenetically different MCG counterparts in the MIS2 sapropel. In the carbon-lean interval, MCG may be incorporating CO_2 into bicarbonates as a part of dark carbon fixation. This ability was shown in lab experiments through cloning of the functional gene acetyl-CoA carboxylase (accC) from MCG and isotopic labelling experiments with ^{14}C-bicarbonate (Lliros, Alonso-Saez et al. 2011).Methanobacterial abundance is influenced by calcium content in the sediments (Fig. 4.5) which needs more investigation.

4.5.2 Role of paleodepositional environment in shaping the subseafloor archaeal microbiome.

The downcore variations in relative abundance and diversity of the different archaeal taxa cannot entirely be explained by the metabolic potential of the presumable living and active archaeal groups as described above. If this was the case, one would expect to find a strong correlation with the downcore distribution of archaeal communities and lithology type. While this correlation was moderately strong (ANOSIM; $P<0.05$; $R=0.48$), a strong correlation ($R=0.73$) was observed between the downcore distribution of archaeal communities and the marine isotope stages and their transitions since the last 140 kyr when lithologies did not necessarily co-vary. This implies that a larger fraction of the subseafloor archaeal

communities was selected by changes in paleoenvironmental conditions that prevailed in the overlying water column at the time of deposition. Even at phylum level, Crenarchaeota were shown to predominate in sediments deposited during glacial periods (MIS6, MIS4, MIS3 and MIS2) while Euryarchaeota predominated during major interglacials (Eemian and the Holocene). A paleodepositional selection of subseafloor archaeal communities has also been reported from other oceanic settings. For example, archaeal communities were found to differ significantly in coastal sediments of the Sea of Okhotsk (Japan) that harboured different geohydrothermal horizons (Inagaki, Suzuki et al. 2003), and archaeal communities in late glacial lake sediments of Hässeldala Port (Sweden) correlated with past changes in lake water temperature and duration of lake ice cover rather than with sediment lithology (Ahmed, Parducci et al. 2018).

In addition, strong correlations were also observed between the vertical distribution of subseafloor archaea and quantitative paleoenvironmental proxy measurements. Notably, past SST played a significant role in shaping Holocene communities which were mainly represented by Thermoplasmata. An increased abundance of Thermoplasmata with with elevated SST is also evident from elevated 16S rRNA gene copy numbers during peak MIS5c at 100ka. Total DNA content declined two orders of magnitude in the first 30,000 year and then remained constant for the rest of the core. A similar trend was observed for the number of archaeal 16S copies per gram of sediment with lowest copy numbers during the early stage of the a-planktonic interval just prior to MIS2. The fact that irrespective of TOC content, both total DNA content and archaeal copy numbers did not decrease exponentially with depth and age of the sediments, indicates that a substantial fraction of archaea may be seeded from the overlying water column and that archaeal activities in sediments older than 30 kyrs are growth limited undergoing weak postburial selection (Orsi et al., 2017). This could explain their strong correlation with the different marine isotope stages and their transitions. Archaeal groups identified through sedimentary 16S profiling that are likely not to be indigenous to the sediments include the dominant crenarchaeotal class Thaumarchaeaota, which comprises known ammonia oxidizing archaea (AOA) and are important primary producers in the ocean (Wuchter et al., 2006) as well as in oxygenated marine surface sediments (Orsi, 2018). These are strictly aerobic archaea and have never been observed living under anaerobic conditions and hence should represent a signal from the past. Other groups normally found in marine waters include the Marine Group II Euryarchaeota, which are the the most abundant archaea in surface waters (Zhang and Rodriquez-Valera, 2015), were recovered at low abundance only in the Holocene sediments. One could argue that the

absence of their DNA in the older sediments is a result of DNA degradation, but increased DNA degradation with sediment depth would not have resulted in a continuous low relative abundance of Marine Group III Euryarchaeota, normally found in low abundance in mid to deep oceanic waters (Zhang and Rodriquez-Valera, 2015), throughout the sediments record. In addition, the co-occurrence of TMEG during increased terrestrial input during MIS2 indicates a paleoenvironmental selection from distant sources.

4.6 CONCLUSIONS

In summary, a highly resolved 16S survey combined with paleo-oceanographic proxy data using well dated sediments from the norther Red Sea suggest that sedimentary DNA originates from both active archaeal communities especially in sediments younger than 30 kyrs and a greater contribution of communities that underwent weak postburial selection in older sediments. Active processes may include methylotrophic methanogenesis by Methanomassiliicoccaceae in the Holocene Sahara dust sediments, proteolytic degradation in the MIS2 sapropel possibly by MCG and MHVG, dark carbon fixation in MIS3, MIS4 and late MIS5 carbonate oozes by different MCG, and formatotrophic methanogensis in MIS5 by Methanobacteria. Evidence that not all DNA was derived from indigenous sedimentary Archaea was provided by the presence of ancient DNA from allochthonous sources – Thaumarchaeota, MGII and MGIII stemming from the overlying water column at the time of deposition as well as terrestrial derived TMEG. Since many of the archaeal groups represent uncultivated groups, future single-cell genomics as well as metatranscriptomic surveys will be required to better elucidate the activity and origin of subseafloor archaea and to increase our understanding of their possible relation to the paleodepositional environment and their suitability as a proxy for past environmental conditions and biogeochemical cycling processes.

Acknowledgements

This work was primarily supported by KAUST-WHOI Special Academic Partnership Program OCRF-SP-WHOI-2013 (grants 7000000463 to XI and 7000000464 to MJLC). Kuldeep More thanks the co-chiefs, scientific participants, captain and crew of the RV Aegaeo. Data has been deposited to SRA (Sequence Read Archive) NCBI under Bio project: PRJNA507921.

4.7 FIGURES

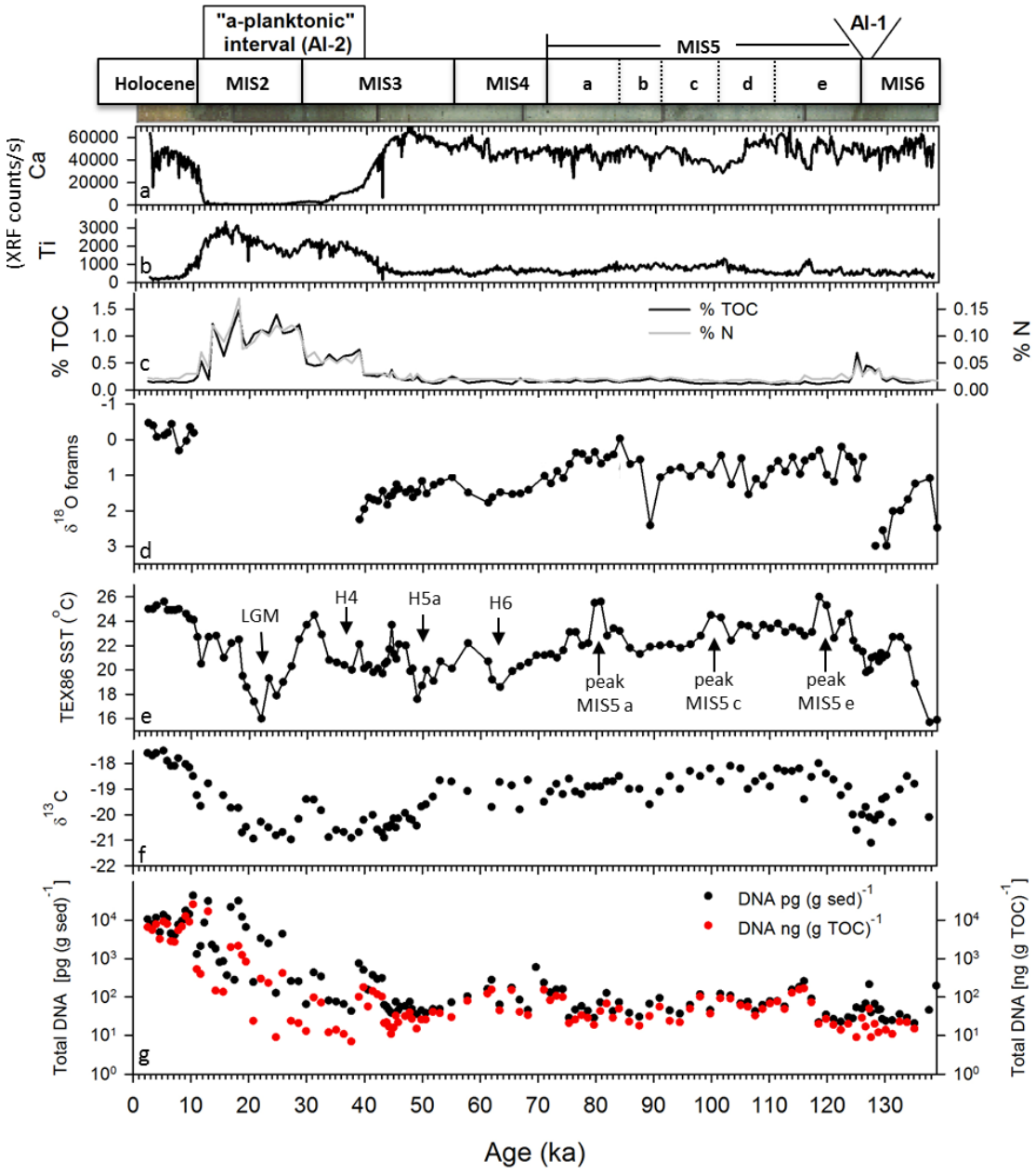

Figure 4.1 Geochemical proxies (a) Calcium and (b) Titanium XRF profiles, (c) TOC content in Black vs %N record in grey (d) foraminiferal δ18O record (e) TEX86 derived SST profile (f) $\delta^{13}C$ content (g) Total DNA content obtained per gram of sediment (black) vs per gram of TOC (red).

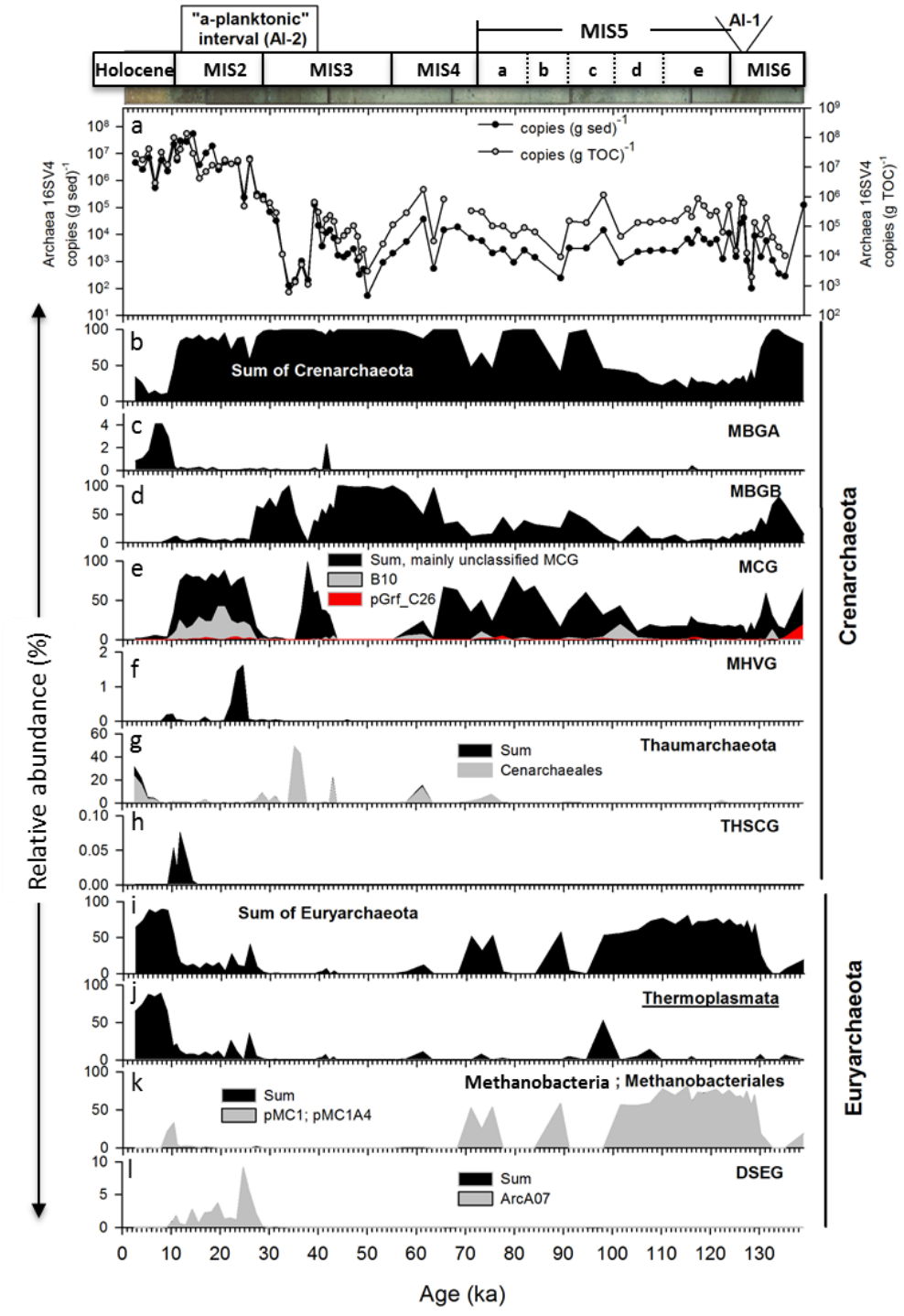

Figure 4.2 Total archaeal distribution throughout the core. (a) Archaeal 16SV4 copies per gram of sediment (black) vs per gram of TOC (grey), (b) Total crenarchaeota. Relative abundance of crenarachaeotal groups (c) Marine Benthic Group A (d) Marine Benthic Group B (e) Marine Crenarchaeota Group (f) Marine Hydrothermal Vent Group (g) Thaumarchaeota (h) Terrestrial Hot Spring Crenarchaeota Group, (i) distribution of total Eukaryota, relative abundance of Euryarchaeotal groups (j) Thermoplasmata (k) Mathanobacteria and (l) Deep Sea Euryarchaeota group.

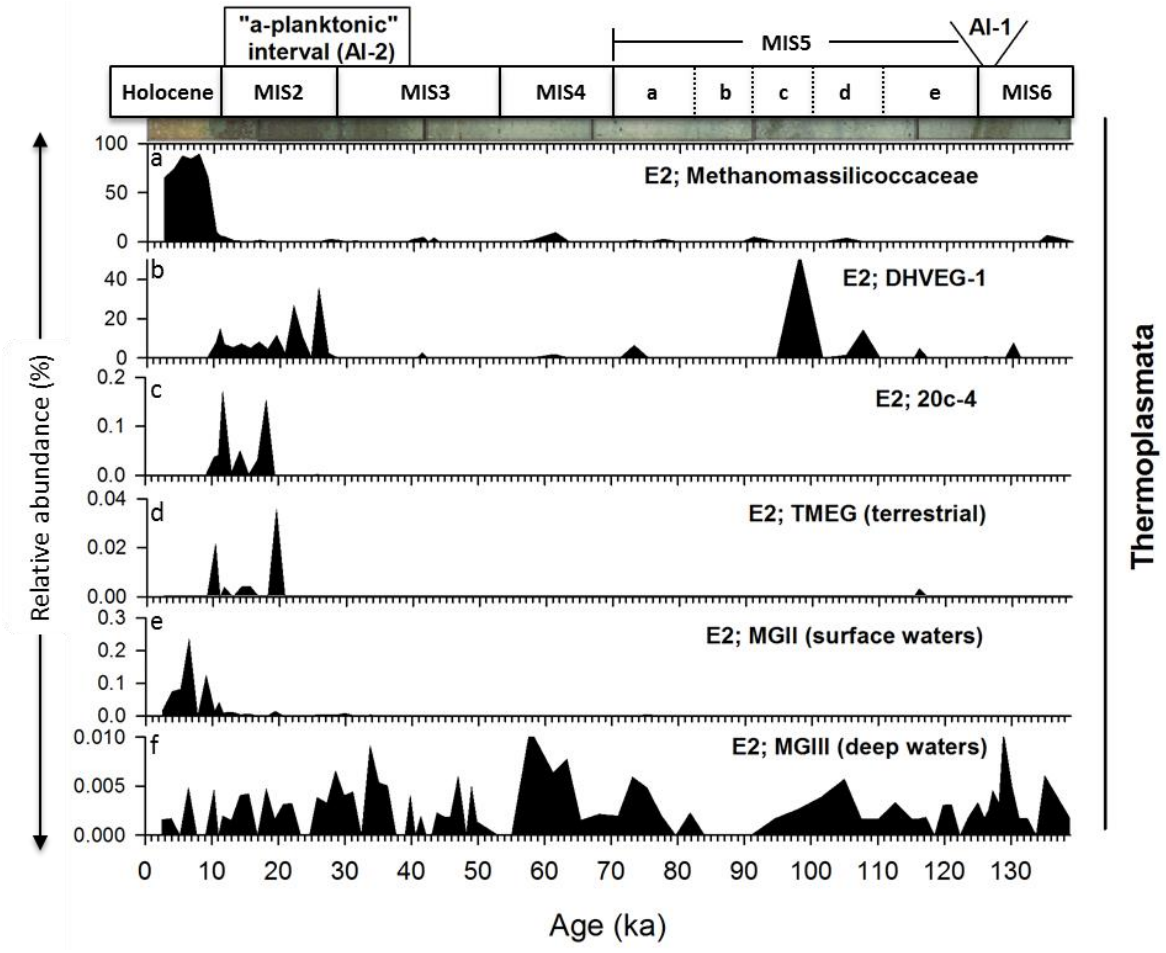

Figure 4.3 Relative abundance of Thermoplasmata groups (a) Methanomassilicoccaceae (b) Deep Hydrothermal Vent Euryarchaeotal Group-1 (c) uncultured group 20c-4 (d) Terrestrial Miscellaneous Euryarchaeota group (e) Marine group II and (f) Marine group III.

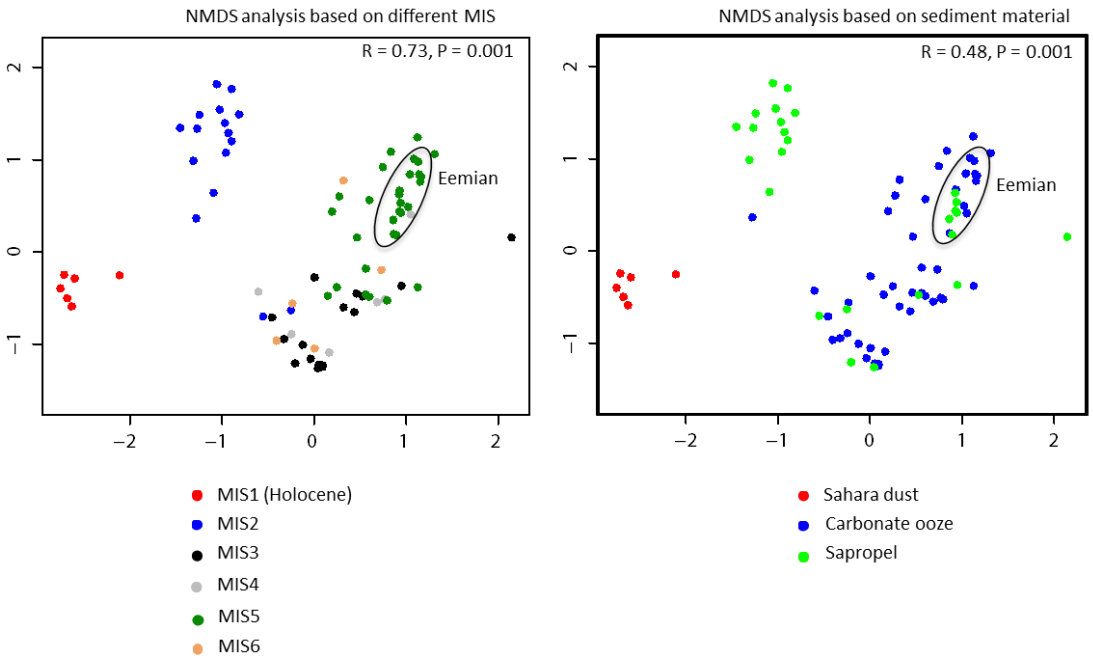

Figure 4.4 NMDS analysis of community compositions of total archaea in two categories. NMDS stress was < 0.05 in all the analyses. R value and P value of each NMDS analysis are indicated at upper right corner. P value indicates significance levels, while R value denotes the strength of the analysed factors on the samples. R value close to 1 indicates high separation between treatment samples, while R value close to 0 indicates no separation. Axes in NMDS are arbitrary.

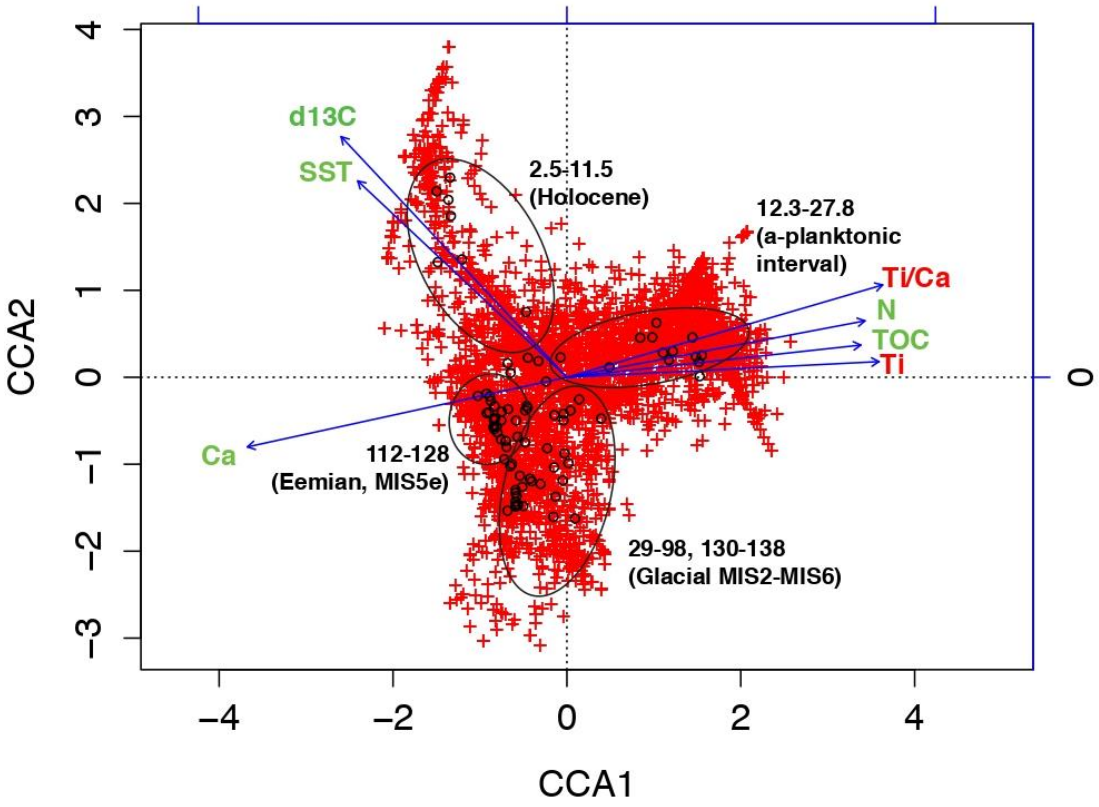

Figure 4.5 Canonical Correspondence Analysis (CCA) plot showing the relationship between archaeal abundance and environmental proxies. Green lables indicate stronger correlation while red lables indicate weak correlation. Axes in CCA are arbitrary.

4.8 TABLES

Indicator species analysis for sediments deposited during different MIS with specificity (A-value) vs. sensitivity (B-value) of each indicator species. A-value of 1 indicates that the indicator species occurs in only one indicator category tested, while a B-value of 1 indicates that this species occurs in all samples of that category. Species names are written in the format "Taxa (r-value)".

Table 4.1 Indicator species for sediments deposited during MIS1

Phylum; class; OTUs (stat value)	A value	B value
Crenarchaeota; Aigarchaeota; 20338 (0.707)	1	0.5
Crenarchaeota; MBGA; 11007 (0.707)	1	0.5
Crenarchaeota; MBGA; 12510 (0.816)	1	0.6667
Crenarchaeota; MBGA; 12960 (0.913)	1	0.8333
Crenarchaeota; MBGA; 1385 (0.803)	0.9665	0.6667
Crenarchaeota; MBGA; 14555 (0.871)	0.9103	0.8333
Crenarchaeota; MBGA; 18143 (0.913)	0.9994	0.8333
Crenarchaeota; MBGA; 2000 (0.707)	1	0.5
Crenarchaeota; MBGA; 20466 (0.707)	1	0.5
Crenarchaeota; MBGA; 2805 (0.707)	1	0.5
Crenarchaeota; MBGA; 3203 (0.999)	0.9984	1
Crenarchaeota; MBGA; 4357 (0.993)	0.9854	1
Crenarchaeota; MBGA; 4598 (1)	0.9992	1
Crenarchaeota; MBGA; 591 (0.707)	1	0.5
Crenarchaeota; MBGA; 7635 (0.996)	0.9929	1
Crenarchaeota; MBGA; 7886 (0.707)	1	0.5
Crenarchaeota; MBGA; 8346 (0.816)	1	0.6667
Crenarchaeota; MBGA; 8918 (0.694)	0.962	0.5
Crenarchaeota; MBGA; 9069 (0.7)	0.9808	0.5
Crenarchaeota; MBGA; 9243 (0.882)	0.933	0.8333
Crenarchaeota; MCG; 11472 (0.816)	0.9995	0.6667
Crenarchaeota; MCG; 11969 (0.707)	1	0.5
Crenarchaeota; MCG; 12538 (0.993)	0.9869	1
Crenarchaeota; MCG; 1439 (0.913)	1	0.8333
Crenarchaeota; MCG; 14633 (0.991)	0.9818	1

Crenarchaeota; MCG; 16372 (0.793)	0.9424	0.6667
Crenarchaeota; MCG; 17420 (0.707)	1	0.5
Crenarchaeota; MCG; 17707 (1)	1	1
Crenarchaeota; MCG; 4052 (0.913)	1	0.8333
Crenarchaeota; MCG; 8018 (1)	1	1
Crenarchaeota; MCG; 8117 (0.996)	0.9913	1
Crenarchaeota; Thaumarchaeota; 10305 (0.816)	0.998	0.6667
Crenarchaeota; Thaumarchaeota; 1066 (0.707)	1	0.5
Crenarchaeota; Thaumarchaeota; 12819 (0.816)	1	0.6667
Crenarchaeota; Thaumarchaeota; 13065 (0.805)	0.9717	0.6667
Crenarchaeota; Thaumarchaeota; 17683 (0.707)	1	0.5
Crenarchaeota; Thaumarchaeota; 2449 (0.91)	0.9942	0.8333
Crenarchaeota; Thaumarchaeota; 4102 (0.707)	1	0.5
Crenarchaeota; Thaumarchaeota; 4173 (0.707)	1	0.5
Crenarchaeota; Thaumarchaeota; 5041 (0.816)	1	0.6667
Crenarchaeota; Thaumarchaeota; 5083 (0.806)	0.9754	0.6667
Crenarchaeota; Thaumarchaeota; 5791 (0.707)	1	0.5
Crenarchaeota; Thaumarchaeota; 6550 (0.851)	0.8689	0.8333
Crenarchaeota; Thaumarchaeota; 8760 (0.707)	1	0.5
Euryarchaeota; Methanobacteria; 13084 (0.707)	1	0.5
Euryarchaeota; Methanobacteria; 2355 (0.707)	1	0.5
Euryarchaeota; Methanobacteria; 5923 (0.707)	1	0.5
Euryarchaeota; Methanobacteria; 893 (0.999)	0.9977	1
Euryarchaeota; Thermoplasmata; 10668 (0.995)	0.9905	1
Euryarchaeota; Thermoplasmata; 11010 (1)	1	1
Euryarchaeota; Thermoplasmata; 11591 (0.913)	1	0.8333
Euryarchaeota; Thermoplasmata; 11771 (1)	1	1
Euryarchaeota; Thermoplasmata; 13201 (0.99)	0.9808	1
Euryarchaeota; Thermoplasmata; 13547 (0.79)	0.9371	0.6667
Euryarchaeota; Thermoplasmata; 14030 (0.987)	0.974	1
Euryarchaeota; Thermoplasmata; 1485 (0.913)	1	0.8333
Euryarchaeota; Thermoplasmata; 1516 (0.794)	0.9459	0.6667
Euryarchaeota; Thermoplasmata; 16188 (0.904)	0.9808	0.8333

Euryarchaeota; Thermoplasmata; 16689 (0.891)	0.9534	0.8333
Euryarchaeota; Thermoplasmata; 17052 (0.967)	0.9346	1
Euryarchaeota; Thermoplasmata; 17201 (0.913)	1	0.8333
Euryarchaeota; Thermoplasmata; 1789 (0.889)	0.9478	0.8333
Euryarchaeota; Thermoplasmata; 18051 (0.913)	1	0.8333
Euryarchaeota; Thermoplasmata; 18385 (0.994)	0.9875	1
Euryarchaeota; Thermoplasmata; 18506 (1)	1	1
Euryarchaeota; Thermoplasmata; 19677 (0.999)	0.9985	1
Euryarchaeota; Thermoplasmata; 19801 (0.802)	0.9639	0.6667
Euryarchaeota; Thermoplasmata; 20792 (0.953)	0.9076	1
Euryarchaeota; Thermoplasmata; 20876 (0.749)	0.8416	0.6667
Euryarchaeota; Thermoplasmata; 21320 (0.994)	0.9876	1
Euryarchaeota; Thermoplasmata; 2876 (0.707)	1	0.5
Euryarchaeota; Thermoplasmata; 2925 (0.816)	1	0.6667
Euryarchaeota; Thermoplasmata; 3258 (0.981)	0.9626	1
Euryarchaeota; Thermoplasmata; 326 (0.816)	1	0.6667
Euryarchaeota; Thermoplasmata; 3814 (0.999)	0.9983	1
Euryarchaeota; Thermoplasmata; 4541 (0.996)	0.992	1
Euryarchaeota; Thermoplasmata; 4884 (0.816)	1	0.6667
Euryarchaeota; Thermoplasmata; 6814 (1)	1	1
Euryarchaeota; Thermoplasmata; 7587 (0.97)	0.9407	1
Euryarchaeota; Thermoplasmata; 7723 (0.988)	0.9756	1
Euryarchaeota; Thermoplasmata; 889 (0.773)	0.7166	0.8333
Euryarchaeota; Thermoplasmata; 9015 (0.913)	1	0.8333
Euryarchaeota; Thermoplasmata; 9126 (1)	1	1
Euryarchaeota; Thermoplasmata; 9225 (0.841)	0.8487	0.8333
Euryarchaeota; Thermoplasmata; 9797 (0.99)	0.9808	1

Table 4.2 Indicator species for sediments deposited during MIS2

Phylum; class; OTUs (stat value)	A value	B value
Crenarchaeota; MBGA; 8378 (0.707)	1	0.5
Crenarchaeota; MBGA; 21083 (0.75)	1	0.5625
Crenarchaeota; MBGB; 2287 (0.707)	1	0.5
Crenarchaeota; MBGB; 2379 (0.702)	0.7163	0.6875
Crenarchaeota; MBGB; 4684 (0.8)	0.9302	0.6875
Crenarchaeota; MBGB; 11844 (0.785)	0.8952	0.6875
Crenarchaeota; MBGB; 14072 (0.829)	1	0.6875
Crenarchaeota; MBGB; 20930 (0.661)	1	0.4375
Crenarchaeota; MCG; 200 (0.831)	0.9212	0.75
Crenarchaeota; MCG; 869 (0.707)	1	0.5
Crenarchaeota; MCG; 1008 (0.778)	0.9686	0.625
Crenarchaeota; MCG; 1083 (0.718)	0.825	0.625
Crenarchaeota; MCG; 1097 (0.829)	1	0.6875
Crenarchaeota; MCG; 1229 (0.866)	1	0.75
Crenarchaeota; MCG; 1308 (0.789)	0.9048	0.6875
Crenarchaeota; MCG; 1571 (0.707)	1	0.5
Crenarchaeota; MCG; 2006 (0.753)	0.8251	0.6875
Crenarchaeota; MCG; 2443 (0.791)	1	0.625
Crenarchaeota; MCG; 2520 (0.707)	1	0.5
Crenarchaeota; MCG; 2944 (0.694)	0.9638	0.5
Crenarchaeota; MCG; 3127 (0.661)	1	0.4375
Crenarchaeota; MCG; 3305 (0.75)	0.9	0.625
Crenarchaeota; MCG; 3712 (0.824)	0.9058	0.75
Crenarchaeota; MCG; 3719 (0.891)	0.793	1
Crenarchaeota; MCG; 3825 (0.741)	0.977	0.5625
Crenarchaeota; MCG; 3973 (0.798)	0.849	0.75
Crenarchaeota; MCG; 3977 (0.791)	1	0.625
Crenarchaeota; MCG; 4077 (0.707)	1	0.5
Crenarchaeota; MCG; 4094 (0.845)	0.9525	0.75
Crenarchaeota; MCG; 4488 (0.8)	0.932	0.6875
Crenarchaeota; MCG; 4787 (0.825)	0.9083	0.75

Crenarchaeota; MCG; 4864 (0.75)	1	0.5625
Crenarchaeota; MCG; 4988 (0.786)	0.9883	0.625
Crenarchaeota; MCG; 5008 (0.75)	1	0.5625
Crenarchaeota; MCG; 5137 (0.865)	0.9972	0.75
Crenarchaeota; MCG; 5465 (0.791)	1	0.625
Crenarchaeota; MCG; 5778 (0.791)	1	0.625
Crenarchaeota; MCG; 6022 (0.829)	0.9989	0.6875
Crenarchaeota; MCG; 6462 (0.823)	0.9859	0.6875
Crenarchaeota; MCG; 6588 (0.789)	0.6642	0.9375
Crenarchaeota; MCG; 6626 (0.71)	0.8077	0.625
Crenarchaeota; MCG; 6862 (0.968)	0.9997	0.9375
Crenarchaeota; MCG; 7026 (0.661)	1	0.4375
Crenarchaeota; MCG; 7070 (0.739)	0.9701	0.5625
Crenarchaeota; MCG; 7134 (0.804)	0.9398	0.6875
Crenarchaeota; MCG; 7469 (0.707)	1	0.5
Crenarchaeota; MCG; 7597 (0.75)	1	0.5625
Crenarchaeota; MCG; 7729 (0.791)	1	0.625
Crenarchaeota; MCG; 8110 (0.699)	0.9762	0.5
Crenarchaeota; MCG; 8204 (0.661)	1	0.4375
Crenarchaeota; MCG; 8652 (0.829)	1	0.6875
Crenarchaeota; MCG; 8685 (0.75)	1	0.5625
Crenarchaeota; MCG; 9012 (0.794)	0.916	0.6875
Crenarchaeota; MCG; 9283 (0.791)	0.9093	0.6875
Crenarchaeota; MCG; 9378 (0.791)	1	0.625
Crenarchaeota; MCG; 9609 (0.707)	1	0.5
Crenarchaeota; MCG; 9646 (0.857)	0.9799	0.75
Crenarchaeota; MCG; 9736 (0.791)	1	0.625
Crenarchaeota; MCG; 10265 (0.924)	0.9116	0.9375
Crenarchaeota; MCG; 10346 (0.75)	1	0.5625
Crenarchaeota; MCG; 10513 (0.661)	1	0.4375
Crenarchaeota; MCG; 10688 (0.952)	0.9067	1
Crenarchaeota; MCG; 11243 (0.788)	0.9946	0.625
Crenarchaeota; MCG; 11352 (0.829)	1	0.6875

Crenarchaeota; MCG; 11429 (0.791)	1	0.625
Crenarchaeota; MCG; 11705 (0.785)	0.8958	0.6875
Crenarchaeota; MCG; 11766 (0.684)	0.7496	0.625
Crenarchaeota; MCG; 11984 (0.856)	0.9768	0.75
Crenarchaeota; MCG; 12078 (0.75)	1	0.5625
Crenarchaeota; MCG; 12268 (0.777)	0.9658	0.625
Crenarchaeota; MCG; 12327 (0.866)	1	0.75
Crenarchaeota; MCG; 12576 (0.739)	0.7936	0.6875
Crenarchaeota; MCG; 12810 (0.75)	1	0.5625
Crenarchaeota; MCG; 12847 (0.791)	1	0.625
Crenarchaeota; MCG; 12861 (0.829)	1	0.6875
Crenarchaeota; MCG; 13236 (0.723)	0.643	0.8125
Crenarchaeota; MCG; 13238 (0.661)	1	0.4375
Crenarchaeota; MCG; 13358 (0.776)	0.8753	0.6875
Crenarchaeota; MCG; 13476 (0.705)	0.9945	0.5
Crenarchaeota; MCG; 13612 (0.781)	0.976	0.625
Crenarchaeota; MCG; 13639 (0.707)	1	0.5
Crenarchaeota; MCG; 13737 (0.866)	1	0.75
Crenarchaeota; MCG; 13853 (0.761)	0.8423	0.6875
Crenarchaeota; MCG; 14194 (0.707)	1	0.5
Crenarchaeota; MCG; 14252 (0.859)	0.9845	0.75
Crenarchaeota; MCG; 15190 (0.785)	0.8207	0.75
Crenarchaeota; MCG; 15237 (0.849)	0.9614	0.75
Crenarchaeota; MCG; 15508 (0.791)	1	0.625
Crenarchaeota; MCG; 15560 (0.829)	1	0.6875
Crenarchaeota; MCG; 15796 (0.776)	0.8755	0.6875
Crenarchaeota; MCG; 15844 (0.822)	0.9828	0.6875
Crenarchaeota; MCG; 15911 (0.96)	0.9207	1
Crenarchaeota; MCG; 15948 (0.75)	1	0.5625
Crenarchaeota; MCG; 16108 (0.748)	0.9936	0.5625
Crenarchaeota; MCG; 16422 (0.822)	0.9828	0.6875
Crenarchaeota; MCG; 16551 (0.707)	1	0.5
Crenarchaeota; MCG; 17029 (0.791)	1	0.625

Crenarchaeota; MCG; 17243 (0.772)	0.9542	0.625
Crenarchaeota; MCG; 17256 (0.707)	1	0.5
Crenarchaeota; MCG; 17515 (0.76)	0.8392	0.6875
Crenarchaeota; MCG; 17527 (0.775)	0.9612	0.625
Crenarchaeota; MCG; 17639 (0.776)	0.9629	0.625
Crenarchaeota; MCG; 17724 (0.661)	1	0.4375
Crenarchaeota; MCG; 17733 (0.829)	0.9161	0.75
Crenarchaeota; MCG; 17766 (0.865)	0.9974	0.75
Euryarchaeota; Thermoplasmata; 20359 (0.661)	1	0.4375
Crenarchaeota; MCG; 17876 (0.791)	1	0.625
Crenarchaeota; MCG; 17968 (0.791)	1	0.625
Crenarchaeota; MCG; 18063 (0.96)	0.9209	1
Crenarchaeota; MCG; 18245 (0.661)	1	0.4375
Crenarchaeota; MCG; 18461 (0.707)	1	0.5
Crenarchaeota; MCG; 18562 (0.817)	0.9707	0.6875
Crenarchaeota; MCG; 18920 (0.791)	1	0.625
Crenarchaeota; MCG; 18966 (0.815)	0.9663	0.6875
Crenarchaeota; MCG; 18983 (0.762)	0.9301	0.625
Crenarchaeota; MCG; 19316 (0.829)	1	0.6875
Crenarchaeota; MCG; 19590 (0.805)	0.943	0.6875
Crenarchaeota; MCG; 19610 (0.841)	0.8705	0.8125
Crenarchaeota; MCG; 19852 (0.767)	0.6725	0.875
Crenarchaeota; MCG; 19913 (0.817)	0.9703	0.6875
Crenarchaeota; MCG; 20013 (0.862)	0.8492	0.875
Crenarchaeota; MCG; 20465 (0.75)	1	0.5625
Crenarchaeota; MCG; 20471 (0.808)	0.9488	0.6875
Crenarchaeota; MCG; 21066 (0.75)	1	0.5625
Crenarchaeota; MHVG; 4062 (0.75)	1	0.5625
Crenarchaeota; Thaumarchaeota; 509 (0.724)	0.839	0.625
Crenarchaeota; Thaumarchaeota; 14667 (0.729)	0.9447	0.5625
Crenarchaeota; Unclassified; 227 (0.784)	0.8952	0.6875
Crenarchaeota; Unclassified; 4969 (0.75)	1	0.5625
Crenarchaeota; Unclassified; 19235 (0.912)	0.8881	0.9375

Euryarchaeota; DSEG; 3601 (0.75)	1	0.5625
Euryarchaeota; DSEG; 8304 (0.866)	1	0.75
Euryarchaeota; DSEG; 9040 (0.79)	0.999	0.625
Euryarchaeota; DSEG; 13672 (1)	0.9997	1
Euryarchaeota; Methanomicrobia; 5471 (0.791)	1	0.625
Euryarchaeota; Methanomicrobia; 18560 (0.791)	1	0.625
Euryarchaeota; Thermoplasmata; 1700 (0.75)	1	0.5625
Euryarchaeota; Thermoplasmata; 2867 (0.707)	1	0.5
Euryarchaeota; Thermoplasmata; 11298 (0.9)	0.9964	0.8125
Euryarchaeota; Thermoplasmata; 12376 (0.707)	0.9995	0.5
Euryarchaeota; Thermoplasmata; 12471 (0.791)	1	0.625
Euryarchaeota; Thermoplasmata; 13528 (0.966)	0.9963	0.9375
Euryarchaeota; Thermoplasmata; 14404 (0.998)	0.9964	1
Euryarchaeota; Thermoplasmata; 18405 (0.968)	0.9991	0.9375
Euryarchaeota; Thermoplasmata; 18440 (0.791)	1	0.625
Euryarchaeota; Thermoplasmata; 19337 (0.707)	1	0.5
Euryarchaeota; Thermoplasmata; 20242 (0.79)	0.9973	0.625

Table 4.3 Indicator species for sediments deposited during MIS3

Phylum; class; OTUs (stat value)	A value	B value
Crenarchaeota; MBGB; 10477 (0.689)	0.8387	0.5652
Crenarchaeota; MBGB; 15772 (0.775)	0.922	0.6522
Crenarchaeota; MBGB; 18764 (0.734)	0.8855	0.6087

Table 4.4 Indicator species for sediments deposited during MIS4

Phylum; class; OTUs (stat value)	A value	B value
Crenarchaeota; MBGB; 4334 (0.696)	0.7273	0.6667
Crenarchaeota; MBGB; 4838 (0.763)	0.5826	1
Crenarchaeota; MBGB; 5244 (0.711)	0.6074	0.8333
Crenarchaeota; MBGB; 5931 (0.726)	0.6326	0.8333
Crenarchaeota; MBGB; 7865 (0.728)	0.6363	0.8333
Crenarchaeota; MBGB; 9903 (0.76)	0.5772	1
Crenarchaeota; MBGB; 15191 (0.708)	0.751	0.6667
Crenarchaeota; MBGB; 16680 (0.709)	0.7549	0.6667
Crenarchaeota; MBGB; 18073 (0.781)	0.7312	0.8333
Crenarchaeota; MBGB; 18271 (0.687)	0.4724	1

Table 4.5 Indicator species for sediments deposited during MIS5

Phylum; class; OTUs (stat value)	A value	B value
Crenarchaeota; MBGB; 13003 (0.799)	0.911	0.7
Crenarchaeota; MBGB; 16430 (0.749)	0.7651	0.7333
Crenarchaeota; MBGB; 17644 (0.805)	0.8839	0.7333
Crenarchaeota; MCG; 810 (0.768)	0.737	0.8
Crenarchaeota; MCG; 3896 (0.781)	0.6098	1
Euryarchaeota; Methanobacteria; 1285 (0.73)	0.6942	0.7667
Euryarchaeota; Methanobacteria; 2439 (0.734)	0.7027	0.7667
Euryarchaeota; Methanobacteria; 4950 (0.709)	0.7928	0.6333
Euryarchaeota; Methanobacteria; 5528 (0.769)	0.7716	0.7667
Euryarchaeota; Methanobacteria; 6013 (0.785)	0.8047	0.7667
Euryarchaeota; Methanobacteria; 8232 (0.877)	0.7688	1
Euryarchaeota; Methanobacteria; 8358 (0.741)	0.7164	0.7667
Euryarchaeota; Methanobacteria; 8754 (0.755)	0.8541	0.6667
Euryarchaeota; Methanobacteria; 10421 (0.73)	1	0.5333
Euryarchaeota; Methanobacteria; 11375 (0.682)	0.8219	0.5667
Euryarchaeota; Methanobacteria; 12464 (0.775)	0.721	0.8333
Euryarchaeota; Methanobacteria; 15180 (0.741)	0.7483	0.7333
Euryarchaeota; Methanobacteria; 15680 (0.741)	0.8229	0.6667
Euryarchaeota; Methanobacteria; 15944 (0.828)	0.8933	0.7667
Euryarchaeota; Methanobacteria; 16226 (0.754)	0.7422	0.7667
Euryarchaeota; Methanobacteria; 18670 (0.785)	0.8799	0.7
Euryarchaeota; Methanobacteria; 19671 (0.696)	0.6927	0.7
Euryarchaeota; Methanobacteria; 20236 (0.762)	0.7566	0.7667

Table 4.6 Indicator species for sediments deposited during MIS6

Phylum; class; OTUs (stat value)	A value	B value
Crenarchaeota; Unclassified; 2483 (0.821)	0.843	0.8
Crenarchaeota; MBGB; 8 (0.828)	0.6857	1
Crenarchaeota; MBGB; 1154 (0.863)	0.9305	0.8
Crenarchaeota; MBGB; 5704 (0.663)	0.4398	1
Crenarchaeota; MBGB; 7427 (0.668)	0.4458	1
Crenarchaeota; MBGB; 8535 (0.695)	0.4828	1
Crenarchaeota; MBGB; 10673 (0.721)	0.8655	0.6
Crenarchaeota; MBGB; 13455 (0.738)	0.9079	0.6
Crenarchaeota; MBGB; 19931 (0.797)	0.7947	0.8
Crenarchaeota; MCG; 19867 (0.73)	0.6658	0.8

4.9 REFERENCES

Ahmed, E., Parducci, L., Unneberg, P., Agren, R., Schenk, F., Rattray, J.E., Han, L., Muschitiello, F., Pedersen, M.W., Smittenberg, R.H., Yamoah, K.A., Slotte, T., Wohlfarth, B., 2018. Archaeal community changes in Lateglacial lake sediments: Evidence from ancient DNA. Quaternary Sci Rev 181, 19-29.

Berg, I.A., Kockelkorn, D., Ramos-Vera, W.H., Say, R.F., Zarzycki, J., Hügler, M., Alber, B.E., Fuchs, G. 2010. Autotrophic carbon fixation in archaea. Nat Rev Microbiol. 2010 Jun;8(6):447-60. doi: 10.1038/nrmicro2365.

Cabello P, Roldán M, Moreno-Vivián C. 2004. Nitrate reduction and the nitrogen cycle in archaea. Microbiology 150(11):3527-3546, doi:10.1099/mic.0.27303-0.

Caporaso, J.G., Kuczynski, J., Stombaugh, J., Bittinger, K., Bushman, F.D., Costello, E.K., Fierer, N., Pena, A.G., Goodrich, J.K., Gordon, J.I., Huttley, G.A., Kelley, S.T., Knights, D., Koenig, J.E., Ley, R.E., Lozupone, C.A., McDonald, D., Muegge, B.D., Pirrung, M., Reeder, J., Sevinsky, J.R., Tumbaugh, P.J., Walters, W.A., Widmann, J., Yatsunenko, T., Zaneveld, J., Knight, R., 2010. QIIME allows analysis of high-throughput community sequencing data. Nat Methods 7, 335-336.

Caporaso, J.G., Lauber, C.L., Walters, W.A., Berg-Lyons, D., Huntley, J., Fierer, N., Owens, S.M., Betley, J., Fraser, L., Bauer, M., Gormley, N., Gilbert, J.A., Smith, G., Knight, R., 2012. Ultra-high-throughput microbial community analysis on the Illumina HiSeq and MiSeq platforms. Isme J 6, 1621-1624.

Clarke, K.R., 1993. Non-parametric multivariate analyses of changes in community structure. Australian Journal of Ecology 18, 117-143.

Coolen, M.J.L., Orsi, W.D., Balkema, C., Quince, C., Harris, K., Sylva, S.P., Filipova-Marinova, M., Giosan, L., 2013. Evolution of the plankton paleome in the Black Sea from the Deglacial to Anthropocene. P Natl Acad Sci USA 110, 8609-8614.

Coolen, M.J.L., Saenz, J.P., Giosan, L., Trowbridge, N.Y., Dimitrov, P., Dimitrov, D., Eglinton, T.I., 2009. DNA and lipid molecular stratigraphic records of haptophyte succession in the Black Sea during the Holocene. Earth Planet Sc Lett 284, 610-621.

Coolen, M.J.L., Cypionka, H., Sass, A.M., Sass, H., Overmann, J. 2002. Ongoing modification of Mediterranean Pleistocene sapropels mediated by prokaryotes. Science. 2002 Jun 28;296(5577):2407-10.

De Caceres, M., Legendre, P., Wiser, S.K., Brotons, L., 2012. Using species combinations in indicator value analyses. Methods Ecol Evol 3, 973-982.

Delong, E.F., 1992. Archaea in Coastal Marine Environments. P Natl Acad Sci USA 89, 5685-5689.

Dridi, B., Fardeau, M.L., Ollivier, B., Raoult, D., Drancourt, M., 2012. Methanomassiliicoccus luminyensis gen. nov., sp nov., a methanogenic archaeon isolated from human faeces. Int J Syst Evol Micr 62, 1902-1907.

Dufrene M, Legendre P (1997) Species assemblages and indicator species: The need for a flexible asymmetrical approach. Ecol Monogr, 67, 345-366.

Durbin, A.M., Teske, A., 2012. Archaea in organic-lean and organic-rich marine subsurface sediments: an environmental gradient reflected in distinct phylogenetic lineages. Front Microbiol 3.

Fenton, M., et al. (2000). "Aplanktonic zones in the Red Sea." Marine Micropaleontology 40(3): 277-294.

Grant, K. M., et al. (2014). "Sea-level variability over five glacial cycles." Nature Communications 5.

Hemleben, C., et al. (1996). "Three hundred eighty thousand year long stable isotope and faunal records from the Red Sea: Influence of global sea level change on hydrography." Paleoceanography 11(2): 147-156.

Hoshino, T., Inagaki, F., 2018. Abundance and distribution of Archaea in the subseafloor sedimentary biosphere. The ISME Journal.

Huguet, C., Hopmans, E.C., Febo-Ayala, W., Thompson, D.H., Damsté, J.S.S. and Schouten, S., 2006. An improved method to determine the absolute abundance of glycerol dibiphytanyl glycerol tetraether lipids. Organic Geochemistry, *37*(9), 1036-1041.

Inagaki, F., Suzuki, M., Takai, K., Oida, H., Sakamoto, T., Aoki, K., Nealson, K.H., Horikoshi, K., 2003. Microbial communities associated with geological horizons in coastal subseafloor sediments from the Sea of Okhotsk. Appl Environ Microb 69, 7224-7235.

Inagaki, F., et al. (2005). "Microbial survival - The paleome: A sedimentary genetic record of past microbial communities." Astrobiology 5(2): 141-153.

Kallmeyer, J., Pockalny, R., Adhikari, R.R., Smith, D.C., D'Hondt, S., 2012. Global distribution of microbial abundance and biomass in subseafloor sediment. P Natl Acad Sci USA 109, 16213-16216.

Lang, K., Schuldes, J., Klingl, A., Poehlein, A., Daniel, R., Brune, A., 2015. New Mode of Energy Metabolism in the Seventh Order of Methanogens as Revealed by Comparative Genome Analysis of "Candidatus Methanoplasma termitum". Appl Environ Microb 81, 1338-1352.

Lliros, M., Alonso-Saez, L., Gich, F., Plasencia, A., Auguet, O., Casamayor, E.O., Borrego, C.M., 2011. Active bacteria and archaea cells fixing bicarbonate in the dark along the water column of a stratified eutrophic lagoon. Fems Microbiol Ecol 77, 370-384.

Lloyd, K.G., Schreiber, L., Petersen, D.G., Kjeldsen, K.U., Lever, M.A., Steen, A.D., Stepanauskas, R., Richter, M., Kleindienst, S., Lenk, S., Schramm, A., Jorgensen, B.B., 2013. Predominant archaea in marine sediments degrade detrital proteins. Nature 496, 215-+.

Morcos, S.A., 1970. Physical and chemical oceanography of the Red Sea. Oceanography and Marine Biology 8, 73-202.

Offre, P., Spang, A., Schleper, C., 2013. Archaea in Biogeochemical Cycles. Annu Rev Microbiol 67, 437-457.

Orsi, W.D., Coolen, M.J.L., Wuchter, C., He, L., More, K.D., Irigoien, X., Chust, G., Johnson, C., Hemingway, J.D., Lee, M., Galy, V., Giosan, L., 2017. Climate oscillations reflected within the microbiome of Arabian Sea sediments. Scientific Reports 7, 6040.

Parkes, R.J., Cragg, B., Roussel, E., Webster, G., Weightman, A., Sass, H. 2014. A review of prokaryotic populations and processes in sub-seafloor sediments, including biosphere, geosphere interactions. Marine Geology, 352, 409-425.

Rashid, H., Hesse, R., Piper, D.J.W., 2003. Evidence for an additional Heinrich event between H5 and H6 in the Labrador Sea. Paleoceanography 18.

Rasul, N. M. A., et al. (2015). Introduction to the Red Sea: Its Origin, Structure, and Environment. The Red Sea: The Formation, Morphology, Oceanography and Environment of a Young Ocean Basin. N. M. A. Rasul and I. C. F. Stewart. Berlin, Heidelberg, Springer Berlin Heidelberg: 1-28.

Reimer, P.J., Baillie, M.G.L., Bard, E., Bayliss, A., Beck, J.W., Bertrand, C.J.H., Blackwell, P.G., Buck, C.E., Burr, G.S., Cutler, K.B., Damon, P.E., Edwards, R.L., Fairbanks, R.G., Friedrich, M., Guilderson, T.P., Hogg, A.G., Hughen, K.A., Kromer, B., McCormac, G., Manning, S., Ramsey, C.B., Reimer, R.W., Remmele, S., Southon, J.R., Stuiver, M., Talamo, S., Taylor, F.W., van der Plicht, J., Weyhenmeyer, C.E., 2004. IntCal04 terrestrial radiocarbon age calibration, 0-26 cal kyr BP. Radiocarbon 46, 1029-1058.

Rohling, E. J. (1994). "Glacial Conditions in the Red-Sea." Paleoceanography 9(5): 653-660.

Schouten, S., Huguet, C., Hopmans, E.C., Kienhuis, M.V. and Sinninghe Damsté, J.S., 2007. Analytical methodology for TEX86 paleothermometry by high-performance liquid chromatography/atmospheric pressure chemical ionization mass spectrometry. *Analytical Chemistry*, *79*(7), 2940-2944.

Schulz, H., von Rad, U., Erlenkeuser, H., von Rad, U., 1998. Correlation between Arabian Sea and Greenland climate oscillations of the past 110,000 years. Nature 393, 54-57.

Sorensen, K.B., Teske, A., 2006. Stratified communities of active archaea in deep marine subsurface sediments. Appl Environ Microb 72, 4596-4603.

Stahl, D.A., Amann, R. , 1991. Development and Application of Nucleic Acid Probes in Bacterial Systematics. in: Stackebrandt, E., Goodfellow, M. (Ed.), Nucleic Acid Techniques in Bacterial Systematics. John Wiley & Sons Ltd., Chichester, 205-248.

Stuiver, M., Reimer, P.J., 1993. Extended C-14 Data-Base and Revised Calib 3.0 C-14 Age Calibration Program. Radiocarbon 35, 215-230.

Tierney, J.E., Tingley, M.P., 2014. A Bayesian, spatially-varying calibration model for the TEX86 proxy. Geochim Cosmochim Ac 127, 83-106.

Tierney, J.E. and Tingley, M.P., 2015. A TEX 86 surface sediment database and extended Bayesian calibration. Scientific data, *2*, p.150029

Vuillemin, A., Ariztegui, D., Leavitt, P.R., Bunting, L., Team, P.S., 2016. Recording of climate and diagenesis through sedimentary DNA and fossil pigments at Laguna Potrok Aike, Argentina. Biogeosciences 13, 2475-2492.

Wuchter, C., Abbas, B., Coolen, M.J.L., Herfort, L., Bleijswijk, J., Timmers, P., Strous, M., Teira, E., Herndl, G.J., Middelburg, J.J., Schouten, S., Sinninghe Damsté., J.S. 2006. Archaeal nitrification in the ocean. Proc.Nat.Aca.Sci., 103, (33) 12317-12322.

Xia, X.M., Guo, W., Liu, H.B., 2017. Basin Scale Variation on the Composition and Diversity of Archaea in the Pacific Ocean. Front Microbiol 8, 2057.

Yang, J., Jiang, H.C., Dong, H.L., Hou, W.G., Li, G.Y., Wu, G., 2015. Sedimentary archaeal amoA gene abundance reflects historic nutrient level and salinity fluctuations in Qinghai Lake, Tibetan Plateau. Scientific Reports 5, 18071.

Zhang, C.L., Xie, W., Martin-Cuadrado, A., Rodriguez-Valera, F., 2015. Marine Group II Archaea, potentially important players in the global ocean carbon cycle. Front Microbiol 6, 1108.

CHAPTER 5

CONCLUSIONS AND FUTURE PERSPECTIVES

5.1 Ancient DNA archives in marine sediments: A key approach

The primary aim of this dissertation was to explore the potential of the paleogenomic analyses of marine sedimentary DNA as a novel approach to reconstruct the response of past ecosystems to the paleoclimate variations when paired with paleoceanographical proxies. This study provided ample evidence for the efficiency of this approach. Most of the taxa (protists, bacteria and archaea) from which the sedimentary DNA originated are not known to produce either fossil or specific biomarkers and, hence, stratigraphic aDNA analysis is the only approach that surpasses the dependence on these more traditional paleobiological proxies. Paleogenomic surveys presented in this dissertation revealed how past OMZ variations affected protist communities in the NE Arabian Sea, how Holocene climate stages shaped the composition of sub-surface bacterial communities in the Black Sea and how different MIS and their transitions affected the sedimentary archaeal distribution of the Red Sea.

5.2 Chapter 2: Past protist response to paleo-OMZ variability

OMZs are increasing worldwide with increase in global temperature (Helm et al., 2011; Keeling et al., 2010) and eutrophication and are affecting the habitat of a variety of marine life ranging from planktonic communities to fish and in turn are disturbing the marine food web. On this prospect, it is critical to know how past OMZ expansions affected the organisms which are directly affected by the OMZ *i.e.* protists. This study demonstrated that 18S rDNA sequencing of sedimentary protist DNA yields a useful long-term record of ecosystem responses to dynamic OMZ conditions including non-fossilizing taxa that traditionally escape microscopic identification in micro-paleontological studies. Results showed that strong OMZ conditions select only those protist communities that are capable of sustaining oxygen depletion either by adapting a parasitic life cycle or by establishing mutualistic relationships

with others or by forming dormant resting stages. This study also revealed that the steady increase in eutrophication triggers decline in the Dia/Dino index, as has been evident in the NE Arabian Sea during the late Holocene. This will likely favour the pelagic component of the marine food web in the context of predicted worldwide expansion of coastal OMZs associated with global climate change. However, this research and these data also show that the marine ecosystem is resilient enough to return to healthy conditions soon after the OMZs cease to exist. If we can stop OMZ spread by controlling the eutrophication levels, there is a chance that the marine ecosystem will recover.

5.3 Chapter 3: Variability in paleodepositional environments reflected in the sedimentary microbiome of the Black Sea

It was recently shown that a subset of subseafloor bacteria originating from surface waters at the time of deposition formed a genetic archive known as “the Paleome” which underwent weak or no post-burial selection and hence directly mirror the variations in the paleodepositional environment. However, additional highly resolved temporal records of such paleomes paired with geochemical proxies were needed to justify this claim. In this study a shotgun metagenomics approach was used to investigate the subseafloor microbial paleome that preserved the signature of changing oceanographic conditions at centennial timescale resolution in up to 13-ka-old Black Sea sediments. This revealed that obligate anaerobic bacteria closely follow the distribution of deposited organic matter. Obligate anaerobic bacterial community changed drastically after the establishment of modern-day conditions at 5.2 ka BP, which coincided with a change in the pelagic plankton community composition as the source of sedimentary organic matter. The functional metagenomic dataset further helped to locate the depth interval where SMTZ occurs in the sediment, based on the activity of anaerobes involved in sulfur and methane cycling. Obligate aerobic bacteria were likely to be seeded from the water column and made the largest contribution to the observed shifts in microbial communities in response to Holocene climate stages. Furthermore, the lack of a significant shift in microbial communities following the marine reconnection at 9 ka BP hints towards a gradual nature of the marine reconnection as opposed to catastrophic flooding. Data generated through this study not only supported the hypothesis that microbes that were present at the time of deposition and are now part of deep subsurface biosphere, capture the response to the changing paleo-depositional conditions but also helped to construct the microbial component of the sulfur cycle in the Black Sea.

5.4 Chapter 4: MIS transitions reflected in the sedimentary archaeal microbiome of the Red Sea

Limited information is available on archaeal responses to long-term environmental changes despite the fact that Archaea contribute on average 35% to the total sub-surface microbiome. This study investigated the potential of archaeal communities to mirror variations in paleodepositional changes during the last six marine isotope stages (i.e., spanning the penultimate and the last glacial cycles) in the Red Sea. The results revealed a strong significant response of subseafloor archaeal communities to changes in paleodepositional conditions associated with MIS stages and their transitions and only a moderately significant response to changes in sediment lithology. The sediments contained a mix of DNA from archaea indigenous to the sediment and were likely involved in biodegradation of labile organic matter and methane cycling as well as ancient DNA originating from from allochthonous sources: Thaumarchaeota, MGII and MGIII stemming from the overlying water column at the time of deposition and terrestrial derived TMEG.

5.5 Future work

OMZs are thought to be expanding in coastal environments world-wide and a similar approach as used in the OMZ of the NE Arabian Sea could be employed at other critical locations which harbour persistent OMZs. Such studies would provide detailed information on how local marine ecosystem have responded to past OMZ expansion. If integrated with observations from modern time series, similar paleogenomic datasets will form the strong feed for models built to study the climate-ecosystem dynamics and will improve the predictions of how long-term OMZ expansion in the future will shape the marine planktonic communities. 16S rDNA profiling and metagenomic surveys paired with paleoceanographic proxies in other anoxic and oxygenated sediments will provide a holistic picture of factors contributing to distribution and abundance of subsurface microbial taxa in the majority of currently unexplored geological settings. This will also help to understand the role of paleodepositional environments in selecting the subsurface microbiome along with other factors such as nutrient availability and sediment lithology. In the Red Sea sediments, many of the archaeal groups detected represented uncultivated groups. Single-cell genomics as well as metatranscriptomic surveys are required to substantially improve our understanding of their role in past and present biogeochemical cycling processes that will help to understand their possible relation to the paleodepositional environment and their suitability as a past climate proxy. In addition, it has been shown that subseafloor microbes subsisting

with extremely low activity actively repair their DNA and can persist to great depths *via* fermentation. These mechanisms of subsistence coupled with weak selection after burial make these paleodepositionally selected bacterial as well as archaeal communities important indicators of paleoclimate variations. Similarly, the rapidly recurring climate-controlled selection of microbial communities in other marine settings that have likely been impacted by past ocean biogeochemistry can serve as climatic feedback mechanisms. However, deeper sediment records are needed to validate if similar approach can be applied for deep biosphere samples to analyse whether deep biosphere micro-organisms also undergo paleo-depositional selection.

Bibliography

"Every reasonable effort has been made to acknowledge the owners of copyright material. I would be please to hear from the copyright owner who has been omitted or incorrectly acknowledged."

Ahmed, E., Parducci, L., Unneberg, P., Agren, R., Schenk, F., Rattray, J.E., Han, L., Muschitiello, F., Pedersen, M.W., Smittenberg, R.H., Yamoah, K.A., Slotte, T., Wohlfarth, B., 2018. Archaeal community changes in Lateglacial lake sediments: Evidence from ancient DNA. Quaternary Sci Rev 181, 19-29.

Altabet, M. A., et al. (1995). "Climate-Related Variations in Denitrification in the Arabian Sea from Sediment N-15/N-14 Ratios." Nature **373**(6514): 506-509.

Altabet, M. A., et al. (2002). "The effect of millennial-scale changes in Arabian Sea denitrification on atmospheric CO2." Nature **415**(6868): 159-162.

Banse, K. (1987). "Seasonality of Phytoplankton Chlorophyll in the Central and Northern Arabian Sea." Deep-Sea Research Part a-Oceanographic Research Papers **34**(5-6): 713-723.

Bemis, B. E., et al. (1998). "Reevaluation of the oxygen isotopic composition of planktonic foraminifera: Experimental results and revised paleotemperature equations." Paleoceanography **13**(2): 150-160.

Billups, K. and D. P. Schrag (2002). "Paleotemperatures and ice volume of the past 27 Myr revisited with paired Mg/Ca and O-18/O-16 measurements on benthic foraminifera." Paleoceanography **17**(1).

Bissett, A., et al. (2005). "Isolation, amplification, and identification of ancient copepod DNA from lake sediments." Limnology and Oceanography-Methods **3**: 533-542.

Blackford, J. C. and P. H. Burkill (2002). "Planktonic community structure and carbon cycling in the Arabian Sea as a result of monsoonal forcing: the application of a generic model." Journal of Marine Systems **36**(3-4): 239-267.

Boere, A. C., et al. (2009). "Late-Holocene succession of dinoflagellates in an Antarctic fjord using a multi-proxy approach: paleoenvironmental genomics, lipid biomarkers and palynomorphs." Geobiology **7**(3): 265-281.

Bond, G., et al. (1992). "Evidence for Massive Discharges of Icebergs into the North-Atlantic Ocean during the Last Glacial Period." Nature **360**(6401): 245-249.

Brassell, S. C. (1993). Applications of Biomarkers for Delineating Marine Paleoclimatic Fluctuations during the Pleistocene. Organic Geochemistry: Principles and Applications. M. H. Engel and S. A. Macko. Boston, MA, Springer US**:** 699-738.

Brinkhoff, T. and G. Muyzer (1997). "Increased species diversity and extended habitat range of sulfur-oxidizing Thiomicrospira spp." Applied and Environmental Microbiology **63**(10): 3789-3796.

Brocks, J. J., et al. (2005). "Biomarker evidence for green and purple sulphur bacteria in a stratified Palaeoproterozoic sea." Nature **437**(7060): 866-870.

Burgoyne, T. W. and J. M. Hayes (1998). "Quantitative production of H-2 by pyrolysis of gas chromatographic effluents." Analytical Chemistry **70**(24): 5136-5141.

Caporaso, J. G., et al. (2010). "QIIME allows analysis of high-throughput community sequencing data." Nature Methods **7**(5): 335-336.

Caporaso, J. G., et al. (2012). "Ultra-high-throughput microbial community analysis on the Illumina HiSeq and MiSeq platforms." Isme Journal **6**(8): 1621-1624.

Ciobanu, M. C., et al. (2012). "Sedimentological imprint on subseafloor microbial communities in Western Mediterranean Sea Quaternary sediments." Biogeosciences **9**(9): 3491-3512.

Clarke, K. R. (1993). "Non-parametric multivariate analyses of changes in community structure." Australian Journal of Ecology **18**(1): 117-143.

Coolen, M. J. L. (2011). "7000 Years of Emiliania huxleyi Viruses in the Black Sea." Science **333**(6041): 451-452.

Coolen, M. J. L., et al. (2004). "Evolution of the methane cycle in Ace Lake (Antarctica) during the Holocene: Response of methanogens and methanotrophs to environmental change." Organic Geochemistry **35**(10): 1151-1167.

Coolen, M.J.L., Cypionka, H., Sass, A.M., Sass, H., Overmann, J. 2002. Ongoing modification of Mediterranean Pleistocene sapropels mediated by prokaryotes. Science. 2002 Jun 28;296(5577):2407-10.

Coolen, M. J. L., et al. (2013). "Evolution of the plankton paleome in the Black Sea from the Deglacial to Anthropocene." Proceedings of the National Academy of Sciences of the United States of America **110**(21): 8609-8614.

Coolen, M. J. L. and J. Overmann (2007). "217 000-year-old DNA sequences of green sulfur bacteria in Mediterranean sapropels and their implications for the reconstruction of the paleoenvironment (vol 9, pg 238, 2007)." Environmental Microbiology **9**(4): 1099-1099.

Coolen, M. J. L., et al. (2009). "DNA and lipid molecular stratigraphic records of haptophyte succession in the Black Sea during the Holocene." Earth and Planetary Science Letters **284**(3-4): 610-621.

Dabney, J., et al. (2013). "Complete mitochondrial genome sequence of a Middle Pleistocene cave bear reconstructed from ultrashort DNA fragments." Proceedings of the National Academy of Sciences of the United States of America **110**(39): 15758-15763.

Damste, J. S. S., et al. (1995). "Evidence for Gammacerane as an Indicator of Water Column Stratification." Geochimica Et Cosmochimica Acta **59**(9): 1895-1900.

De Caceres, M., et al. (2012). "Using species combinations in indicator value analyses." Methods in Ecology and Evolution **3**(6): 973-982.

De Man, E. and S. Van Simaeys (2004). "Late Oligocene Warming Event in the southern North Sea Basin: benthic foraminifera as paleotemperature proxies." Netherlands Journal of Geosciences-Geologie En Mijnbouw **83**(3): 227-239.

Degens, E. T. and D. A. Ross (1972). "Chronology of the Black Sea over the last 25,000 years." Chemical Geology **10**(1): 1-16.

Delong, E. F. (1992). "Archaea in Coastal Marine Environments." Proceedings of the National Academy of Sciences of the United States of America **89**(12): 5685-5689.

Dridi, B., et al. (2012). "Methanomassiliicoccus luminyensis gen. nov., sp nov., a methanogenic archaeon isolated from human faeces." International Journal of Systematic and Evolutionary Microbiology **62**: 1902-1907.

Dufrene M, Legendre P (1997) Species assemblages and indicator species: The need for a flexible asymmetrical approach. Ecol Monogr, 67, 345-366.

Durbin, A. M. and A. Teske (2012). "Archaea in organic-lean and organic-rich marine subsurface sediments: an environmental gradient reflected in distinct phylogenetic lineages." Frontiers in Microbiology **3**.

Elderfield, H. and G. Ganssen (2000). "Past temperature and delta O-18 of surface ocean waters inferred from foraminiferal Mg/Ca ratios." Nature **405**(6785): 442-445.

Fenton, M., et al. (2000). "Aplanktonic zones in the Red Sea." Marine Micropaleontology **40**(3): 277-294.

Giosan, L., et al. (2012). "Early Anthropogenic Transformation of the Danube-Black Sea System." Scientific Reports **2**.

Giosan, L., et al. (2009). "Was the Black Sea catastrophically flooded in the early Holocene?" Quaternary Science Reviews **28**(1-2): 1-6.

Grant, K. M., et al. (2014). "Sea-level variability over five glacial cycles." Nature Communications **5**.

Grice, K., et al. (2005). "Photic zone euxinia during the Permian-Triassic superanoxic event." Science **307**(5710): 706-709.

Gross, M. G. (1974). "DEGENS, E. T., AND D. A. ROSS [EDS.]. 1974. The Black Sea—Geology, chemistry, and biology. American Association of Petroleum Geologists, Tulsa, Oklahoma, ix + 633 p. $33.00." Limnology and Oceanography **19**(6): 1016-1017.

Hemleben, C., et al. (1996). "Three hundred eighty thousand year long stable isotope and faunal records from the Red Sea: Influence of global sea level change on hydrography." Paleoceanography **11**(2): 147-156.

Hiscott, R. N., et al. (2007). "A gradual drowning of the southwestern Black Sea shelf: Evidence for a progressive rather than abrupt Holocene reconnection with the eastern Mediterranean Sea through the Marmara Sea Gateway." Quaternary International **167**: 19-34.

Hofreiter, M., et al. (2001). "Ancient DNA." Nature Reviews Genetics **2**(5): 353-359.

Hoshino, T. and F. Inagaki (2018). "Abundance and distribution of Archaea in the subseafloor sedimentary biosphere." The ISME Journal.

Inagaki, F., et al. (2015). "Exploring deep microbial life in coal-bearing sediment down to similar to 2.5 km below the ocean floor." Science **349**(6246): 420-424.

Inagaki, F., et al. (2005). "Microbial survival - The paleome: A sedimentary genetic record of past microbial communities." Astrobiology **5**(2): 141-153.

Inagaki, F., et al. (2003). "Microbial communities associated with geological horizons in coastal subseafloor sediments from the Sea of Okhotsk." Applied and Environmental Microbiology **69**(12): 7224-7235.

Jiang, H., et al. (2002). "Late-Holocene summer sea-surface temperatures based on a diatom record from the north Icelandic shelf." Holocene **12**(2): 137-147.

Johns, R. B. (1986). Biological markers in the sedimentary record. Amsterdam ; New York : New York, NY, Elsevier ; Distributors for the United States and Canada, Elsevier Science Pub. Co.

Jones, G. A. and A. R. Gagnon (1994). "Radiocarbon Chronology of Black-Sea Sediments." Deep-Sea Research Part I-Oceanographic Research Papers **41**(3): 531-557.

Kallmeyer, J., et al. (2012). "Global distribution of microbial abundance and biomass in subseafloor sediment." Proceedings of the National Academy of Sciences of the United States of America **109**(40): 16213-16216.

Kaplin, P. A. and A. O. Selivanov (2004). "Lateglacial and Holocene sea level changes in semi-enclosed seas of North Eurasia: examples from the contrasting Black and White Seas." Palaeogeography, Palaeoclimatology, Palaeoecology **209**(1): 19-36.

Kirkpatrick, J. B., et al. (2016). "Fossil DNA persistence and decay in marine sediment over hundred-thousand-year to million-year time scales." Geology **44**(8): 615-618.

Lang, K., et al. (2015). "New Mode of Energy Metabolism in the Seventh Order of Methanogens as Revealed by Comparative Genome Analysis of "Candidatus Methanoplasma termitum"." Applied and Environmental Microbiology **81**(4): 1338-1352.

Lear, C. H., et al. (2000). "Cenozoic deep-sea temperatures and global ice volumes from Mg/Ca in benthic foraminiferal calcite." Science **287**(5451): 269-272.

Lindahl, T. (1993). "Instability and Decay of the Primary Structure of DNA." Nature **362**(6422): 709-715.

Lliros, M., et al. (2011). "Active bacteria and archaea cells fixing bicarbonate in the dark along the water column of a stratified eutrophic lagoon." Fems Microbiology Ecology **77**(2): 370-384.

Lloyd, K. G., et al. (2013). "Predominant archaea in marine sediments degrade detrital proteins." Nature **496**(7444): 215-+.

Lyra, C., et al. (2013). "Sediment Bacterial Communities Reflect the History of a Sea Basin." Plos One **8**(1).

Madhupratap, M., et al. (1996). "Mechanism of the biological response to winter cooling in the northeastern Arabian Sea." Nature **384**(6609): 549-552.

Major, C., et al. (2002). "Constraints on Black Sea outflow to the Sea of Marmara during the last glacial-interglacial transition." Marine Geology **190**(1-2): 19-34.

Major, C. O., et al. (2006). "The co-evolution of Black Sea level and composition through the last deglaciation and its paleoclimatic significance." Quaternary Science Reviews **25**(17-18): 2031-2047.

Marcus, N. H. (1996). "Ecological and evolutionary significance of resting eggs in marine copepods: Past, present, and future studies." Hydrobiologia **320**(1-3): 141-152.

Marlowe, I. T., et al. (1984). "Long chain (n-C37–C39) alkenones in the Prymnesiophyceae. Distribution of alkenones and other lipids and their taxonomic significance." British Phycological Journal **19**(3): 203-216.

Marret, F., et al. (2009). "A Holocene dinocyst record of a two-step transformation of the Neoeuxinian brackish water lake into the Black Sea." Quaternary International **197**: 72-86.

Morcos, S. A. (1970). "Physical and chemical oceanography of the Red Sea." Oceanography and Marine Biology **8**: 73-202.

Murray, J. W. and E. Yakushev (2006). THE SUBOXIC TRANSITION ZONE IN THE BLACK SEA. Past and Present Water Column Anoxia, Dordrecht, Springer Netherlands.

Offre, P., et al. (2013). "Archaea in Biogeochemical Cycles." Annual Review of Microbiology, Vol 67 **67**: 437-457.

Orcutt, B. N., et al. (2011). "Microbial Ecology of the Dark Ocean above, at, and below the Seafloor." Microbiology and Molecular Biology Reviews **75**(2): 361-+.

Orlando, L., et al. (2013). "Recalibrating Equus evolution using the genome sequence of an early Middle Pleistocene horse." Nature **499**(7456): 74-+.

Orsi, W. D., et al. (2017). "Climate oscillations reflected within the microbiome of Arabian Sea sediments." Scientific Reports **7**(1): 6040.

Parkes, R. J., et al. (2000). "Recent studies on bacterial populations and processes in subseafloor sediments: A review." Hydrogeology Journal **8**(1): 11-28.

Parmesan, C. (2006). "Ecological and evolutionary responses to recent climate change." Annual Review of Ecology Evolution and Systematics **37**: 637-669.

Pedgley, D. E. (1974). An outline of the weather and climate of the Red Sea. Actes du Colloques, Publications Centre National pour l'Exploitation des Oceans

Poinar, H. N., et al. (1996). "Amino acid racemization and the preservation of ancient DNA." Science **272**(5263): 864-866.

Pross, J. (2001). "Paleo-oxygenation in Tertiary epeiric seas: evidence from dinoflagellate cysts." Palaeogeography Palaeoclimatology Palaeoecology **166**(3-4): 369-381.

Rammig, A. and M. D. Mahecha (2015). "ECOLOGY Ecosystem responses to climate extremes." Nature **527**(7578): 315-+.

Rashid, H., et al. (2003). "Evidence for an additional Heinrich event between H5 and H6 in the Labrador Sea." Paleoceanography **18**(4).

Rasul, N. M. A., et al. (2015). Introduction to the Red Sea: Its Origin, Structure, and Environment. The Red Sea: The Formation, Morphology, Oceanography and Environment of a Young Ocean Basin. N. M. A. Rasul and I. C. F. Stewart. Berlin, Heidelberg, Springer Berlin Heidelberg**:** 1-28.

Rebata-Landa, V. and J. C. Santamarina (2006). "Mechanical limits to microbial activity in deep sediments." Geochemistry Geophysics Geosystems **7**.

Reichart, G. J., et al. (1998). "Temporal variability in the northern Arabian Sea Oxygen Minimum Zone (OMZ) during the last 225,000 years." Paleoceanography **13**(6): 607-621.

Reimer, P. J., et al. (2004). "IntCal04 terrestrial radiocarbon age calibration, 0-26 cal kyr BP." Radiocarbon **46**(3): 1029-1058.

Rohling, E. J. (1994). "Glacial Conditions in the Red-Sea." Paleoceanography **9**(5): 653-660.

Ross, D. A., et al. (1970). "Black Sea: Recent Sedimentary History." Science **170**(3954): 163-165.

Ryan, W. B. F., et al. (2003). "Catastrophic flooding of the Black Sea." Annual Review of Earth and Planetary Sciences **31**: 525-554.

Sancetta, C. and S. Silvestri (1986). "Pliocene-Pleistocene Evolution of the North Pacific Ocean-Atmosphere System, Interpreted from Fossil Diatoms." Paleoceanography **1**(2): 163-180.

Schulte, S. and P. J. Muller (2001). "Variations of sea surface temperature and primary productivity during Heinrich and Dansgaard-Oeschger events in the northeastern Arabian Sea." Geo-Marine Letters **21**(3): 168-175.

Schulz, H., et al. (1998). "Correlation between Arabian Sea and Greenland climate oscillations of the past 110,000 years." Nature **393**(6680): 54-57.

Schulz, H., et al. (2002). "Planktic foraminifera, particle flux and oceanic productivity off Pakistan, NE Arabian Sea: modern analogues and application to the palaeoclimatic record." Geological Society, London, Special Publications **195**(1): 499-516.

Schulz, H., et al. (1996). "Laminated sediments from the oxygen-minimum zone of the northeastern Arabian Sea." Geological Society, London, Special Publications **116**(1): 185-207.

Sessions, A. L., et al. (2001). "Correction of H-3(+) contributions in hydrogen isotope ratio monitoring mass spectrometry." Analytical Chemistry **73**(2): 192-199.

Simoneit, B. R. T. (2004). "Biomarkers (molecular fossils) as geochemical indicators of life." Space Life Sciences: Search for Signatures of Life, and Space Flight Environmental Effects on the Nervous System **33**(8): 1255-1261.

Sluijs, A., et al. (2005). "From greenhouse to icehouse; organic-walled dinoflagellate cysts as paleoenvironmental indicators in the Paleogene." Earth-Science Reviews **68**(3-4): 281-315.

Song, S., et al. (2013). Chapter Three - Our Second Genome—Human Metagenome: How Next-Generation Sequencer Changes our Life Through Microbiology. Advances in Microbial Physiology. R. K. Poole, Academic Press. **62:** 119-144.

Sorensen, K. B. and A. Teske (2006). "Stratified communities of active archaea in deep marine subsurface sediments." Applied and Environmental Microbiology **72**(7): 4596-4603.

Soulet, G., et al. (2010). "Glacial hydrologic conditions in the Black Sea reconstructed using geochemical pore water profiles." Earth and Planetary Science Letters **296**(1-2): 57-66.

Soulet, G., et al. (2011). "A revised calendar age for the last reconnection of the Black Sea to the global ocean." Quaternary Science Reviews **30**(9-10): 1019-1026.

Stahl, D. A., Amann, R. (1991). Development and Application of Nucleic Acid Probes in Bacterial Systematics.

Nucleic Acid Techniques in Bacterial Systematics. E. Stackebrandt, Goodfellow, M. Chichester, John Wiley & Sons Ltd.**:** 205-248.

Starnawski, P., et al. (2017). "Microbial community assembly and evolution in subseafloor sediment." Proceedings of the National Academy of Sciences of the United States of America **114**(11): 2940-2945.

Stuiver, M. and P. J. Reimer (1993). "Extended C-14 Data-Base and Revised Calib 3.0 C-14 Age Calibration Program." Radiocarbon **35**(1): 215-230.

Summons, R. E. and T. G. Powell (1986). "Chlorobiaceae in Palaeozoic seas revealed by biological markers, isotopes and geology." Nature **319**: 763.

Svetlichny, L., et al. (2010). "Salinity tolerance of Calanus euxinus in the Black and Marmara Seas." Marine Ecology Progress Series **404**: 127-138.

Taylor, F. J. R. (1987). The Biology of dinoflagellates. Oxford, Blackwell Scientific.

van der Meer, M. T. J., et al. (2008). "Molecular isotopic and dinoflagellate evidence for Late Holocene freshening of the Black Sea." Earth and Planetary Science Letters **267**(3-4): 426-434.

Volkman, J.K., Barrett, S.M., Dunstan, G.A., Jeffrey, S.W. 1993. Geochemical significance of the occurrence of dinosterol and other 4-methyl sterols in a marine diatom. Organic Geochemistry 20(1): 7-15.

von Rad, U., et al. (1999). "Multiple monsoon-controlled breakdown of oxygen-minimum conditions during the past 30,000 years documented in laminated sediments off Pakistan." Palaeogeography, Palaeoclimatology, Palaeoecology **152**(1–2): 129-161.

Vonrad, U., et al. (1995). "Sampling the Oxygen Minimum Zone Off Pakistan - Glacial Interglacial Variations of Anoxia and Productivity (Preliminary-Results, Sonne-90 Cruise)." Marine Geology **125**(1-2): 7-19.

Vuillemin, A., et al. (2016). "Recording of climate and diagenesis through sedimentary DNA and fossil pigments at Laguna Potrok Aike, Argentina." Biogeosciences **13**(8): 2475-2492.

Walther, G. R. (2010). "Community and ecosystem responses to recent climate change." Philosophical Transactions of the Royal Society B-Biological Sciences **365**(1549): 2019-2024.

Walther, G. R., et al. (2002). "Ecological responses to recent climate change." Nature **416**(6879): 389-395.

Willerslev, E., et al. (2004). "Isolation of nucleic acids and cultures from fossil ice and permafrost." Trends in Ecology & Evolution **19**(3): 141-147.

William, A. S. S. (1986). "Sporopollenin Dinoflagellate Cysts. Their Morphology and Interpretation " Micropaleontology **32**(3): 282-285.

Xia, X. M., et al. (2017). "Basin Scale Variation on the Composition and Diversity of Archaea in the Pacific Ocean." Frontiers in Microbiology **8**.

Yang, J., et al. (2015). "Sedimentary archaeal amoA gene abundance reflects historic nutrient level and salinity fluctuations in Qinghai Lake, Tibetan Plateau." Scientific Reports **5**.

Yun, S. M., et al. (2017). "Fossil Diatom Assemblages as Paleoecological Indicators of Paleo-water Environmental Change in the Ulleung Basin, East Sea, Republic of Korea." Ocean Science Journal **52**(3): 345-357.

Zhang, C.L., Xie, W., Martin-Cuadrado, A., Rodriguez-Valera, F., 2015. Marine Group II Archaea, potentially important players in the global ocean carbon cycle. Front Microbiol 6, 1108.

Zonneveld, K. A. F., et al. (1997). "Preservation of organic-walled dinoflagellate cysts in different oxygen regimes: A 10,000 year natural experiment." Marine Micropaleontology **29**(3-4): 393-405.

Appendix

Following pages contain documents stating the rights, granted by Elsevier and Wiley publishing groups to the first author of the publications that forms the chapter 2 and 3 of this thesis respectively, to reproduce their articles in full or in part, for a wide range of scholarly, non-commercial purposes, including in a thesis (provided that this is not to be published commercially).

Personal use

Authors can use their articles, in full or in part, for a wide range of scholarly, non-commercial purposes as outlined below:

- Use by an author in the author's classroom teaching (including distribution of copies, paper or electronic)
- Distribution of copies (including through e-mail) to known research colleagues for their personal use (but not for Commercial Use)
- Inclusion in a thesis or dissertation (provided that this is not to be published commercially)
- Use in a subsequent compilation of the author's works
- Extending the Article to book-length form
- Preparation of other derivative works (but not for Commercial Use)
- Otherwise using or re-using portions or excerpts in other works

These rights apply for all Elsevier authors who publish their article as either a subscription article or an open access article. In all cases we require that all Elsevier authors always include a full acknowledgement and, if appropriate, a link to the final published version hosted on Science Direct.

JOHN WILEY AND SONS LICENSE TERMS AND CONDITIONS

May 13, 2019

This Agreement between Kuldeep More ("You") and John Wiley and Sons ("John Wiley and Sons") consists of your license details and the terms and conditions provided by John Wiley and Sons and Copyright Clearance Center.

License Number	4586880746915
License date	May 13, 2019
Licensed Content Publisher	John Wiley and Sons
Licensed Content Publication	Geobiology
Licensed Content Title	Holocene paleodepositional changes reflected in the sedimentary microbiome of the Black Sea
Licensed Content Author	Kuldeep D. More, Liviu Giosan, Kliti Grice, et al
Licensed Content Date	Mar 6, 2019
Licensed Content Volume	0
Licensed Content Issue	0
Licensed Content Pages	13
Type of use	Dissertation/Thesis
Requestor type	Author of this Wiley article
Format	Electronic
Portion	Full article
Will you be translating?	No
Title of your thesis / dissertation	Ancient DNA archives in marine sediments
Expected completion date	May 2019
Expected size (number of pages)	150
Requestor Location	Kuldeep More 8 Tarun Court Cannington, WA 6107 Australia Attn: Kuldeep More
Publisher Tax ID	EU826007151
Total	0.00 AUD
Terms and Conditions	

TERMS AND CONDITIONS

This copyrighted material is owned by or exclusively licensed to John Wiley & Sons, Inc. or one of its group companies (each a"Wiley Company") or handled on behalf of a society with which a Wiley Company has exclusive publishing rights in relation to a particular work (collectively "WILEY"). By clicking "accept" in connection with completing this licensing transaction, you agree that the following terms and conditions apply to this transaction (along with the billing and payment terms and conditions established by the Copyright Clearance Center Inc., ("CCC's Billing and Payment terms and conditions"), at the time that you opened your RightsLink account (these are available at any time at http://myaccount.copyright.com).

Terms and Conditions

- The materials you have requested permission to reproduce or reuse (the "Wiley Materials") are protected by copyright.

- You are hereby granted a personal, non-exclusive, non-sub licensable (on a stand-alone basis), non-transferable, worldwide, limited license to reproduce the Wiley Materials for the purpose specified in the licensing process. This license, **and any CONTENT (PDF or image file) purchased as part of your order,** is for a one-time use only and limited to any maximum distribution number specified in the license. The first instance of republication or reuse granted by this license must be completed within two years of the date of the grant of this license (although copies prepared before the end date may be distributed thereafter). The Wiley Materials shall not be used in any other manner or for any other purpose, beyond what is granted in the license. Permission is granted subject to an appropriate acknowledgement given to the author, title of the material/book/journal and the publisher. You shall also duplicate the copyright notice that appears in the Wiley publication in your use of the Wiley Material. Permission is also granted on the understanding that nowhere in the text is a previously published source acknowledged for all or part of this Wiley Material. Any third party content is expressly excluded from this permission.

- With respect to the Wiley Materials, all rights are reserved. Except as expressly granted by the terms of the license, no part of the Wiley Materials may be copied, modified, adapted (except for minor reformatting required by the new Publication), translated, reproduced, transferred or distributed, in any form or by any means, and no derivative works may be made based on the Wiley Materials without the prior permission of the respective copyright owner.**For STM Signatory Publishers clearing permission under the terms of the STM Permissions Guidelines only, the terms of the license are extended to include subsequent editions and for editions in other languages, provided such editions are for the work as a whole in situ and does not involve the separate exploitation of the permitted figures or extracts,** You may not alter, remove or suppress in any manner any copyright, trademark or other notices displayed by the Wiley Materials. You may not license, rent, sell, loan, lease, pledge, offer as security, transfer or assign the Wiley Materials on a stand-alone basis, or any of the rights granted to you hereunder to any other person.

- The Wiley Materials and all of the intellectual property rights therein shall at all times remain the exclusive property of John Wiley & Sons Inc, the Wiley Companies, or their respective licensors, and your interest therein is only that of having possession of and the right to reproduce the Wiley Materials pursuant to Section 2 herein during the continuance of this Agreement. You agree that you own no right, title or interest in or to the Wiley Materials or any of the intellectual property rights therein. You shall have no rights hereunder other than the license as provided for above in Section 2. No right, license or interest to any trademark, trade name, service mark or other branding ("Marks") of WILEY or its licensors is granted hereunder, and you agree that you shall not assert any such right, license or interest with respect thereto

- NEITHER WILEY NOR ITS LICENSORS MAKES ANY WARRANTY OR REPRESENTATION OF ANY KIND TO YOU OR ANY THIRD PARTY, EXPRESS, IMPLIED OR STATUTORY, WITH RESPECT TO THE MATERIALS OR THE ACCURACY OF ANY INFORMATION CONTAINED IN THE MATERIALS, INCLUDING, WITHOUT LIMITATION, ANY IMPLIED WARRANTY OF MERCHANTABILITY, ACCURACY, SATISFACTORY QUALITY, FITNESS FOR A PARTICULAR PURPOSE, USABILITY, INTEGRATION OR NON-INFRINGEMENT AND ALL SUCH WARRANTIES ARE HEREBY EXCLUDED BY WILEY AND ITS LICENSORS AND WAIVED

BY YOU.

- WILEY shall have the right to terminate this Agreement immediately upon breach of this Agreement by you.

- You shall indemnify, defend and hold harmless WILEY, its Licensors and their respective directors, officers, agents and employees, from and against any actual or threatened claims, demands, causes of action or proceedings arising from any breach of this Agreement by you.

- IN NO EVENT SHALL WILEY OR ITS LICENSORS BE LIABLE TO YOU OR ANY OTHER PARTY OR ANY OTHER PERSON OR ENTITY FOR ANY SPECIAL, CONSEQUENTIAL, INCIDENTAL, INDIRECT, EXEMPLARY OR PUNITIVE DAMAGES, HOWEVER CAUSED, ARISING OUT OF OR IN CONNECTION WITH THE DOWNLOADING, PROVISIONING, VIEWING OR USE OF THE MATERIALS REGARDLESS OF THE FORM OF ACTION, WHETHER FOR BREACH OF CONTRACT, BREACH OF WARRANTY, TORT, NEGLIGENCE, INFRINGEMENT OR OTHERWISE (INCLUDING, WITHOUT LIMITATION, DAMAGES BASED ON LOSS OF PROFITS, DATA, FILES, USE, BUSINESS OPPORTUNITY OR CLAIMS OF THIRD PARTIES), AND WHETHER OR NOT THE PARTY HAS BEEN ADVISED OF THE POSSIBILITY OF SUCH DAMAGES. THIS LIMITATION SHALL APPLY NOTWITHSTANDING ANY FAILURE OF ESSENTIAL PURPOSE OF ANY LIMITED REMEDY PROVIDED HEREIN.

- Should any provision of this Agreement be held by a court of competent jurisdiction to be illegal, invalid, or unenforceable, that provision shall be deemed amended to achieve as nearly as possible the same economic effect as the original provision, and the legality, validity and enforceability of the remaining provisions of this Agreement shall not be affected or impaired thereby.

- The failure of either party to enforce any term or condition of this Agreement shall not constitute a waiver of either party's right to enforce each and every term and condition of this Agreement. No breach under this agreement shall be deemed waived or excused by either party unless such waiver or consent is in writing signed by the party granting such waiver or consent. The waiver by or consent of a party to a breach of any provision of this Agreement shall not operate or be construed as a waiver of or consent to any other or subsequent breach by such other party.

- This Agreement may not be assigned (including by operation of law or otherwise) by you without WILEY's prior written consent.

- Any fee required for this permission shall be non-refundable after thirty (30) days from receipt by the CCC.

- These terms and conditions together with CCC's Billing and Payment terms and conditions (which are incorporated herein) form the entire agreement between you and WILEY concerning this licensing transaction and (in the absence of fraud) supersedes all prior agreements and representations of the parties, oral or written. This Agreement may not be amended except in writing signed by both parties. This Agreement shall be binding upon and inure to the benefit of the parties' successors, legal representatives, and authorized assigns.

- In the event of any conflict between your obligations established by these terms and conditions and those established by CCC's Billing and Payment terms and conditions, these terms and conditions shall prevail.

- WILEY expressly reserves all rights not specifically granted in the combination of (i) the license details provided by you and accepted in the course of this licensing transaction, (ii) these terms and conditions and (iii) CCC's Billing and Payment terms and conditions.

- This Agreement will be void if the Type of Use, Format, Circulation, or Requestor Type was misrepresented during the licensing process.

- This Agreement shall be governed by and construed in accordance with the laws of the State of New York, USA, without regards to such state's conflict of law rules. Any legal action, suit or proceeding arising out of or relating to these Terms and Conditions or the breach thereof shall be instituted in a court of competent jurisdiction in New York County in the State of New York in the United States of America and each party hereby consents and submits to the personal jurisdiction of such court, waives any objection to venue in such court and consents to service of process by registered or certified mail, return receipt requested, at the last known address of such party.

WILEY OPEN ACCESS TERMS AND CONDITIONS

Wiley Publishes Open Access Articles in fully Open Access Journals and in Subscription journals offering Online Open. Although most of the fully Open Access journals publish open access articles under the terms of the Creative Commons Attribution (CC BY) License only, the subscription journals and a few of the Open Access Journals offer a choice of Creative Commons Licenses. The license type is clearly identified on the article.

The Creative Commons Attribution License

The Creative Commons Attribution License (CC-BY) allows users to copy, distribute and transmit an article, adapt the article and make commercial use of the article. The CC-BY license permits commercial and non-

Creative Commons Attribution Non-Commercial License

The Creative Commons Attribution Non-Commercial (CC-BY-NC)License permits use, distribution and reproduction in any medium, provided the original work is properly cited and is not used for commercial purposes.(see below)

Creative Commons Attribution-Non-Commercial-NoDerivs License

The Creative Commons Attribution Non-Commercial-NoDerivs License (CC-BY-NC-ND) permits use, distribution and reproduction in any medium, provided the original work is properly cited, is not used for commercial purposes and no modifications or adaptations are made. (see below)

Use by commercial "for-profit" organizations

Use of Wiley Open Access articles for commercial, promotional, or marketing purposes requires further explicit permission from Wiley and will be subject to a fee.

Further details can be found on Wiley Online Library

http://olabout.wiley.com/WileyCDA/Section/id-410895.html

Other Terms and Conditions:

v1.10 Last updated September 2015

Questions? customercare@copyright.com or +1-855-239-3415 (toll free in the US) or +1-978-646-2777.